

BIOMEDICAL PHOTONICS

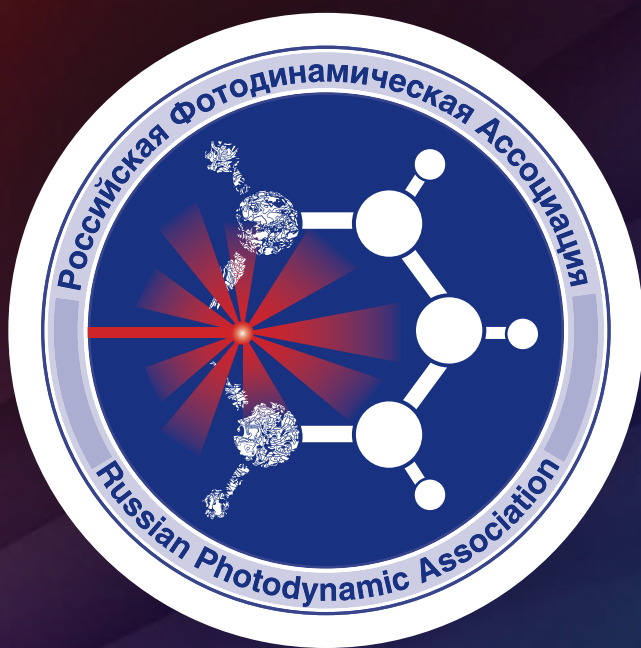
Volume 13, # 2, 2024

In the issue:

- Evaluation of the quality of electrochemical study in the diagnosis of infection of pancreatic cysts
- Photodynamic therapy with methylene blue and chlorin e6 photosensitizers: study on Ehrlich carcinoma mice model
- Effect of the composition of combined solid lipid particles with gefitinib and a photosensitizer on their size, stability and cytotoxic activity
- Bactericidal effectiveness of high-intensity pulsed broadband irradiation in treating infected wounds
- Effectiveness of palliative photodynamic therapy for unresectable biliary cancer. Systematic review and meta-analysis
- The role of membrane transport proteins in 5-ALA-induced accumulation of protoporphyrin IX in tumor cells

BMP

Российская Фотодинамическая Ассоциация



www.pdt-association.com

BIOMEDICAL PHOTONICS

FOUNDERS:

Russian Photodynamic Association
P.A. Herzen Moscow Cancer Research Institute

EDITOR-IN-CHIEF:

Filonenko E.V., Dr. Sci. (Med.), professor, head of the Centre of laser and photodynamic diagnosis and therapy of tumors in P.A. Herzen Moscow Cancer Research Institute (Moscow, Russia)

DEPUTY CHIEF EDITOR:

Grin M.A., Dr. Sci. (Chem.), professor, chief of department of Chemistry and technology of biological active substances named after Preobragenskiy N.A. in Moscow Technological University (Moscow, Russia)

Loschenov V.B., Dr. Sci. (Phys and Math), professor, chief of laboratory of laser biospectroscopy in the Natural Sciences Center of General Physics Institute of the Russian Academy of Sciences (Moscow, Russia)

EDITORIAL BOARD:

Kaprin A.D., Academician of the Russian Academy of Sciences, Dr. Sci. (Med.), professor, general director of National Medical Research Radiological Centre of the Ministry of Health of the Russian Federation (Moscow, Russia)

Romanko Yu.S., Dr. Sci. (Med.), professor of the department of Oncology, radiotherapy and plastic surgery named after L.L. Lyovshina in I.M. Sechenov First Moscow State Medical University (Moscow, Russia)

Stranadko E.Ph., Dr. Sci. (Med.), professor, chief of department of laser oncology and photodynamic therapy of State Research and Clinical Center of Laser Medicine named by O.K. Skobelcin of FMBA of Russia (Moscow, Russia)

Blondel V., PhD, professor at University of Lorraine, joint-Head of the Health-Biology-Signal Department (SBS) (Nancy, France)

Bolotine L., PhD, professor of Research Center for Automatic Control of Nancy (Nancy, France)

Douplik A., PhD, professor in Ryerson University (Toronto, Canada)

Steiner R., PhD, professor, the honorary director of Institute of Laser Technologies in Medicine and Metrology at Ulm University (Ulm, Germany)

BIOMEDICAL PHOTONICS –

research and practice, peer-reviewed, multidisciplinary journal.

The journal is issued 4 times per year.

The circulation – 1000 copies., on a quarterly basis.

The journal is included into the List of peer-reviewed science press of the State Commission for Academic Degrees and Titles of Russian Federation
The journal is indexed in the international abstract and citation database – Scopus.

The publisher «Agentstvo MORE».
Moscow, Khokhlovskiy lane., 9

Editorial staff:

Chief of the editorial staff	Ivanova-Radkevich V.I.
Science editor professor	Mamontov A.S.
Literary editor	Moiseeva R.N.
Translators	Kalyagina N.A.
Computer design	Kreneva E.I.
Desktop publishing	Shalimova N.M.

The Address of Editorial Office:

Russia, Moscow, 2nd Botkinskiy proezd, 3
Tel. 8 (495) 945–86–60
www: PDT-journal.com
E-mail: PDT-journal@mail.ru

Corresponding to:

125284, Moscow, p/o box 13

Registration certificate ПИ № ФС 77–51995, issued on 29.11.2012 by the Federal Service for Supervision of Communications, Information Technology, and Mass Media of Russia

The subscription index

of «Rospechat» agency – 70249

The editorial staff is not responsible for the content of promotional material. Articles represent the authors' point of view, which may be not consistent with view of the journal's editorial board. Editorial Board admits for publication only the articles prepared in strict accordance with guidelines for authors. Whole or partial presentation of the material published in the Journal is acceptable only with written permission of the Editorial board.

BIOMEDICAL PHOTONICS

BIOMEDICAL PHOTONICS –

научно-практический, рецензируемый,
мультидисциплинарный журнал.
Выходит 4 раза в год.
Тираж – 1000 экз., ежеквартально.

Входит в Перечень ведущих рецензируемых
научных журналов ВАК РФ.
Индексируется в международной
реферативной базе данных Scopus.

Издательство «Агентство МОРЕ».
Москва, Хохловский пер., д. 9

Редакция:

Зав. редакцией	Иванова-Радкевич В.И.
Научный редактор	проф. Мамонтов А.С.
Литературный редактор	Моисеева Р.Н.
Переводчики	Калягина Н.А.
Компьютерный дизайн	Кренева Е.И.
Компьютерная верстка	Шалимова Н.М.

Адрес редакции:

Россия, Москва, 2-й Боткинский пр., д. 3
Тел. 8 (495) 945–86–60
www: PDT-journal.com
E-mail: PDT-journal@mail.ru

Адрес для корреспонденции:

125284, Москва, а/я 13

Свидетельство о регистрации ПИ
№ ФС 77–51995, выдано 29.11.2012 г.
Федеральной службой по надзору в сфере
связи, информационных технологий
и массовых коммуникаций (Роскомнадзор)

Индекс по каталогу агентства

«Роспечать» – 70249

Редакция не несет ответственности за содержа-
ние рекламных материалов.

В статьях представлена точка зрения авторов,
которая может не совпадать с мнением редак-
ции журнала.

К публикации принимаются только статьи, под-
готовленные в соответствии с правилами для
авторов, размещенными на сайте журнала.

Полное или частичное воспроизведение матери-
алов, опубликованных в журнале, допускается
только с письменного разрешения редакции.

УЧРЕДИТЕЛИ:

Российская Фотодинамическая Ассоциация
Московский научно-исследовательский онкологический институт
им. П.А. Герцена

ГЛАВНЫЙ РЕДАКТОР:

Филоненко Е.В., доктор медицинских наук, профессор, руководитель
Центра лазерной и фотодинамической диагностики и терапии опухолей
Московского научно-исследовательского онкологического института
им. П.А. Герцена (Москва, Россия)

ЗАМ. ГЛАВНОГО РЕДАКТОРА:

Грин М.А., доктор химических наук, профессор, заведующий
кафедрой химии и технологии биологически активных соединений
им. Н.А. Преображенского Московского технологического университета
(Москва, Россия)

Лощенов В.Б., доктор физико-математических наук, профессор,
заведующий лабораторией лазерной биоспектроскопии в Центре
естественно-научных исследований Института общей физики
им. А.М. Прохорова РАН (Москва, Россия)

РЕДАКЦИОННАЯ КОЛЛЕГИЯ:

Каприн А.Д., академик РАН, доктор медицинских наук, профессор,
генеральный директор Национального медицинского исследовательского
центра радиологии Минздрава России (Москва, Россия)

Романко Ю.С., доктор медицинских наук, профессор кафедры онкологии,
радиотерапии и пластической хирургии им. Л.Л. Лёвшина Первого Москов-
ского государственного медицинского университета имени И.М. Сеченова
(Москва, Россия)

Странадко Е.Ф., доктор медицинских наук, профессор, руководитель Отде-
ления лазерной онкологии и фотодинамической терапии ФГБУ «Государствен-
ный научный центр лазерной медицины им. О.К.Скобелкина ФМБА России»

Blondel V., профессор Университета Лотарингии, руководитель отделения
Здравоохранение-Биология-Сигналы (SBS) (Нанси, Франция)

Bolotine L., профессор научно-исследовательского центра автоматизации
и управления Нанси (Нанси, Франция)

Douplik A., профессор Университета Райерсона (Торонто, Канада)

Steiner R., профессор, почетный директор Института лазерных технологий
в медицине и измерительной технике Университета Ульма (Ульм, Германия)

ORIGINAL ARTICLES

Evaluation of the quality of electrochemical study in the diagnosis of infection of pancreatic cysts

Gerasimov A.V., Nikolskiy V.I., Mitroshin A.N., Sergatskiy K.I.

4

Photodynamic therapy with methylene blue and chlorin e6 photosensitizers: study on Ehrlich carcinoma mice model

Pominova D.V., Ryabova A.V., Skobeltsin A.S., Markova I.V., Romanishkin I.D.

9

Effect of the composition of combined solid lipid particles with gefitinib and a photosensitizer on their size, stability and cytotoxic activity

Nikolaeva L.L., Sanarova E.V., Kolpaksidi A.P., Shcheglov S.D., Rudakova A.A., Baryshnikova M.A., Lantsova A.V.

19

Bactericidal effectiveness of high-intensity pulsed broadband irradiation in treating infected wounds

Abduvosidov Kh.A., Chudnykh S.M., Egorov V.S., Filimonov A.Yu., Korolyova I.A., Kamrukov A.S., Bagrov V.V., Kondrat'ev A.V.

26

REVIEWS OF LITERATURE

Effectiveness of palliative photodynamic therapy for unresectable biliary cancer. Systematic review and meta-analysis

Tseimakh A.E., Mitshenko A.N., Kurtukov V.A., Shoikhet Ia.N., Kuleshova I.V.

34

The role of membrane transport proteins in 5-ALA-induced accumulation of protoporphyrin IX in tumor cells

Ivanova-Radkevich V.I., Kuznetsova O.M., Filonenko E.V.

43

ОРИГИНАЛЬНЫЕ СТАТЬИ

Оценка качества электрохимического исследования в диагностике инфицирования кист поджелудочной железы

А.В. Герасимов, В.И. Никольский, А.Н. Митрошин, К.И. Сергацкий

4

Фотодинамическая терапия с фотосенсибилизаторами метиленовый синий и хлорин е6: исследование на мышинной модели карциномы Эрлиха

Д.В. Поминова, А.В. Рябова, А.С. Скобельцин, И.В. Маркова, И.Д. Романишкин

9

Влияние состава комбинированных твердых липидных частиц с gefitinibом и фотосенсибилизатором на их размер, стабильность и цитотоксическую активность

Л.Л. Николаева, Е.В. Санарова, А.П. Колпаксиди, С.Д. Щеглов, А.А. Рудакова, М.А. Барышникова, А.В. Ланцова

19

Бактерицидная эффективность использования высокоинтенсивного импульсного широкополосного облучения при лечении инфицированных ран

Х.А. Абдувосидов, С.М. Чудных, В.С. Егоров, А.Ю. Филимонов, И.А. Корольова, А.С. Камруков, В.В. Багров, А.В. Кондратьев

26

ОБЗОРЫ ЛИТЕРАТУРЫ

Эффективность паллиативной фотодинамической терапии нерезектабельных злокачественных новообразований желчевыводящей системы. Систематический обзор и метаанализ

А.Е. Цеймах, А.Н. Мищенко, В.А. Куртуков, Я.Н. Шойхет, И.В. Кулешова

34

Роль трансмембранных переносчиков в накоплении 5-АЛК-индуцированного протопорфирина IX в опухолевых клетках

В.И. Иванова-Радкевич, О.М. Кузнецова, Е.В. Филоненко

43

EVALUATION OF THE QUALITY OF ELECTROCHEMICAL STUDY IN THE DIAGNOSIS OF INFECTION OF PANCREATIC CYSTS

Gerasimov A.V., Nikolskiy V.I., Mitroshin A.N., Sergatskiy K.I.

Medical Institute, Penza State University, Penza, Russia

Abstract

The formation of pancreatic cysts is a serious complication of acute pancreatitis, chronic pancreatitis and pancreatic injuries. Joulemetry is an integral method for evaluating the electrochemical properties of biological objects. To date, this method has not been used in the study of the electrochemical properties of the contents of pancreatic cysts. The purpose of this study was to evaluate the effectiveness of electrochemical analysis in the detection of infection in the contents of necrotic pancreatic cysts. An electrochemical study of contents of necrotic pancreatic cysts carried out on 106 patients. Group 1 included 84 patients without signs of infection of pancreatic cysts; group 2 included 22 patients with signs of infection of pancreatic cysts. The electrochemical study was conducted as follows: 10 ml of the contents of a pancreatic cyst was injected into a liquid flow sensor of a joule meter, where it was exposed to an electrical current for a short period of time. The resulting data was analyzed using a diagnostic research complex. During the study of the electrochemical properties of the contents of postnecrotic pancreatic cysts by using joulemetry, it was revealed that the current work in patients of group 1 ranged from 0.92 to 18.31 mJ (on average 5.86 ± 5.02 mJ), in patients of group 2 – from 19.01 to 26.3 mJ (on average 22.32 ± 1.92 mJ). When evaluating the quality of the joulemetric study in determining the early signs of inflammation of the contents of postnecrotic pancreatic cysts, it was proved that the threshold differential diagnostic value of 19.1 mJ provides 81.8% sensitivity of the proposed method and 80.7% specificity (AUC = 91.3) with a statistically significant difference in current work ($p < 0.001$).

Keywords: Postnecrotic pancreatic cysts, pancreatitis, joulemetry, infection, electrochemical properties.

Contacts: Gerasimov A. V., gerasimov-av30@yandex.ru

For citations: Gerasimov A.V., Nikolskiy V.I., Mitroshin A.N., Sergatskiy K.I. Evaluation of the quality of electrochemical study in the diagnosis of infection of pancreatic cysts, *Biomedical Photonics*, 2024, vol. 13, no. 2, pp. 4–8. doi: 10.24931/2413–9432–2024–13–2–4–8.

ОЦЕНКА КАЧЕСТВА ЭЛЕКТРОХИМИЧЕСКОГО ИССЛЕДОВАНИЯ В ДИАГНОСТИКЕ ИНФИЦИРОВАНИЯ КИСТ ПОДЖЕЛУДОЧНОЙ ЖЕЛЕЗЫ

А.В. Герасимов, В.И. Никольский, А.Н. Митрошин, К.И. Сергачкий

ФГБОУ ВО «Пензенский государственный университет», Медицинский институт, г. Пенза, Россия

Резюме

Образование кист поджелудочной железы является серьёзным осложнением острого и хронического панкреатита, а также травм поджелудочной железы. Джоульметрия – интегральный метод оценки электрохимических свойств биологических объектов. На сегодняшний день этот метод еще не использовали в изучении электрохимических свойств содержимого кист поджелудочной железы. Целью исследования явилась оценка качества электрохимического исследования в диагностике инфицирования содержимого постнекротических кист поджелудочной железы. Электрохимическое исследование выполнили 106 пациентам с постнекротическими кистами поджелудочной железы. В 1-ю группу вошли 84 пациента без признаков инфицирования кист поджелудочной железы, во 2-ю группу – 22 пациента с признаками инфицирования кист поджелудочной железы. Электрохимическое исследование выполняли следующим образом: содержимое кисты поджелудочной железы забирали в количестве 10 мл и вводили внутрь жидкостного проточного датчика джоульметрического прибора, где за короткий промежуток времени на него действовал ток. Посредством диагностического исследовательского комплекса оценивали полученные результаты. В ходе исследования электрохимических свойств содержимого постнекротических кист поджелудочной железы с помощью джоульметрии было выявлено, что показатель работы тока у больных 1-й группы колебался в пределах от 0,92 до 18,31 мкДж (в среднем $5,86 \pm 5,02$ мкДж), у пациентов 2-й группы – от 19,01 до 26,3 мкДж (в среднем $22,32 \pm 1,92$ мкДж). При оценке качества джоульметрического исследования в определении ранних признаков воспаления содержимого постнекротических кист поджелудочной железы доказано, что пороговое дифференциально-диагностическое значение равно 19,1 мкДж обеспечивает чувствительность предложенного метода в 81,8% и специфичность в 80,7% (AUC = 91,3) при статистически значимой разнице показателей работы тока ($p < 0,001$).

Ключевые слова. Постнекротические кисты поджелудочной железы, панкреатит, джоульметрия, инфицирование, электрохимические свойства.

Контакты: Герасимов А.В., gerasimov-av30@yandex.ru

Для цитирования: Герасимов А.В., Никольский В.И., Митрошин А.Н., Сергачкий К.И. Оценка качества электрохимического исследования в диагностике инфицирования кист поджелудочной железы // *Biomedical photonics*. – 2024. – Т.13, № 2. – С. 4–8. doi: 10.24931/2413–9432–2024–13–2–4–8.

Introduction

Formation of pancreatic cysts is a serious complication of acute and chronic pancreatitis, as well as pancreatic injuries [1, 2, 3, 4]. Formation of cysts in acute pancreatitis is observed in almost 20% of cases, and this indicator increases 4 times in destructive forms. In chronic pancreatitis, the incidence of pancreatic cysts is between 20% and 40% and in pancreatic injuries, cysts occur in 20-30% of cases [4, 5]. It is worth noting that during the formation of a cyst, quite serious complications can be observed, occurring in almost 40% of cases: bleeding into the cyst cavity, suppuration, perforation, compression of adjacent organs with the corresponding clinical picture.

A tactical approach to the treatment of patients in this category includes identifying early signs of infection of the contents of the pancreatic cyst and the presence of a connection between the cyst and the duct system of the pancreas [4, 5, 6]. However, the currently existing methods for diagnosing infection of postnecrotic pancreatic cysts have a number of disadvantages: a long period of time before obtaining the result (up to 3-5 days for bacteriological examination), low information content, limitations in use due to contraindications, etc.

It has been proven that under the influence of various factors of the external and internal environment of the body, such as changes in temperature, volume, concentration of electrolytes, the appearance of signs of suppuration or blood elements, etc., the electrical properties of any biological objects change [7]. At the same time, when using microcurrents of 10-100 μ A, there are no changes in the physico-chemical processes of the object under study. Joulemetry is an integral method based on the assessment of the values of the current work expended by an external source of electrical energy at the time when the state of the object under study changes.

The advantages of joulemetry include: simplicity of implementation of the method, low time costs, wide application (for all types of biological tissues), high sensitivity of the method, which allows to increase the number of necessary informative features.

It should be noted that it is the timely and accurate diagnosis of early signs of inflammation of the contents of postnecrotic pancreatic cysts that allows to correctly select the necessary method of surgical treatment and determine the tactical approach as a whole [5, 6].

The aim of the study was to assess the quality of electrochemical study in the diagnosis of infection of the contents of postnecrotic pancreatic cysts.

Materials and methods

To determine early signs of inflammation of the contents of postnecrotic pancreatic cysts, a method of express diagnostics based on a joulemetric study was developed and introduced into clinical practice (Patent of the Russian Federation for Invention No. 2684424 dated 04/09/2019).

The study was conducted at the Medical Institute of the Federal State Budgetary Educational Institution of Higher Education "Penza State University" and the surgical departments of the State Budgetary Healthcare Institution "Penza Regional Clinical Hospital named after N.N. Burdenko".

For the period from 2016 to 2023 inclusive, 106 patients with postnecrotic pancreatic cysts were treated in the surgical departments of the State Budgetary Healthcare Institution "Penza Regional Clinical Hospital named after N.N. Burdenko".

Depending on the presence of signs of inflammation, the patients were divided into two groups. Group 1 included 84 (79.2%) patients with pancreatic cysts without signs of inflammation, and Group 2 included 22 (20.8%) patients with pancreatic cysts and signs of inflammation. This division was based on clinical and laboratory data and instrumental research data (ultrasound, CT, MRI).

Scientists from Penza State University have developed a joulemetry method and a device for diagnosing the state of biological objects (Patent of the Russian Federation No. 2033606 dated 20/04/95), and received permission from the Ministry of Health of the Russian Federation (minutes of the meeting of the commission on new medical equipment No. 10 dated 18/11/93) for use in clinical practice (Gerashchenko S.I., Nikolsky V.I., Volchikhin V.I., 1993). The Divo joulemeter and IPC 2000 software were developed by the staff of the Medical Devices and Equipment Department of the Penza State University.

Electrochemical (another name is joulemetric) study of the contents of postnecrotic pancreatic cysts was performed as follows: 10 ml of the contents of the patient's pancreatic cyst, obtained by puncture or external drainage under ultrasound control, were taken; these contents were then introduced into the liquid flow sensor of the Divo joulemetric device (Penza); a current of 0.1 mA was passed through the liquid flow sensor of the joulemetric device for less than 8 s. The results were evaluated using a diagnostic research complex (Fig. 1), which included a joulemetric device, a liquid flow sensor, and a computer program for information analysis (IPC 2000).

The IPC 2000 program was used to evaluate the obtained dependencies, which were curves with certain values of potential change over time. Based on the obtained dependencies, the work for each current value was calculated, and graphs were constructed that allowed to analyze the activity of the inflammatory process of pancreatic cysts.

Statistical analysis was performed on an IBM-PC compatible computer using the licensed program BioStat 2010 5.8.3.0 and IBM SPSS Statistics for Windows, Version 25.0. ROC analysis (receiver operating characteristic) was performed to assess the quality of the model of the proposed method for express diagnostics of pancreatic cyst infection based on joulemetry.

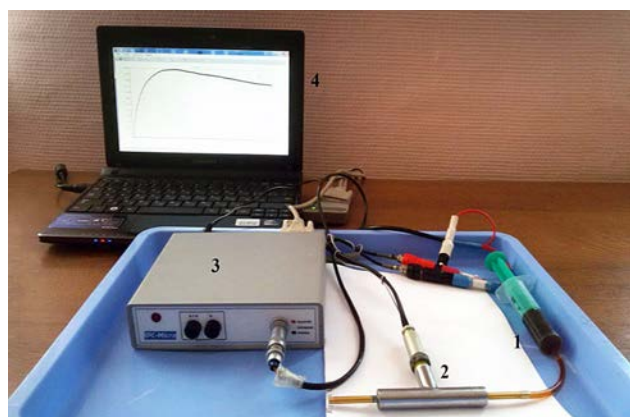


Рис. 1. Диагностический исследовательский комплекс: 1 – шприц для нагнетания содержимого кисты; 2 – жидкостной проточный датчик; 3 – джоульметрический прибор; 4 – компьютер с установленной программой IPC 2000.

Fig. 1. Diagnostic research complex: 1 – a syringe for pumping cyst contents; 2 – a liquid flow sensor; 3 – a joule meter; 4 – a computer with the IPC 2000 program installed.

Results and Discussion

To form two groups of patients with a preliminary assessment of infection or absence of infection of pancreatic cysts, criteria were defined based on clinical, laboratory and instrumental data.

The following criteria of clinical, laboratory and instrumental research methods were considered as signs of inflammation of postnecrotic pancreatic cysts:

- increased body temperature;
- the presence of peritoneal symptoms;
- leukocytosis with a shift in the leukocyte formula to the left;
- according to ultrasound: heterogeneous cyst contents (finely dispersed hyperechoic suspension with the

presence of partitions), uneven thickening of the cyst wall, signs of infiltration of the parapancreatic tissue;

- according to SCT: heterogeneous structure with hypodense inclusions (density of contents from +20 to +30 HU units), edema and stringiness of the parapancreatic tissue;
- according to MRI: a formation with an increased MR signal on T_2 -weighted images and an increased MR signal on T_1 -weighted images, the parapancreatic tissue is heterogeneous with signs of edema.

Postnecrotic pancreatic cysts without signs of inflammation had the following clinical, laboratory and instrumental features:

- no constant hyperthermia was observed;
- no peritoneal symptoms;
- no signs of inflammation in the clinical blood test;
- according to ultrasound: homogeneous anechoic contents of the cyst cavity or heterogeneous contents with a parietal component, smooth clear contour of the formation, no signs of infiltration of the parapancreatic tissue;
- according to SCT: homogeneous structure of the cyst (density of the contents from +5 to +18 HU), no signs of infiltration of the parapancreatic tissue;
- according to MRI: a formation with an increased MR signal on T_2 -weighted images and a decreased MR signal on T_1 -weighted images, without edema of the parapancreatic tissue.

During the study of the electrochemical properties of the contents of postnecrotic pancreatic cysts using joulemetry, it was revealed that the current work index (Table 1) in patients of the 1st Group was in the range from 0.92 to 18.31 μJ (on average $5.86 \pm 5.02 \mu\text{J}$), in patients of the 2nd Group – from 19.01 to 26.3 μJ (on average $22.32 \pm 1.92 \mu\text{J}$).

Таблица 1

Работа тока у больных с признаками воспаления кист поджелудочной железы и без признаков воспаления кист поджелудочной железы

Table 1

Electric current work in patients with signs of inflammation of pancreatic cysts and without signs of inflammation of pancreatic cysts

Исследуемые группы пациентов The studied groups of patients	Количество пациентов, n=106 Number of patients, n=106		Работа тока, мкДж Electric current work, μJ	Среднее значение The average value
	Абс.	%		
1 группа – больные без признаков воспаления кист поджелудочной железы 1 group – patients without signs of inflammation of pancreatic cysts	84	79,2	от 0,92 до 18,31	$5,86 \pm 5,02$
2 группа – больные с признаками воспаления кист поджелудочной железы 2 group – patients with signs of inflammation of pancreatic cysts	22	20,8	от 19,01 до 26,3	$22,32 \pm 1,92$
Итого Total	106	100	-	-
Достоверность Reliability	-	-	-	< 0,001

Consequently, statistically significant data on infection of postnecrotic pancreatic cysts were obtained ($p < 0.001$): in patients of the 1st group without signs of inflammation of the contents of the pancreatic cysts, a low current work rate was diagnosed (on average $5.86 \pm 5.02 \mu\text{J}$), whereas in patients of the 2nd group with signs of inflammation of the contents of the pancreatic cysts, a high current work rate was detected (on average $22.32 \pm 1.92 \mu\text{J}$).

Fig. 2 and 3 present the measured electrochemical parameters in graphical form, which indicated the presence or absence of signs of inflammation of the contents of postnecrotic pancreatic cysts.

Fig. 2 shows that the saturation point is reached at a time of 3.8 s, the potential value at this point is 4200 mV, whereas in Fig. 3 the saturation point is reached at a time of 0.9 s, the potential value at this point is 2850 mV. Thus, for the electrochemical reaction in patients with infected pancreatic cysts, a higher voltage, amount of time and, as a result, more current work is required to reach the saturation point than in patients with pancreatic cysts without signs of inflammation, which is confirmed by the above data.

All the obtained results of the electrochemical study of the contents of pancreatic cysts were confirmed by

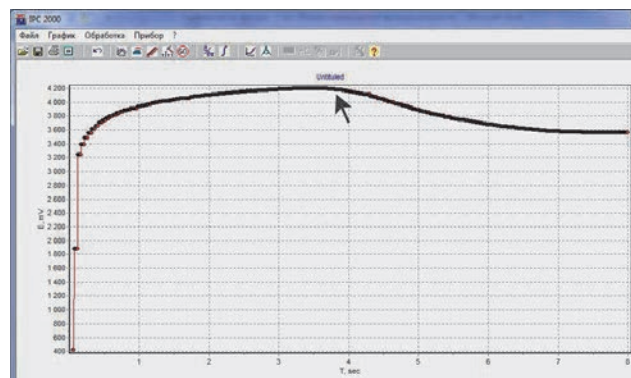


Рис. 2. Характерная кривая для кисты с признаками воспаления; стрелкой указана точка насыщения.

Fig. 2. A typical curve for a cyst with signs of inflammation, with the arrow indicating the saturation point.

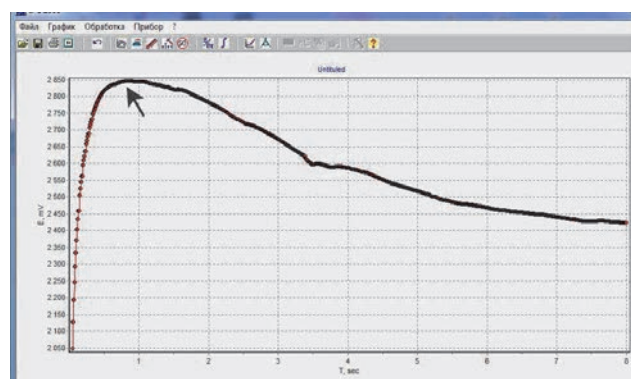


Рис. 3. Характерная кривая для кисты без признаками воспаления; стрелкой указана точка насыщения.

Fig. 3. A typical curve for a cyst without signs of inflammation, with the arrow indicating the saturation point.

bacteriological examination: in 22 patients with signs of inflammation of pancreatic cysts and a high current work rate (on average $22.32 \pm 1.92 \mu\text{J}$), growth of microorganisms was observed, in 84 patients without signs of inflammation of pancreatic cysts and a low current work rate (on average $5.86 \pm 5.02 \mu\text{J}$), there was no growth of microflora.

The quality of the model of the proposed method for express diagnostics of infection of postnecrotic pancreatic cysts using joulemetry was analyzed. For this purpose, ROC curves were evaluated (Fig. 4).

The presented graph clearly demonstrates that the numerical indicator of the area under the curve ($\text{AUC} = 91.3$) tends to 1.0, which characterizes the excellent quality of the model of the proposed method based on joulemetry.

Fig. 5 shows a graph of the dependence of signs of infection of postnecrotic cysts of the pancreas on the indicators of the current work obtained by joulemetry.

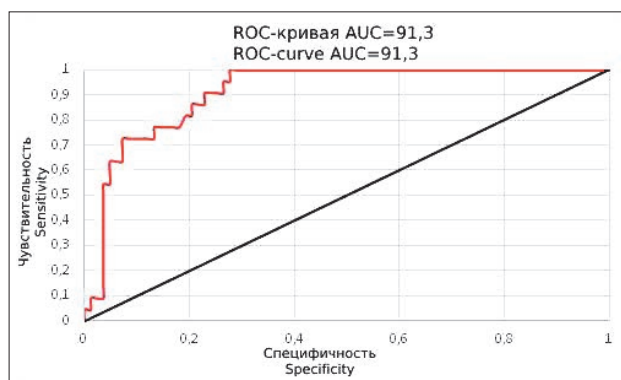


Рис. 4. ROC-кривая исследования работы тока у больных с постнекротическими кистами поджелудочной железы при определении их инфицирования на основе джоульметрии. На графике красным цветом показана ROC-кривая, черным – положительная диагональ.

Fig. 4. The ROC curve of the study of the electrical current in patients with postnecrotic pancreatic cysts in determining their infection based on joulemetry. The graph shows the ROC-curve in red, and the positive diagonal in black.

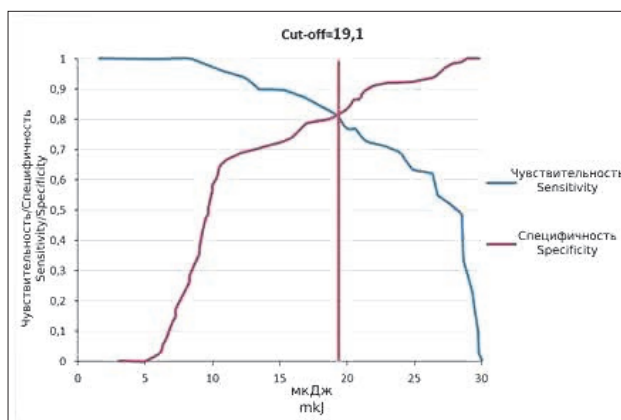


Рис. 5. Значение точки отсечения (cut-off) наличия/отсутствия признаков инфицирования содержимого постнекротической кисты ПЖ при джоульметрии.

Fig. 5. The value of the cut-off point for the presence/absence of signs of infection of the contents of a postnecrotic pancreatic cyst during joulemetry.

During the study, the cut-off point value for the presence/absence of signs of infection of the contents of a postnecrotic pancreatic cyst was determined: 19.1 μJ (if the current work value is $> 19.1 \mu\text{J}$, then the cyst has signs of infection; if the current work value is $\leq 19.1 \mu\text{J}$, then the cyst is not infected).

Table 2 shows a fragment of the ROC-curve coordinate table for the study of current work in patients with postnecrotic pancreatic cysts when determining infection of their contents using the joulemetric method.

Based on the table of coordinates of the ROC curve of the study of the current work in patients with postnecrotic cysts of the pancreas when determining their infection based on joulemetry, the threshold differential diagnostic value was taken to be the current work index equal to 19.1 μJ . This value ensures the sensitivity of the proposed method of express diagnostics of exudate infection in local pancreatogenic peritonitis based on joulemetry equal to 81.8%, and specificity equal to 80.7% (AUC = 91.3).

All the obtained results of the electrochemical study of the contents of pancreatic cysts were confirmed by bacteriological examination: in 22 patients with signs of inflammation of pancreatic cysts and a high current work rate (on average $22.32 \pm 1.92 \mu\text{J}$), growth of microorganisms was observed; in 84 patients without signs of inflammation of pancreatic cysts and a low current work rate (on average $5.86 \pm 5.02 \mu\text{J}$), growth of microflora was not observed.

Conclusion

During the electrochemical study of the contents of postnecrotic pancreatic cysts, statistically significant data on infection of the cyst contents were obtained ($p < 0.001$). When the current work was from 19.01 to 26.3 μJ

Таблица 2

Фрагмент таблицы координат ROC-кривой исследования работы тока у пациентов с постнекротическими кистами ПЖ при определении инфицирования их содержимого

Table 2

A fragment of the coordinate table of the ROC-curve of the study of electrical current work in patients with postnecrotic pancreatic cysts in determining infection of their contents

Работа тока, мкДж Electric current work, μJ	Чувствитель- ность Sensitivity	Специфич- ность Specificity
10,1	0,9789	0,6378
13,42	0,9213	0,7066
16,91	0,8708	0,7853
19,1	0,8182	0,8072
20,14	0,7835	0,8113
22,76	0,7412	0,8810
23,1	0,7244	0,9227

(on average $22.32 \pm 1.92 \mu\text{J}$), infection of the postnecrotic pancreatic cyst was diagnosed; the current work indicator from 0.92 to 18.31 μJ (on average $5.86 \pm 5.02 \mu\text{J}$) indicates the absence of infection.

When assessing the quality of the joulemetric study in determining the early signs of inflammation of the contents of postnecrotic cysts of the pancreas, it was proven that the threshold differential diagnostic value of 19.1 μJ provides the sensitivity of the proposed method at 81.8% and specificity at 80.7% (AUC = 91.3) with a statistically significant difference in the current work indicators ($p < 0.001$).

REFERENCES

- Korymasov E.A., Khoroshilov M.Yu. "Fulminant" acute pancreatitis: diagnosis, prognosis, treatment, *Annals of Surgical Hepatology*, 2021, vol. 26(2), pp. 50-59. doi: 10.16931/1995-5464.2021-2-50-60.
- Zurnadzhlyants V.A., Khibekov E.A., Gasanov K.G. et al. Optimization of diagnostic approaches for destructive pancreatitis, *Perm Medical Journal*, 2023, vol. 40(4), pp. 82-91. doi: 10.17816/pmj40482-91.
- Styazhkina S.N., Vorobyova A.S., Naumova O.N. Frequency of occurrence of the diagnosis "Acute pancreatitis" among patients of the surgical department of the 1st RCH UR, *Science and Education Today*, 2019, vol. 1, pp. 89-92.
- Ramsey M.L., Conwell D.L., Hart P.A. Complications of chronic pancreatitis, *Dig. Dis. Sci.*, 2017, vol. 32(7), pp. 1746-1750. doi: 10.1007/s10620-017-4518-x
- Sobolev Yu.A., Belyaeva A.I. Efficiency of transcutaneous puncture drainage of pancreatic cysts under ultrasound control, *Bulletin of the Volgograd State Medical University*, 2021, vol. 77, pp. 52-55. doi: 10.19163/1994-9480-2021-1(77)-52-55.
- García de Paredes A.G., López-Durán S., José Olcina R.F., et al. Management of pancreatic collections: an update, *Rev. Esp. Enferm. Dig.*, 2020, vol. 112(6), pp. 483-490. doi: 10.17235/reed.2020.6814/2019.
- Gerashchenko, S.I. Joulemetry and joulemetric systems: theory and application: monograph, Penza: PSU Publishing House, 2002, 184 p.

ЛИТЕРАТУРА

- Корымасов Е.А., Хорошилов М.Ю. «Молниеносный» острый панкреатит: диагностика, прогнозирование, лечение // *Анналы хирургической гепатологии*. – 2021. – Т. 26, № 2. – С. 50-59. doi: 10.16931/1995-5464.2021-2-50-60.
- Зурнаджянц В.А., Кхибеков Э.А., Гасанов К.Г. и др. Оптимизация диагностических подходов деструктивного панкреатита // *Пермский медицинский журнал*. – 2023. – Т. 40, №4. – С. 82-91. doi: 10.17816/pmj40482-91.
- Стяжкина С.Н., Воробьева А.С., Наумова О.Н. Частота встречаемости диагноза «Острый панкреатит» среди пациентов хирургического отделения 1 РКБ УР // *Наука и образование сегодня*. – 2019. – №1. – С. 89-92.
- Ramsey M.L., Conwell D.L., Hart P.A. Complications of chronic pancreatitis // *Dig. Dis. Sci.* – 2017. – Vol. 32(7). – P. 1746-1750. doi: 10.1007/s10620-017-4518-x
- Соболев Ю.А., Беляева А.И. Эффективность транскутанного пункционного дренирования кист поджелудочной железы под ультразвуковым контролем // *Вестник Волгоградского Государственного Медицинского университета*. – 2021. – №77. – С. 52-55. doi: 10.19163/1994-9480-2021-1(77)-52-55.
- García de Paredes A.G., López-Durán S., José Olcina R.F., et al. Management of pancreatic collections: an update // *Rev. Esp. Enferm. Dig.* – 2020. – Vol. 112(6). – P. 483-490. doi: 10.17235/reed.2020.6814/2019.
- Герашченко, С. И. Джоульметрия и джоульметрические системы: теория и приложение: монография // Пенза: Изд-во ПГУ, 2002. – 184 с.

PHOTODYNAMIC THERAPY WITH METHYLENE BLUE AND CHLORIN e6 PHOTSENSITIZERS: STUDY ON EHRlich CARCINOMA MICE MODEL

Pominova D.V.^{1,2}, Ryabova A.V.^{1,2}, Skobeltsin A.S.¹, Markova I.V.², Romanishkin I.D.¹

¹Prokhorov General Physics Institute of Russian Academy of Sciences, Moscow, Russia

²National Research Nuclear University MEPhI (Moscow Engineering Physics Institute), Moscow, Russia

Abstract

Hypoxia negatively affects the effectiveness of all types of anticancer therapy, in particular photodynamic therapy (PDT). In this regard, various approaches to overcome the limitations associated with hypoxia are widely discussed in the literature, one of them is the use of photosensitizers (PS) operating through the first mechanism of the photodynamic reaction, such as methylene blue (MB). Previously, we have demonstrated that MB can have a positive effect on tumor oxygenation. In this work, we investigated the photodynamic activity of MB and a combination of MB with chlorin e6 on a tumor in vivo using a model of Ehrlich carcinoma. PDT was studied with the joint and separate administration of chlorin e6 and MB. The accumulation and localization of MB and its combination with chlorin e6 in vivo was assessed using video fluorescence and spectroscopic methods, and the effect of laser exposure on accumulation was analyzed. After the PDT with chlorin e6, MB and a combination of MB with chlorin e6, a good therapeutic effect and a decrease in the tumor growth rate were observed compared to the control, especially in groups with PDT with MB and with the simultaneous administration of chlorin e6 and MB. The level of tumor oxygenation on days 3 and 5 after PDT was higher for groups with irradiation, the highest oxygenation on the 5th day after PDT was observed in the group with PDT only with MB. Phasor diagrams of tumors after PDT show a deviation from the metabolic trajectory and a shift towards a longer lifetimes compared to the control tumor, which indicates the presence of lipid peroxidation products. Thus, tumor regression after PDT is associated with the direct destruction of tumor cells under the influence of reactive oxygen species formed during PDT. Thus, the effectiveness of PDT with the combined use of MB and chlorin e6 has been demonstrated, and the main mechanisms of the antitumor effect of the combination of these PS have been studied.

Keywords: photodynamic therapy, methylene blue, inhibition of tumor growth.

Contacts: Pominova D.V., e-mail: pominovadv@gmail.com

For citations: Pominova D.V., Ryabova A.V., Skobeltsin A.S., Markova I.V., Romanishkin I.D. Photodynamic therapy with methylene blue and chlorin e6 photosensitizers: study on Ehrlich carcinoma mice model, *Biomedical Photonics*, 2024, vol. 13, no. 2, pp. 9–18. doi: 10.24931/2413-9432-2024-13-2-9-18.

ФОТОДИНАМИЧЕСКАЯ ТЕРАПИЯ С ФОТОСЕНСИБИЛИЗАТОРАМИ МЕТИЛЕНОВЫЙ СИНИЙ И ХЛОРИН e6: ИССЛЕДОВАНИЕ НА МЫШИНОЙ МОДЕЛИ КАРЦИНОМЫ ЭРЛИХА

Д.В. Поминова^{1,2}, А.В. Рябова^{1,2}, А.С. Скобельцин¹, И.В. Маркова², И.Д. Романишкин¹

¹Институт общей физики им. А. М. Прохорова Российской академии наук, Москва, Россия

²Национальный исследовательский ядерный университет «МИФИ», Москва, Россия

Резюме

Гипоксия негативно влияет на эффективность всех видов противоопухолевой терапии, в частности фотодинамической терапии (ФДТ). В связи с этим в литературе широко обсуждаются разные подходы для преодоления ограничений, связанных с гипоксией. Одним из них является использование фотосенсибилизаторов (ФС), работающих по первому механизму фотодинамической реакции, таких как метиленовый синий (МС). Ранее нами было показано, что МС может положительно влиять на оксигенацию опухоли. В данной работе мы провели исследование фотодинамической активности МС и МС в комбинации с хлорином e6 на опухоли *in vivo* на модели карциномы Эрлиха. Была исследована ФДТ при совместном и раздельном введении хлорина e6 и МС. Выполнена оценка накопления и локализации МС и МС в комбинации с хлорином e6 *in vivo* при помощи видеофлуоресцентных и спектроскопических методов, проанализировано влияние лазерного воздействия на накопление. После проведения ФДТ с хлорином e6, МС и комбинации МС с хлорином e6 отмечен хороший терапевтический эффект и уменьшение скорости роста опухоли по сравнению с контролем, особенно

в группах с ФДТ с МС и при одновременном введении хлорина е6 и МС. Уровень оксигенации опухоли на 3-е и 5-е сутки после ФДТ был выше в группах с облучением, самая высокая оксигенация на 5-е сутки после ФДТ отмечена в группе с ФДТ с МС. На фазовых диаграммах опухолей после проведения ФДТ наблюдается отклонение от метаболической траектории и сдвиг в сторону более длинного времени жизни по сравнению с контрольной опухолью, что указывает на наличие продуктов перекисного окисления липидов. Следовательно, регрессия опухоли после ФДТ связана с прямым разрушением опухолевых клеток под воздействием активных форм кислорода, образующихся при ФДТ. Таким образом, продемонстрирована эффективность ФДТ при совместном применении МВ и хлорина е6 и исследованы основные механизмы противоопухолевого действия комбинации этих ФС.

Ключевые слова: фотодинамическая терапия, метиленовый синий, подавление роста опухоли.

Контакты: Поминова Д.В., e-mail: pominovadv@gmail.com

Для цитирования: Поминова Д.В., Рябова А.В., Скобельцин А.С., Маркова И.В., Романишкин И.Д. Фотодинамическая терапия с фотосенсибилизаторами метиленовый синий и хлорин е6: исследование на мышиной модели карциномы Эрлиха // Biomedical Photonics. – 2024. – Т. 13, № 2. – С. 9–18.. doi: 10.24931/2413-9432-2024-13-2-9-18.

Introduction

Hypoxia is commonly associated with poor outcome in most cancer types and treatment modalities [1, 2, 3]. In recent years, it was shown that hypoxia plays an important role in the interaction between cancer cells, stroma and immune cells [4, 5, 6]. Hypoxia inducible factors (HIFs) are the major regulators of cancer cell survival [7, 8, 9, 10] and the role of hypoxia can be crucial in treatment resistance [11, 12].

Strategies to overcome hypoxia are widely discussed in many papers and reviews [13, 14, 15]. Strategies to increase oxygenation during photodynamic therapy (PDT), a promising approach for cancer treatment with low systemic toxicity and minimal invasiveness that has already demonstrated efficacy and safety in clinical use, are gaining increasing attention [16, 17, 18, 19]. During PDT, a special drug – photosensitizer (PS) – generates reactive oxygen species (ROS) under the action of light, which can damage biological structures and act as regulators of cell proliferation, metabolism, and apoptosis [20]. There are two types of reactions that result in the formation of ROS: the participation of PS in electron transfer reactions initiating the formation of hydroxyl radicals and hydroperoxides (type I photochemical reaction) and the energy transfer from PS to molecular oxygen, which results in the creation of singlet oxygen (type II photochemical reaction) [21]. The majority of clinically approved photosensitizers utilize the type II photochemical reaction, but less oxygen-dependent type I PDT is discussed as a strategy for the treatment of hypoxic tumors [22, 23]. Other strategies to overcome tumor hypoxia for enhancing PDT efficacy were summarized in recent review [24] and include delivering exogenous oxygen to tumor, generation of oxygen in tumor, reducing tumor oxygen consumption, normalizing tumor vasculature and inhibiting HIF-1 signaling pathway to relieve tumor hypoxia.

Our previous studies have shown that the methylene blue (MB) PS can be used to increase oxygenation of tumors via its redox properties [25, 26]. We assume that

the changes in oxygenation are caused by interaction of MB with NADH [26, 27, 28]. A high ratio NADH/NAD⁺ has been reported to be a key feature of malignant cells [29] and can reflect the inhibition of the electron transport chain [30]. When interacting with NADH, MB is reduced to the leucoform, while NADH is oxidized to NAD⁺, providing an increase of pyruvate:lactate (associated with shift from glycolysis to oxidative phosphorylation) and alpha-ketoglutarate (α-KG) to 2- hydroxyglutarate (HG) ratio (associated with decrease of reductive stress), suppression of 2-HG production [31] and reactivation of electron transport chain [30, 32]. The negative aspect is that the leucoform lacks absorption in the red part of the spectrum, making it photodynamically inactive. Consequently, the idea of utilizing a combination of two photosensitizers, MB and chlorin e6, to enhance the effectiveness of PDT arose. The intent is to increase the tumor oxygenation through the use of MB, and then carry out PDT with chlorin e6. In addition, the mutual influence of photosensitizers when administered together was studied, in particular, the effect of chlorin e6 on the transition of MB to the leucoform, as well as the synergistic effects caused by the use of two PS.

According to systematic review of preclinical studies [33] photodynamic therapy with MB is effective against different types of cancer including colorectal tumor, carcinoma, and melanoma. However, the results were promising not for all tumor types, a modest decrease in tumor size was observed for breast cancer and HeLa models, as well as no inhibition of osteosarcoma growth in mice [34]. Authors of review hypothesized that the bioavailability of MB in different target tissues is not equal. We assume that this may also be due to the transition of MB to the leucoform, which reduces its photodynamic activity.

Chlorin e6 is a second generation photosensitizer approved by FDA which has demonstrated high ROS generation ability and anticancer potency against many types of cancer [35]. It is commercially available and widely used for PDT in medical institutions in Russia [36, 37, 38].

Interest in the combined use of MB and chlorin e6 is due to the proximity of their absorption wavelengths in the near-infrared I part of the spectrum: 660 nm for chlorin e6 [39] and 664 nm for MB [40]. Excitation in this range allows for the reduction of autofluorescence and scattering from the biological tissue, thus facilitating deeper penetration into the tumor. The use of a single laser wavelength for both PS excitation is convenient and results in a production of a large number of ROS in the tumor cells and more effectively induces apoptosis, as was shown by Alimu et al [41]. However, this study was conducted on cells *in vitro* under normoxia conditions. In addition, liposomes loaded with two PS were studied, which, on the one hand, ensures simultaneous accumulation of drugs in the target area, but excludes the possibility of taking advantage of the effect of MB on tumor metabolism.

In this work, we conducted a study of PDT with the use of a combination of MB and chlorin e6 *in vivo* in a mouse model of Ehrlich carcinoma. *In vivo* research is of great importance because the oxygen distribution in tumors is highly heterogeneous, with hypoxia levels ranging from mild, almost non-hypoxic, to severe and anoxic levels [42]. The dynamic pattern of hypoxia levels that induces cellular responses and controls interactions between tumor cells, stroma and immune cells in the microenvironment cannot be simulated *in vitro* and at the same time is critical for assessing the effectiveness of photodynamic treatment. Intravenous joint and separate administration makes it possible to study the effect of each PS on the microenvironment and oxygenation, as well as the synergistic effects when two PS are used together.

Materials and methods

The photosensitizer used was a 0.35% solution of radachlorin (OOO RADAPHARMA, Russia) and a 1% aqueous solution of methylene blue (OJSC Samaramedprom, Russia).

Male BALB/c mice weighing 25–30 g and aged 8–10 weeks were used in experiments. The mice were kept in standard cages at a temperature of 21°C with a 12-hour light-dark cycle. They were given *ad libitum* access to standard laboratory feed and water. Ehrlich carcinoma was used as a model tumor; experiments were carried out on the 12th day after intramuscular grafting of the tumor onto the right hind paw. Tumor size was determined by direct measurement of its dimensions, and the volume was calculated using the formula: $V = 0.5 (L \times W^2)$, where V – volume, L – length and W – width. Tumor growth was assessed at the beginning of the experiment and on the third and fifth days after therapy. All measurements were done in triplicate. At the beginning of the experiment, the tumor size for all mice was about 1 cm³.

The mice were divided into five groups based on concentrations of MB and chlorin e6 and irradiation dose.

There were 4 groups with irradiation (wavelength 660 nm, light dose 60 J/cm²): 1) with intravenous injection of 10 mg/kg of MB, 2) 5 mg/kg of e6, 3) 10 mg/kg of MB and 5 mg/kg of e6 simultaneously, 4) 5 mg/kg of e6 and 10 mg/kg of MB separately with the time interval between injection. The 200 µl of photosensitizer aqueous solution in saline with concentration calculated to achieve a total dose were administered intravenously into the tail vein under fluorescence control. Irradiation was carried out an hour after the introduction of photosensitizers. In the group with separate administration of MB and e6, chlorin e6 was first administered intravenously, an hour later MB and immediately irradiated. Groups with administration of 10 mg/kg MB, 5 mg/kg e6 without irradiation, as well as mice without administration of photosensitizers and irradiation were used as controls. Each group consisted of three mice.

The accumulation of MB, e6 and its combination in tumor was measured spectroscopically using a LESA-01-Biospec fiber-optic spectrometer (Biospec, Russia) with fiber-optic probe, consisting of a central illuminating fiber and six peripheral collecting fibers for the scattered and fluorescence radiation. MB fluorescence was excited with a He-Ne laser at 632.8 nm and 5 mW. Using an optical filter, the fluorescence was observed in the same dynamic range as the backscattered laser radiation. Fluorescence measurements were taken at five locations in tumor. After this, the data was averaged and STD was calculated. As a quantitative characteristic, we used the fluorescence index, calculated as the ratio of the area under the fluorescence peak in the range of 660–800 nm to the area under the laser peak in the range of 620–645 nm. The concentration of the PS in the tissues was calculated by matching the fluorescence index to the values from optical phantoms that mimic the scattering and absorption properties of biological tissues and contain a 0 to 10 mg/kg and 0 to 5 mg/kg range of MB and e6 concentrations, respectively.

For *in vivo* video imaging the PS fluorescence was excited using 660 nm laser radiation and detected by a black-and-white MQ013RG-ON camera (Ximea, Korea) with a 700–750 nm bandpass optical filter. The fluorescent signal was recorded in a video file, which was further processed. After the injection of the PS, the mouse remained under low-intensity laser irradiation for 5 minutes, during which the fluorescence signal was recorded to the video file. For the selected time-frames of the recorded video file, the average brightness in the tumor area was calculated. The brightness value in a pixel was normalized and took values from zero to one.

The degree of hemoglobin oxygenation *in vivo* was examined using a hemoglobin optical absorption method [43] with a halogen lamp as a light source. LESA-01-Biospec fiber-optic spectrometer was used to register the diffuse reflectance spectra. The degree of hemoglobin

oxygenation was calculated as the ratio of oxygenated hemoglobin absorption to total hemoglobin absorption, derived from the absorption spectrum. Oxygenation measurements were taken at five locations in both tumor and normal muscle tissue for each mouse.

The used spectroscopic methods and setup are described in more detail in the work [25].

To evaluate the effect of photodynamic therapy at the cellular level, the fluorescence microscopy and fluorescence lifetime imaging microscopy (FLIM) were used. Mice were euthanized on the fifth day after PDT. Tumors, subcutaneous tissue, skin, and muscle were excised en bloc and frozen. Sections of 50 μm were examined on a laser scanning confocal microscope LSM-710-NLO (Carl Zeiss AG, Oberkochen, Germany). The spectrally resolved images were acquired under simultaneous 488 nm and 633 nm laser excitation. Acridine orange (AO) and propidium iodide (PI) staining was used to assess the number of dead cells.

Time-resolved images of autofluorescence and MB fluorescence were recorded under two-photon 740 nm excitation with a Chameleon Ultra II femtosecond laser (Coherent, Saxonburg, Pennsylvania, USA), with a pulse width of 140 fs and a repetition rate of 80 MHz. Optical bandpass filters FB450-40 (Thorlabs, Newton New Hersey, USA) and BP 640/30 (Carl Zeiss AG, Oberkochen, Germany) were used to isolate fluorescence signals from NADH and MB, respectively. The images were processed with SPCLImage 8.0 software (Becker & Hickl GmbH, Berlin, Germany). NADH metabolic index was calculated as a_1/a_2 ratio with fixed lifetimes: $\tau_1 = 0.4$ ns, $\tau_2 = 2.5$ ns [44].

Results and discussions

The therapeutic effects of MB and MB with chlorin e6 on tumors were investigated. *In vivo* fluorescence video imaging has shown that after intravenous administration, MB accumulates very quickly both in the tumor and in normal tissue, and then rapidly decreases in tumor, Fig. 1.

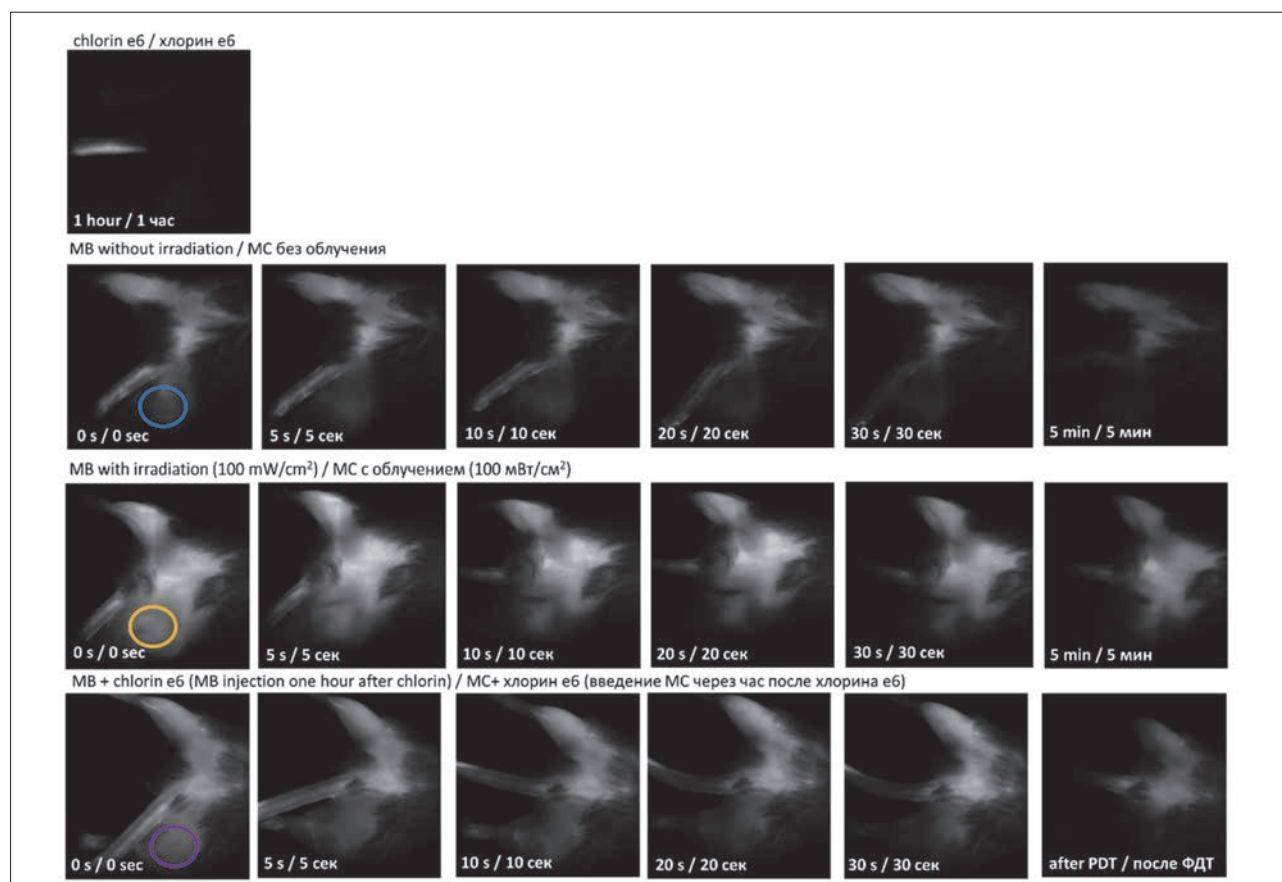


Рис. 1. Флуоресцентная визуализация MC *in vivo* с использованием возбуждения 660 нм: изображения, полученные через 5, 10, 20, 30 с и 5 мин после внутривенного введения MC в дозе 10 мг/кг и MC в комбинации с хлорином е6 (10 мг/кг + 5 мг/кг, введение MC произведено через 1 ч после введения хлорина е6). В группе с облучением каждые 5 с включали второй источник излучения с длиной волны 660 нм, плотность мощности 100 мВт/см². Цветные круги показывают области, в которых была рассчитана яркость.

Fig. 1. Fluorescence imaging of MB *in vivo* using 660 nm excitation: images obtained at 5, 10, 20, 30 seconds and 5 minutes after intravenous administration of MB at a dose of 10 mg/kg and MB in combination with chlorin e6 (10 mg/kg + 5 mg/kg, injection of MB was performed one hour after chlorin e6). In the irradiation group, a second radiation source with a wavelength of 660 nm and a power density of 100 mW/cm² was turned on every 5 seconds. The colored circles show the areas in which the brightness was calculated.

The fluorescence intensity of MB in normal tissues decreases slightly and remains constant throughout the entire measurement (5 minutes). These results are similar to the MB pharmacokinetics obtained in experiments on Lewis lung carcinoma [26].

The effect of laser irradiation and the second PS on the transition of MB to the leucoform was also analyzed. For quantitative assessment, the average brightness normalized to the initial value was used. The time dependences of the average brightness of tumor areas, normalized to the initial value, are presented in Fig. 2.

It can be seen that under the laser irradiation of MB, the decrease in fluorescence intensity occurs more slowly than for MB without irradiation. The same effect, but even more pronounced, was observed when MB is administered in combination with chlorin e6. We assume that irradiation prevents the transition of MB to the leucoform; during irradiation, the leucoform is reoxidized back to the MB upon interaction with reactive oxygen species.

Quantitative assessment of the accumulation of MB and chlorin e6 in the tumor was carried out using spectroscopic methods based on the fluorescence intensity in the red region of the spectrum recorded *in vivo*. The dependence of the fluorescence index on the accumulation time for tumors with intravenous administration is shown in Fig. 3.

The fluorescence intensity of chlorin e6 in the tumor gradually increases over time and reaches a plateau an hour after intravenous administration. The accumulation time of 1 hour for chlorin e6 was chosen for further experiments. The concentration of chlorin e6 in the tumor, determined by spectroscopic methods one hour after administration, was 0.7 mg/kg. An increase in the concentration of MB in the tumor was observed

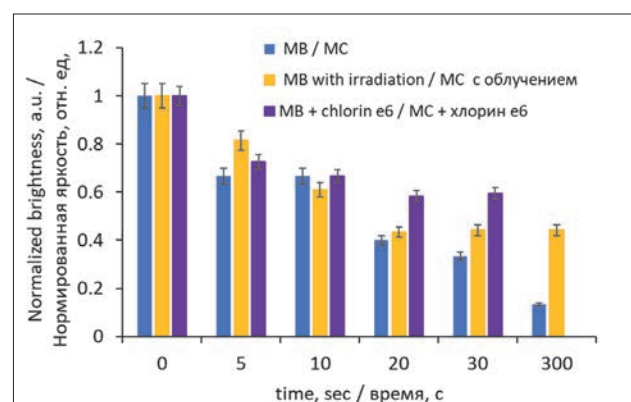


Рис. 2. Временные зависимости средней яркости опухоли, нормированной на начальное значение, для МС без облучения, МС с облучением (каждые 5 с включали второй источник излучения с длиной волны 660 нм, плотность мощности 100 мВт/см²) и комбинации МС с хлорином е6.

Fig. 2. Time dependences of the average tumor brightness normalized to the initial value for MB without irradiation, MB with irradiation (every 5 seconds a second radiation source with a wavelength of 660 nm was turned on, power density 100 mW/cm²) and a combination of MB with chlorin e6.

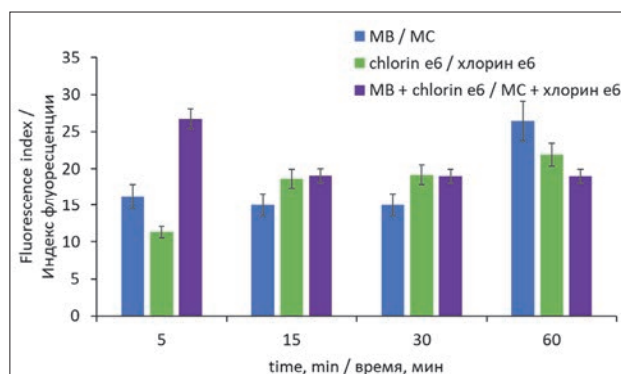


Рис. 3. Зависимость индекса флуоресценции МС, хлорина е6 и их комбинации в опухоли от времени накопления.

Fig. 3. Dependence of the fluorescence index for MB chlorin e6 and their combination in the tumor on the accumulation time.

only an hour after intravenous administration, which is presumably due to the transition to the leucoform 5 in minutes after administration, recorded using video fluorescent methods.

An interesting effect was observed for the combination of chlorin e6 and MB. Maximum of MB fluorescence was recorded immediately after the administration of PS, which corresponds to the data obtained using video fluorescent methods. The prevention of MB transition to the leucoform may also be due to the photodamaging effect of chlorin e6 on blood vessels, which occurred under low-intensity laser illumination during fluorescence imaging of PS accumulation. Another explanation for this effect could be a change in mitochondrial potential under the influence of chlorin e6, which leads to a disruption of MB reduction to the leucoform.

Changes in tumor oxygenation *in vivo* during PS accumulation were also assessed. For this study, a large tumor size was chosen; the volume before therapy was about 1 cm³, oxygenation was significantly reduced relative to normal tissues and amounted to about 35%. The dependence of tumor oxygenation on PS accumulation time is shown in Fig. 4.

It has been shown that for Ehrlich carcinoma after intravenous administration of MB and a combination of MB with chlorin e6, a temporary decrease in oxygenation is observed, and then an increase in the level of oxygenation above the initial one. For the combination of chlorin e6 and MB, the increase in oxygenation levels occurred more quickly, as early as 30 minutes after administration, which correlates with faster accumulation of the PS combination. At the same time, the change in the level of oxygenation with the joint administration of MB and chlorin e6 was more pronounced, which confirms the assumption of the vascular effects of chlorin e6. Thus, it was previously shown that preliminary irradiation of a tumor with low-intensity laser radiation promotes more efficient accumulation of chlorin e6 [45].

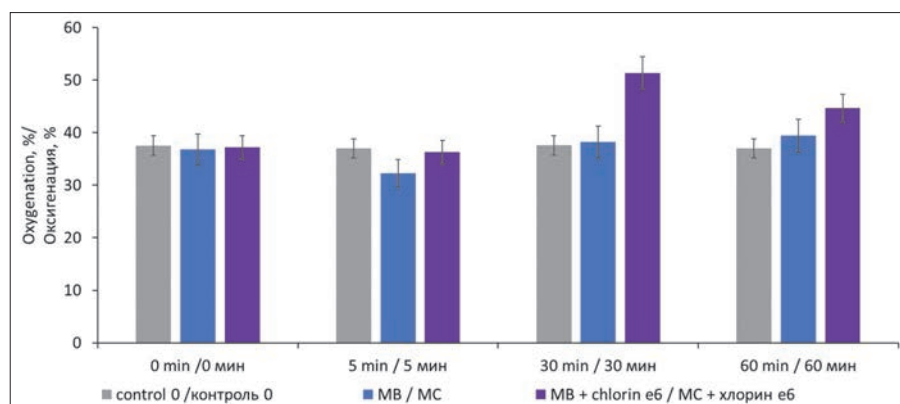


Рис. 4. Оксигенация опухоли, определенная по поглощению гемоглобина до, через 5, 30 мин и через 1 ч после внутривенного введения МС в дозе 10 мг/кг и комбинации МС с хлорином е6 (10 мг/кг + 5 мг/кг). Контроль – без введения ФС.

Fig. 4. Tumor oxygenation, determined by hemoglobin absorption before, after 5, 30 minutes and 1 hour after intravenous administration of MB at a dose of 10 mg/kg and a combination of MB with chlorin e6 (10 mg/kg + 5 mg/kg). Control – without administration of PS.

We have studied PDT with the combined use of chlorin e6 and MB. Based on the results obtained on the accumulation and effect on oxygenation, the following options for the joint use of drugs were chosen: joint administration of MB and chlorin e6 and laser irradiation an hour after administration (an increase in the tumor oxygenation and a more pronounced photodynamic effect was expected) and separate administration of PS, first chlorin e6 was injected, after an hour MB and immediately after MB administration was performed irradiation, until MB passes into a colorless form (an enhanced photodynamic effect was assumed due to a higher concentration of PS). In addition, the generation of singlet oxygen by chlorin e6 can lead to the oxidation of the colorless leucoform of MB back to blue, and chlorin e6 can have an effect on blood vessels.

The characteristic appearance of tumors in groups on days 3 and 5 after PDT is presented in Fig. 5.

The effectiveness of therapy was assessed by the rate of tumor growth. After therapy, the fastest growth of tumors was observed in the control group; on day 5 the tumor volume exceeded 3.5 cm³, Fig. 6.

In the groups without irradiation, there was no significant decrease in tumor growth rate compared to the control group without any therapy. We hypothesize that the effect of MB on tumor oxygenation after a single administration is too short-lived for therapeutic effect.

A good therapeutic effect was observed in all groups with irradiation. After PDT with chlorin e6, MB and a combination of MB with chlorin e6 a decrease in the tumor growth rate were observed compared to the control. The most pronounced therapeutic effect was observed

	3 days / 3 дня	5 days / 5 дней	lambda coded/цветовая кодировка по длинам волн	AO and PI staining/окрашивание АО и ПИ
Control 0 / Контроль 0				
chlorin e6 / хлорин е6			NA	NA
MB / МС				
MB PDT / МС ФДТ				
chlorin e6 PDT / хлорин е6 ФДТ				
MB+e6 separately PDT / МС+е6 раздельное введение ФДТ				
MB+e6 simultaneously / МС+е6 совместное введение ФДТ				

Рис. 5. Характерный вид опухоли в группах на 3-й и 5-й день после ФДТ. Флуоресцентные изображения криосрезов опухолей в режиме цветовой кодировки по длинам волн и после окрашивания акридиновым оранжевым и иодидом пропидия (АО и ПИ).

Fig. 5. Characteristic appearance in groups on the 3rd and 5th day after PDT. Fluorescent images of cryosections of tumors in wavelength-color-coded mode (lambda mode) and after staining with acridine orange and propidium iodide (AO and PI).

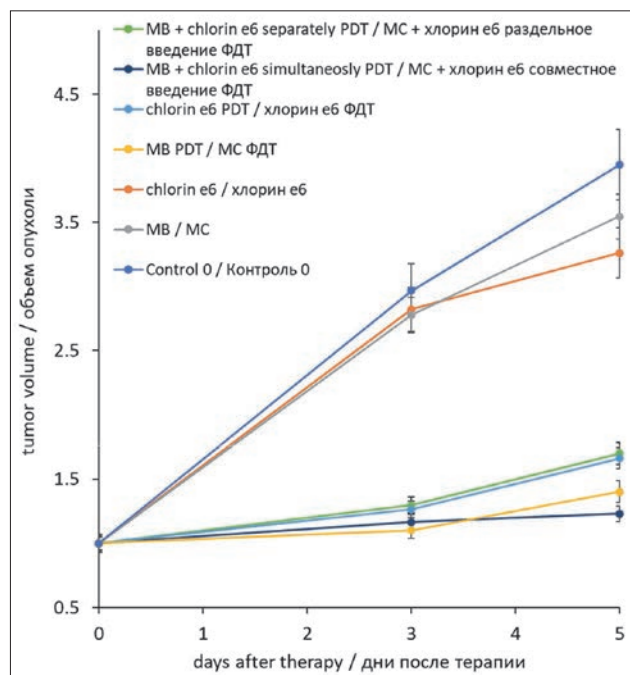


Рис. 6. Характерный размер опухоли в группах на 3-й и 5-й дни после ФДТ.

Fig. 6. Characteristic tumor size in groups on the 3rd and 5th day after PDT.

in groups with PDT with MB and with the simultaneous administration of chlorin e6 and MB (to increase tumor oxygenation before therapy) followed by irradiation an hour later. In both groups with the introduction of chlorin e6 and MB, the appearance of ulcers and more pronounced tissue necrosis in the area of photodynamic exposure were observed, however, the suppression of tumor growth was more significant in the group with the combined administration of MB and chlorin e6.

Oxygenation measurements were used as an additional parameter to assess the effectiveness of the therapy. The dependence of tumor oxygenation on time after PDT is shown in Fig. 7.

In all groups with irradiation, the level of tumor oxygenation on days 3 and 5 was higher than in the control group and groups without irradiation. The highest oxygenation on day 5 after PDT was observed for the group with MB and irradiation of 60 J/cm². The lower oxygenation for groups receiving chlorin e6 alone or in combination with MB is presumably due to the photodamaging effect of chlorin e6 on blood vessels.

Also, after animal euthanasia and preparation of cryosections of the studied tumors, FLIM was performed to study the effect of MB administration on the metabolic type of tumor tissues. The distribution of MB fluorescence

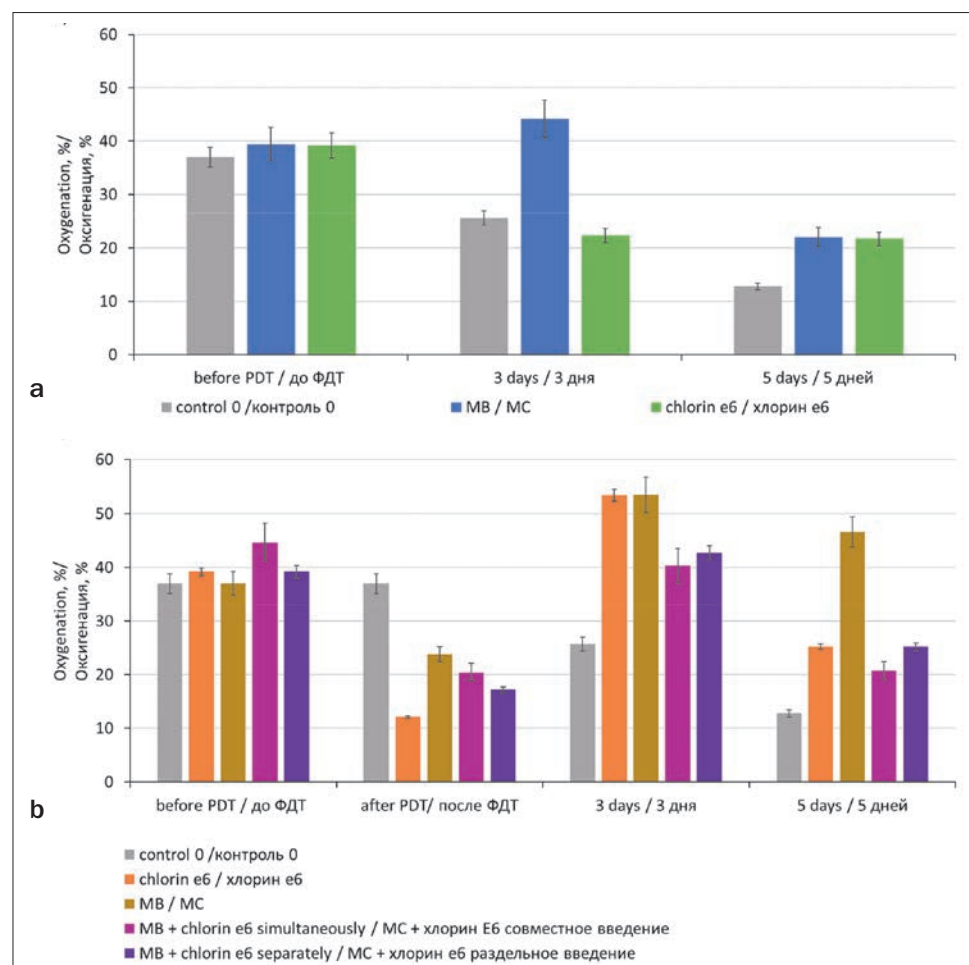


Рис. 7. Оксигенации опухоли, определенная по поглощению гемоглобина до ФДТ, сразу, на 3-й и 5-й дни после ФДТ для групп:

a – с облучением;

b – без облучения.

Fig. 7. The tumor oxygenation, determined by hemoglobin absorption before PDT, immediately, on days 3 and 5 after PDT for groups:

a – without irradiation;

b – with irradiation.

and the lifetime of the metabolic cofactor NADH were analyzed on cryosections of tumors.

Fig. 8 shows phasor diagrams of fluorescence in the spectral range of NADH from tumor sections.

Phasor diagrams of the FLIM for tumors after PDT show a deviation from the metabolic trajectory and a shift towards a longer lifetime compared to the control tumor without any therapy. This shift in the metabolic index indicates the presence of lipid peroxidation products [46]. Thus, tumor regression after PDT with studied PS is associated with the direct destruction of tumor cells under the influence of reactive oxygen species formed during PDT. Interestingly, more severe damage does not contribute to more effective suppression of tumor growth. Thus, in the group with PDT only with MB, for which the smallest shift in phasor was observed relative to the control, the suppression of tumor growth was most pronounced, along with the highest level of oxygenation on day 5 after therapy.

Conclusion

A study was conducted of the therapeutic effects of MB and MB in combination with chlorin e6 on tumors *in vivo*.

Using spectroscopic methods, the optimal time for chlorin e6 accumulation in the tumor was estimated to be 1 hour. For MB, a smooth increase in concentration was observed with increasing accumulation time, which corresponds to the time dependence of MB concentration obtained previously for Lewis lung carcinoma. For the combination of chlorin e6 and MB, maximum accumulation was observed already 5 minutes after co-administration of the drugs, which is possibly due to the vascular effect of chlorin e6 during irradiation. Another explanation for this effect could be a change in mitochondrial potential under the influence of chlorin e6, which leads to a disruption in the reduction of MB to the leukemic form.

Study with help of video fluorescent methods confirmed previously obtained for Lewis carcinoma results: after intravenous administration, MB very quickly accumulates both in the tumor and in normal tissue. Irradiation of MB prevents the transition of MB to the leucoform, which is presumably due to the oxidation of LMB to MB upon interaction with reactive oxygen species. The same effect, but even more pronounced, is observed when MB is administered in combination with chlorin e6.

A study of the photodynamic activity of MB and MB in combination with chlorin e6 has demonstrated a good therapeutic effect and a decrease in the tumor growth rate for groups with PDT with chlorin e6, MB and a combination of MB with chlorin e6, a decrease in the tumor growth rate were observed in all groups with PDT compared to the control and groups without irradiation. The most pronounced therapeutic effect was observed in groups with MB and irradiation and with the combined

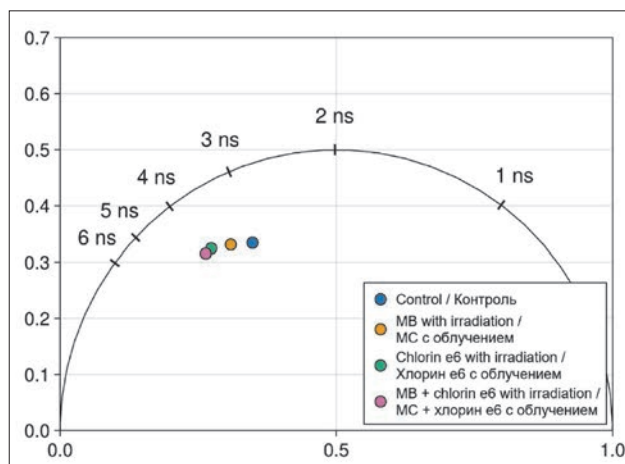


Рис. 8. Средние фазорные значения на разрешенных во времени флуоресцентных изображениях НАДН в срезах опухоли после терапии.

Fig. 8. Mean phasor values for time-resolved fluorescence images of NADH in tumor cryosections after therapy.

administration of chlorin e6 and MB (to increase tumor oxygenation before therapy) followed by irradiation an hour later. In both groups with the introduction of chlorin e6 and MB, the appearance of ulcers and more pronounced tissue necrosis in the area of photodynamic exposure were observed, however, the suppression of tumor growth was more significant in the group with the combined administration of MB and chlorin e6.

The level of tumor oxygenation on days 3 and 5 was higher in groups with PDT compared to control and groups without irradiation. The highest oxygenation on day 5 after PDT was observed for the group with PDT with MB. The lower oxygenation for groups receiving chlorin e6 alone or in combination with MB is presumably due to the photodamaging effect of chlorin e6 on blood vessels.

Phasor diagrams of the FLIM for tumors after PDT show a deviation from the metabolic trajectory and a shift towards a longer lifetime compared to the control tumor. This shift in the metabolic index indicates the presence of lipid peroxidation products. Thus, tumor regression after PDT with studied PS is associated with the direct destruction of tumor cells under the influence of reactive oxygen species formed during PDT.

Thus, the effectiveness of PDT with combined use of MB and chlorin e6 was demonstrated. According to obtained results, the most promising approach among studied is the combined administration of chlorin e6 and MB to increase tumor oxygenation before therapy followed by irradiation an hour later. Further study is needed to optimize MB and chlorin e6 concentrations and accumulation time, as well as irradiation dose.

Acknowledgment

The study was funded by a grant from the Russian Science Foundation (project N 22-72-10117).

REFERENCES

- Hockel M., Vaupel P. Tumor Hypoxia: Definitions and Current Clinical, Biologic, and Molecular Aspects, *JNCI Journal of the National Cancer Institute*, 2001, vol. 93 (4), pp. 266–276. doi:10.1093/jnci/93.4.266.
- Vaupel P., Harrison L. Tumor Hypoxia: Causative Factors, Compensatory Mechanisms, and Cellular Response, *The Oncologist*, 2004, vol. 9 (S5), pp. 4–9. doi:10.1634/theoncologist.9-90005-4.
- Robert Grimes D., Partridge M. A Mechanistic Investigation of the Oxygen Fixation Hypothesis and Oxygen Enhancement Ratio, *Biomed. Phys. Eng. Express*, 2015, vol. 1 (4), pp. 045209. doi:10.1088/2057-1976/1/4/045209.
- Casazza A., Di Conza G., Wenes M. et al. Tumor Stroma: A Complexity Dictated by the Hypoxic Tumor Microenvironment, *Oncogene*, 2014, vol. 33 (14), pp. 1743–1754. doi:10.1038/ncr.2013.121.
- Bader S.B., Dewhirst M.W., Hammond E.M. Cyclic Hypoxia: An Update on Its Characteristics, Methods to Measure It and Biological Implications in Cancer, *Cancers*, 2020, vol. 13 (1), pp. 23. doi:10.3390/cancers13010023.
- Vaupel P., Flood A.B., Swartz H.M. Oxygenation Status of Malignant Tumors vs. Normal Tissues: Critical Evaluation and Updated Data Source Based on Direct Measurements with pO₂ Microsensors, *Appl Magn Reson*, 2021, vol. 52 (10), pp. 1451–1479. doi:10.1007/s00723-021-01383-6.
- Zhang Q., Yan Q., Yang H. et al. Oxygen Sensing and Adaptability Won the 2019 Nobel Prize in Physiology or Medicine, *Genes & Diseases*, 2019, vol. 6 (4), pp. 328–332. doi:10.1016/j.gendis.2019.10.006.
- Rankin E.B., Giaccia A.J. Hypoxic Control of Metastasis, *Science*, 2016, vol. 352 (6282), pp. 175–180. doi:10.1126/science.aaf4405.
- LaGory E.L., Giaccia A.J. The Ever-Expanding Role of HIF in Tumour and Stromal Biology, *Nat Cell Biol*, 2016, vol. 18 (4), pp. 356–365. doi:10.1038/ncb3330.
- Semenza G.L. Hypoxia-Inducible Factors in Physiology and Medicine, *Cell*, 2012, vol. 148 (3), pp. 399–408. doi:10.1016/j.cell.2012.01.021.
- Jin M.-Z., Jin W.-L. The Updated Landscape of Tumor Microenvironment and Drug Repurposing, *Sig Transduct Target Ther*, 2020, vol. 5 (1), pp. 166. doi:10.1038/s41392-020-00280-x.
- Krisnawan V.E., Stanley J.A., Schwarz J.K. et al. Tumor Microenvironment as a Regulator of Radiation Therapy: New Insights into Stromal-Mediated Radioresistance, *Cancers*, 2020, vol. 12 (10), pp. 2916. doi:10.3390/cancers12102916.
- Sahu A., Kwon I., Tae G. Improving Cancer Therapy through the Nanomaterials-Assisted Alleviation of Hypoxia, *Biomaterials*, 2020, vol. 228, pp. 119578. doi:10.1016/j.biomaterials.2019.119578.
- Ravichandran G., Yadav D.N., Murugappan S. et al. "Nano Effects": A Review on Nanoparticle-Induced Multifarious Systemic Effects on Cancer Theranostic Applications, *Mater. Adv.*, 2022, vol. 3 (22), pp. 8001–8011. doi:10.1039/D2MA00784C.
- Zhao L., Fu C., Tan L. et al. Advanced Nanotechnology for Hypoxia-Associated Antitumor Therapy, *Nanoscale*, 2020, vol. 12 (5), pp. 2855–2874. doi:10.1039/C9NR09071A.
- Mansoori B., Mohammadi A., Amin Doustvandi M. et al. Photodynamic Therapy for Cancer: Role of Natural Products, *Photodiagnosis and Photodynamic Therapy*, 2019, vol. 26, pp. 395–404. doi:10.1016/j.pdpdt.2019.04.033.
- Correia J.H., Rodrigues J.A., Pimenta S. et al. Photodynamic Therapy Review: Principles, Photosensitizers, Applications, and Future Directions, *Pharmaceutics*, 2021, vol. 13 (9), pp. 1332. doi:10.3390/pharmaceutics13091332.
- Jiang W., Liang M., Lei Q. et al. The Current Status of Photodynamic Therapy in Cancer Treatment, *Cancers*, 2023, vol. 15 (3), pp. 585. doi:10.3390/cancers15030585.
- Olyushin V.E., Kukanov K.K., Nechaeva A.S. et al. Photodynamic Therapy in Neurooncology, *Biomedical photonics*, 2023, vol. 12 (3), pp. 25–35. doi:10.24931/2413-9432-2023-12-3-25-35.
- Villalpando-Rodriguez G.E., Gibson S.B. Reactive Oxygen Species (ROS) Regulates Different Types of Cell Death by Acting as a Rheostat, *Oxidative Medicine and Cellular Longevity*, 2021, vol. 2021, pp. 1–17. doi:10.1155/2021/9912436.
- Krasnovskii A.A. [Photodynamic activity and singlet oxygen], *Biofizika*, 2004, vol. 49 (2), pp. 305–321.
- Zhao X., Liu J., Fan J. et al. Recent Progress in Photosensitizers for Overcoming the Challenges of Photodynamic Therapy: From Molecular Design to Application, *Chem. Soc. Rev.*, 2021, vol. 50 (6), pp. 4185–4219. doi:10.1039/D0CS00173B.
- Baptista M.S., Indig G.L. Effect of BSA Binding on Photophysical and Photochemical Properties of Triarylmethane Dyes, *J. Phys. Chem. B*, 1998, vol. 102 (23), pp. 4678–4688. doi:10.1021/jp981185n.

ЛИТЕРАТУРА

- Hockel M., Vaupel P. Tumor Hypoxia: Definitions and Current Clinical, Biologic, and Molecular Aspects. // *JNCI Journal of the National Cancer Institute*. – 2001. – Т. 93, № 4. – С. 266–276.
- Vaupel P., Harrison L. Tumor Hypoxia: Causative Factors, Compensatory Mechanisms, and Cellular Response. // *The Oncologist*. – 2004. – Т. 9, № 55. – С. 4–9.
- Robert Grimes D., Partridge M. A mechanistic investigation of the oxygen fixation hypothesis and oxygen enhancement ratio. // *Biomedical Physics & Engineering Express*. – 2015. – Т. 1, № 4. – С. 045209.
- Casazza A., Di Conza G., Wenes M., Finisguerra V., Deschoemaeker S., Mazzone M. Tumor stroma: a complexity dictated by the hypoxic tumor microenvironment. // *Oncogene*. – 2014. – Т. 33, № 14. – С. 1743–1754.
- Bader S. B., Dewhirst M. W., Hammond E. M. Cyclic Hypoxia: An Update on Its Characteristics, Methods to Measure It and Biological Implications in Cancer. // *Cancers*. – 2020. – Т. 13, № 1. – С. 23.
- Vaupel P., Flood A. B., Swartz H. M. Oxygenation Status of Malignant Tumors vs. Normal Tissues: Critical Evaluation and Updated Data Source Based on Direct Measurements with pO₂ Microsensors. // *Applied Magnetic Resonance*. – 2021. – Т. 52, № 10. – С. 1451–1479.
- Zhang Q., Yan Q., Yang H., Wei W. Oxygen sensing and adaptability won the 2019 Nobel Prize in Physiology or medicine. // *Genes & Diseases*. – 2019. – Т. 6, № 4. – С. 328–332.
- Rankin E. B., Giaccia A. J. Hypoxic control of metastasis. // *Science*. – 2016. – Т. 352, № 6282. – С. 175–180.
- LaGory E. L., Giaccia A. J. The ever-expanding role of HIF in tumour and stromal biology. // *Nature Cell Biology*. – 2016. – Т. 18, № 4. – С. 356–365.
- Semenza G. L. Hypoxia-Inducible Factors in Physiology and Medicine. // *Cell*. – 2012. – Т. 148, № 3. – С. 399–408.
- Jin M.-Z., Jin W.-L. The updated landscape of tumor microenvironment and drug repurposing. // *Signal Transduction and Targeted Therapy*. – 2020. – Т. 5, № 1. – С. 166.
- Krisnawan V. E., Stanley J. A., Schwarz J. K., DeNardo D. G. Tumor Microenvironment as a Regulator of Radiation Therapy: New Insights into Stromal-Mediated Radioresistance. // *Cancers*. – 2020. – Т. 12, № 10. – С. 2916.
- Sahu A., Kwon I., Tae G. Improving cancer therapy through the nanomaterials-assisted alleviation of hypoxia. // *Biomaterials*. – 2020. – Т. 228. – С. 119578.
- Ravichandran G., Yadav D. N., Murugappan S., Sankaranarayanan S. A., Revi N., Rengan A. K. "Nano effects": a review on nanoparticle-induced multifarious systemic effects on cancer theranostic applications. // *Materials Advances*. – 2022. – Т. 3, № 22. – С. 8001–8011.
- Zhao L., Fu C., Tan L., Li T., Zhong H., Meng X. Advanced nanotechnology for hypoxia-associated antitumor therapy. // *Nanoscale*. – 2020. – Т. 12, № 5. – С. 2855–2874.
- Mansoori B., Mohammadi A., Amin Doustvandi M., Mohammadnejad F., Kamari F., Gjerstorff M. F., Baradaran B., Hamblin M. R. Photodynamic therapy for cancer: Role of natural products. // *Photodiagnosis and Photodynamic Therapy*. – 2019. – Т. 26. – С. 395–404.
- Correia J. H., Rodrigues J. A., Pimenta S., Dong T., Yang Z. Photodynamic Therapy Review: Principles, Photosensitizers, Applications, and Future Directions. // *Pharmaceutics*. – 2021. – Т. 13, № 9. – С. 1332.
- Jiang W., Liang M., Lei Q., Li G., Wu S. The Current Status of Photodynamic Therapy in Cancer Treatment. // *Cancers*. – 2023. – Т. 15, № 3. – С. 585.
- Olyushin V. E., Kukanov K. K., Nechaeva A. S., Sklyar S. S., Vershinin A. E., Dikonenko M. V., Golikova A. S., Mansurov A. S., Safarov B. I., Rynda A. Y., Papayan G. V. Photodynamic therapy in neurooncology. // *Biomedical Photonics*. – 2023. – Т. 12, № 3. – С. 25–35.
- Villalpando-Rodriguez G. E., Gibson S. B. Reactive Oxygen Species (ROS) Regulates Different Types of Cell Death by Acting as a Rheostat. // *Oxidative Medicine and Cellular Longevity*. – 2021. – Т. 2021. – С. 1–17.
- Krasnovskii A. A. [Photodynamic activity and singlet oxygen]. // *Biofizika*. – 2004. – Т. 49, № 2. – С. 305–321.
- Zhao X., Liu J., Fan J., Chao H., Peng X. Recent progress in photosensitizers for overcoming the challenges of photodynamic therapy: from molecular design to application. // *Chemical Society Reviews*. – 2021. – Т. 50, № 6. – С. 4185–4219.
- Baptista M. S., Indig G. L. Effect of BSA Binding on Photophysical and Photochemical Properties of Triarylmethane Dyes. // *The Journal of Physical Chemistry B*. – 1998. – Т. 102, № 23. – С. 4678–4688.
- Wan Y., Fu L., Li C., Lin J., Huang P. Conquering the Hypoxia Limitation for Photodynamic Therapy. // *Advanced Materials*. – 2021. – Т. 33, № 48. – С. 2103978.

24. Wan Y., Fu L., Li C. et al. Conquering the Hypoxia Limitation for Photodynamic Therapy, *Advanced Materials*, 2021, vol. 33 (48), pp. 2103978. doi:10.1002/adma.202103978.
25. Pominova D.V., Ryabova A.V., Skobeltsin A.S. et al. Spectroscopic Study of Methylene Blue in Vivo: Effects on Tissue Oxygenation and Tumor Metabolism, *Biomedical photonics*, 2023, vol. 12 (1), pp. 4–13. doi:10.24931/2413-9432-2023-12-1-4-13.
26. Pominova D., Ryabova A., Skobeltsin A. et al. The Use of Methylene Blue to Control the Tumor Oxygenation Level, *Photodiagnosis and Photodynamic Therapy*, 2024, vol. 46, pp. 104047. doi:10.1016/j.pdpdt.2024.104047.
27. Sevcik P., Dunford H.B. Kinetics of the Oxidation of NADH by Methylene Blue in a Closed System, *J. Phys. Chem.*, 1991, vol. 95 (6), pp. 2411–2415. doi:10.1021/j100159a054.
28. Engbersen J.F.J., Koudijs A., Van Der Plas H.C. Reaction of NADH Models with Methylene Blue, *Recl. Trav. Chim. Pays-Bas*, 2010, vol. 104 (5), pp. 131–138. doi:10.1002/recl.19851040503.
29. Chiarugi A., Dölle C., Felici R. et al. The NAD Metabolome — a Key Determinant of Cancer Cell Biology, *Nat Rev Cancer*, 2012, vol. 12 (11), pp. 741–752. doi:10.1038/nrc3340.
30. Jiang H., Jedoui M., Ye J. The Warburg Effect Drives Dedifferentiation through Epigenetic Reprogramming, *Cancer Biol Med*, 2024, vol. 20 (12), pp. 891–897. doi:10.20892/j.issn.2095-3941.2023.0467.
31. Jiang H., Greathouse R.L., Tiche S.J. et al. Mitochondrial Uncoupling Induces Epigenome Remodeling and Promotes Differentiation in Neuroblastoma, *Cancer Research*, 2023, vol. 83 (2), pp. 181–194. doi:10.1158/0008-5472.CAN-22-1029.
32. Komlódi T., Tretter L. Methylene Blue Stimulates Substrate-Level Phosphorylation Catalysed by Succinyl-CoA Ligase in the Citric Acid Cycle, *Neuropharmacology*, 2017, vol. 123, pp. 287–298. doi:10.1016/j.neuropharm.2017.05.009.
33. Taldaev A., Terekhov R., Nikitin I. et al. Methylene Blue in Anticancer Photodynamic Therapy: Systematic Review of Preclinical Studies, *Front. Pharmacol.*, 2023, vol. 14, pp. 1264961. doi:10.3389/fphar.2023.1264961.
34. Matsubara T., Kusuzaki K., Matsumine A. et al. Methylene Blue in Place of Acridine Orange as a Photosensitizer in Photodynamic Therapy of Osteosarcoma, *In Vivo*, 2008, vol. 22 (3), pp. 297–303.
35. Hak A., Ali M.S., Sankaranarayanan S.A. et al. Chlorin E6: A Promising Photosensitizer in Photo-Based Cancer Nanomedicine, *ACS Appl. Bio Mater.*, 2023, vol. 6 (2), pp. 349–364. doi:10.1021/acsabm.2c00891.
36. Rynda A.Yu., Rostovtsev D.M., Olyushin V.E. et al. Therapeutic Pathomorphosis in Malignant Glioma Tissues after Photodynamic Therapy with Chlorin E6 (Reports of Two Clinical Cases), *Biomedical photonics*, 2020, vol. 9 (2), pp. 45–54. doi:10.24931/2413-9432-2020-9-2-45-54.
37. Filonenko E.V. Clinical Implementation and Scientific Development of Photodynamic Therapy in Russia in 2010-2020, *Biomedical photonics*, 2022, vol. 10 (4), pp. 4–22. doi:10.24931/2413-9432-2021-9-4-4-22.
38. Panaseykin Y.A., Kapinus V.N., Filonenko E.V. et al. Photodynamic Therapy Treatment of Oral Cavity Cancer in Patients with Comorbidities, *Biomedical photonics*, 2023, Vol. 11 (4), pp. 19–24. doi:10.24931/2413-9432-2022-11-4-19-24.
39. Adimoolam M.G., A.V., Nalam M.R. et al. Chlorin E6 Loaded Lactoferrin Nanoparticles for Enhanced Photodynamic Therapy, *J. Mater. Chem. B*, 2017, vol. 5 (46), pp. 9189–9196. doi:10.1039/C7TB02599H.
40. Lim D.-J. Methylene Blue-Based Nano and Microparticles: Fabrication and Applications in Photodynamic Therapy, *Polymers*, 2021, vol. 13 (22), pp. 3955. doi:10.3390/polym13223955.
41. Alimu G., Yan T., Zhu L. et al. Liposomes Loaded with Dual Clinical Photosensitizers for Enhanced Photodynamic Therapy of Cervical Cancer, *RSC Adv.*, 2023, Vol. 13 (6), pp. 3459–3467. doi:10.1039/D2RA03055A.
42. Hompland T., Fjeldbo C.S., Lyng H. Tumor Hypoxia as a Barrier in Cancer Therapy: Why Levels Matter, *Cancers*, 2021, vol. 13 (3), pp. 499. doi:10.3390/cancers13030499.
43. Strattonnikov A.A., Loschenov V.B. Evaluation of Blood Oxygen Saturation in Vivo from Diffuse Reflectance Spectra, *J. Biomed. Opt.*, 2001, vol. 6 (4), pp. 457. doi:10.1117/1.1411979.
44. Atamna H., Kumar R. Protective Role of Methylene Blue in Alzheimer's Disease via Mitochondria and Cytochrome c Oxidase, *JAD*, 2010, vol. 20 (s2), pp. S439–S452. doi:10.3233/JAD-2010-100414.
45. Efendiev K.T., Alekseeva P.M., Shiryayev A.A. et al. Preliminary Low-Dose Photodynamic Exposure to Skin Cancer with Chlorin E6 Photosensitizer, *Photodiagnosis and Photodynamic Therapy*, 2022, vol. 38, pp. 102894. doi:10.1016/j.pdpdt.2022.102894.
46. Datta R., Alfonso-García A., Cinco R. et al. Fluorescence Lifetime Imaging of Endogenous
25. Pominova D. V., Ryabova A. V., Skobeltsin A. S., Markova I. V., Romanishkin I. D., Loschenov V. B. Spectroscopic study of methylene blue in vivo: effects on tissue oxygenation and tumor metabolism. // *Biomedical Photonics*. – 2023. – T. 12, № 1. – С. 4–13.
26. Pominova D., Ryabova A., Skobeltsin A., Markova I., Linkov K., Romanishkin I. The use of methylene blue to control the tumor oxygenation level. // *Photodiagnosis and Photodynamic Therapy*. – 2024. – T. 46. – С. 104047.
27. Sevcik P., Dunford H. B. Kinetics of the oxidation of NADH by methylene blue in a closed system. // *The Journal of Physical Chemistry*. – 1991. – T. 95, № 6. – С. 2411–2415.
28. Engbersen J. F. J., Koudijs A., Van Der Plas H. C. Reaction of NADH models with methylene blue. // *Recueil des Travaux Chimiques des Pays-Bas*. – 2010. – T. 104, № 5. – С. 131–138.
29. Chiarugi A., Dölle C., Felici R., Ziegler M. The NAD metabolome — a key determinant of cancer cell biology. // *Nature Reviews Cancer*. – 2012. – T. 12, № 11. – С. 741–752.
30. Jiang H., Jedoui M., Ye J. The Warburg effect drives dedifferentiation through epigenetic reprogramming. // *Cancer Biology & Medicine*. – 2024. – T. 20, № 12. – С. 891–897.
31. Jiang H., Greathouse R. L., Tiche S. J., Zhao M., He B., Li Y., Li A. M., Forgo B., Yip M., Li A., Shih M., Banuelos S., Zhou M.-N., Gruber J. J., Rankin E. B., Hu Z., Shimada H., Chiu B., Ye J. Mitochondrial Uncoupling Induces Epigenome Remodeling and Promotes Differentiation in Neuroblastoma. // *Cancer Research*. – 2023. – T. 83, № 2. – С. 181–194.
32. Komlódi T., Tretter L. Methylene blue stimulates substrate-level phosphorylation catalysed by succinyl-CoA ligase in the citric acid cycle. // *Neuropharmacology*. – 2017. – T. 123. – С. 287–298.
33. Taldaev A., Terekhov R., Nikitin I., Melnik E., Kuzina V., Klochko M., Reshetov I., Shiryayev A., Loschenov V., Ramenskaya G. Methylene blue in anticancer photodynamic therapy: systematic review of preclinical studies. // *Frontiers in Pharmacology*. – 2023. – T. 14. – С. 1264961.
34. Matsubara T., Kusuzaki K., Matsumine A., Satonaka H., Shintani K., Nakamura T., Uchida A. Methylene blue in place of acridine orange as a photosensitizer in photodynamic therapy of osteosarcoma. // *In Vivo (Athens, Greece)*. – 2008. – T. 22, № 3. – С. 297–303.
35. Hak A., Ali M. S., Sankaranarayanan S. A., Shinde V. R., Rengan A. K. Chlorin e6: A Promising Photosensitizer in Photo-Based Cancer Nanomedicine. // *ACS Applied Bio Materials*. – 2023. – T. 6, № 2. – С. 349–364.
36. Rynda A. Yu., Rostovtsev D. M., Olyushin V. E., Zabrodskaya Yu. M. Therapeutic pathomorphosis in malignant glioma tissues after photodynamic therapy with chlorin e6 (reports of two clinical cases). // *Biomedical Photonics*. – 2020. – T. 9, № 2. – С. 45–54.
37. Filonenko E. V. Clinical implementation and scientific development of photodynamic therapy in Russia in 2010-2020. // *Biomedical Photonics*. – 2022. – T. 10, № 4. – С. 4–22.
38. Panaseykin Y. A., Kapinus V. N., Filonenko E. V., Polkin V. V., Sevrukov F. E., Isaev P. A., Ivanov S. A., Kaprin A. D. Photodynamic therapy treatment of oral cavity cancer in patients with comorbidities. // *Biomedical Photonics*. – 2023. – T. 11, № 4. – С. 19–24.
39. Adimoolam M. G., A. V., Nalam M. R., Sunkara M. V. Chlorin e6 loaded lactoferrin nanoparticles for enhanced photodynamic therapy. // *Journal of Materials Chemistry B*. – 2017. – T. 5, № 46. – С. 9189–9196.
40. Lim D.-J. Methylene Blue-Based Nano and Microparticles: Fabrication and Applications in Photodynamic Therapy. // *Polymers*. – 2021. – T. 13, № 22. – С. 3955.
41. Alimu G., Yan T., Zhu L., Du Z., Ma R., Fan H., Chen S., Alifu N., Zhang X. Liposomes loaded with dual clinical photosensitizers for enhanced photodynamic therapy of cervical cancer. // *RSC Advances*. – 2023. – T. 13, № 6. – С. 3459–3467.
42. Hompland T., Fjeldbo C. S., Lyng H. Tumor Hypoxia as a Barrier in Cancer Therapy: Why Levels Matter. // *Cancers*. – 2021. – T. 13, № 3. – С. 499.
43. Strattonnikov A. A., Loschenov V. B. Evaluation of blood oxygen saturation in vivo from diffuse reflectance spectra. // *Journal of Biomedical Optics*. – 2001. – T. 6, № 4. – С. 457.
44. Atamna H., Kumar R. Protective Role of Methylene Blue in Alzheimer's Disease via Mitochondria and Cytochrome c Oxidase. // *Journal of Alzheimer's Disease*. – 2010. – T. 20, № s2. – С. S439–S452.
45. Efendiev K. T., Alekseeva P. M., Shiryayev A. A., Skobeltsin A. S., Solonina I. L., Fatyanova A. S., Reshetov I. V., Loschenov V. B. Preliminary low-dose photodynamic exposure to skin cancer with chlorin e6 photosensitizer. // *Photodiagnosis and Photodynamic Therapy*. – 2022. – T. 38. – С. 102894.
46. Datta R., Alfonso-García A., Cinco R., Gratton E. Fluorescence lifetime imaging of endogenous biomarker of oxidative stress. // *Scientific Reports*. – 2015. – T. 5, № 1. – С. 9848.

EFFECT OF THE COMPOSITION OF COMBINED SOLID LIPID PARTICLES WITH GEFITINIB AND A PHOTSENSITIZER ON THEIR SIZE, STABILITY AND CYTOTOXIC ACTIVITY

Nikolaeva L.L.^{1,2}, Sanarova E.V.¹, Kolkaksidi A.P.¹, Shcheglov S.D.^{1,2}, Rudakova A.A.¹, Baryshnikova M.A.¹, Lantsova A.V.¹

¹N.N. Blokhin National Medical Research Center of Oncology, Ministry of Health of Russia, Moscow, Russia

²I.M. Sechenov First Moscow State Medical University (Sechenov University), Moscow, Russia

Abstract

The creation of combined nanomedicines and their controlled release under the influence of photoinduction is an actively developing branch of scientific research. This work is devoted to the development of models of solid lipid nanoparticles for a well-known antitumor drug – gefitinib in combination with a photoindicating agent – a photosensitizer from the phthalocyanine group. Nanoparticles were obtained by several methods: hot homogenization with stearic acid, sesame oil and Tween 80 and by one-step dispersion with copolymers of lactic and glycolic acids and polyvinyl alcohol. In vitro experiments when irradiating particles with a laser in the near-infrared range (about 730 nm) proved the advantage of using combined nanoparticles with gefitinib and a photosensitizer compared to monotherapy, while the activity in terms of IC_{50} was 5.1-8.7 times higher for gefitinib and 1.5-1.8 times for the photosensitizer.

Key words: solid lipid nanoparticles, aluminum phthalocyanine, gefitinib, in vitro, photoinduced activity

Contacts: Nikolaeva L.L., e-mail: alima91@yandex.ru

For citation: Nikolaeva L.L., Sanarova E.V., Kolkaksidi A.P., Shcheglov S.D., Rudakova A.A., Baryshnikova M.A., Lantsova A.V. Effect of the composition of combined solid lipid particles with gefitinib and a photosensitizer on their size, stability and cytotoxic activity, *Biomedical Photonics*, 2024, vol. 13, no. 1, pp. 19–25. doi: 10.24931/2413–9432–2023–13-1-19–25.

ВЛИЯНИЕ СОСТАВА КОМБИНИРОВАННЫХ ТВЕРДЫХ ЛИПИДНЫХ ЧАСТИЦ С ГЕФИТИНИБОМ И ФОТОСЕНСИБИЛИЗАТОРОМ НА ИХ РАЗМЕР, СТАБИЛЬНОСТЬ И ЦИТОТОКСИЧЕСКУЮ АКТИВНОСТЬ

Л.Л. Николаева^{1,2}, Е.В. Санарова¹, А.П. Колпаксиди¹, С.Д. Щеглов^{1,2}, А.А. Рудакова¹, М.А. Барышникова¹, А.В. Ланцова¹

¹ФГБУ «НМИЦ онкологии им. Н.Н. Блохина» Минздрава России, Москва, Россия

²ФГАОУ ВО Первый МГМУ им. И.М. Сеченова Минздрава России (Сеченовский Университет), Москва, Россия

Резюме

Создание комбинированных нанолекарств и их контролируемое высвобождение под воздействием фотоиндукции активно развивающаяся отрасль научных исследований. Данная работа посвящена разработке моделей твердых липидных наночастиц для известного противоопухолевого препарата – гефитиниба в комбинации с фотоиндицирующим агентом – фотосенсибилизатор из группы фталоцианинов. Наночастицы получали несколькими методами: горячей гомогенизацией со стеариновой кислотой, кунжутным маслом и твином 80 и путем одностадийного диспергирования с сополимерами молочной и гликолевой кислот и поливиниловым спиртом. В опытах *in vitro* при облучении частиц лазером в ближнем инфракрасном диапазоне (около 730 нм) было доказано преимущество применения комбинированных наночастиц с гефитинибом и фотосенсибилизатором по сравнению с монотерапией, при этом активность по показателю IC_{50} была выше в 5,1-8,7 раз для гефитиниба и в 1,5-1,8 раз для фотосенсибилизатора.

Ключевые слова: твердые липидные наночастицы, алюминия фталоцианин, гефитиниб, *in vitro*, фотоиндуцированная активность

Контакты: Николаева Л.Л., e-mail: alima91@yandex.ru

Для цитирования: Николаева Л.Л., Санарова Е.В., Колпаксиди А.П., Щеглов С.Д., Рудакова А.А., Барышникова М.А., Ланцова А.В. Влияние состава комбинированных твердых липидных частиц с гефитинибом и фотосенсибилизатором на их размер, стабильность и цитотоксическую активность // *Biomedical Photonics*. – 2024. – Т. 13, № 2. – С. 19–25. doi: 10.24931/2413–9432–2024–13-2-19–25.

Introduction

After the discovery of the first tyrosine kinase inhibitor (TKI), imatinib, studies on the synthesis of various substances with a similar mechanism of action followed. Most TKIs are antitumor agents, and some are used as anti-inflammatory agents. However, in the process of studying TKIs, it was found that despite their efficacy, these compounds are hepatotoxic, extensively metabolized and have limited bioavailability, and resistance develops rapidly when administered. These negative aspects can be mitigated by developing new generations of TKIs or by creating the most effective and safe dosage forms (DF), including selective action [1]. In addition, the activity of TKIs can be increased by using in combination with other antitumor drugs.

Various nano- and microstructures, including hybrid ones [2], have shown great potential for the development of biomarkers and chemotherapeutic agents due to their multifunctional adjustability and biocompatibility [3, 4]. One of the promising areas of development of antitumor therapy is the creation of nanosystems with controlled discharge. For example, photoinduced discharge, due to the inclusion of a photosensitizer (PS) in the nanocarrier, which is activated when exposed to light with a wavelength absorbed by this PS, can lead to the release of a chemotherapeutic agent, exerting a combined effect on the tumor. The most preferable approach to the development of such nanostructures is to use a PS with radiation in the near IR range of 700–850 nm as a photoinducer, which has the greatest ability to penetrate into biological tissues and needs low intensity below 30 mW/cm² [5].

The aim of this study was to develop a nanosystem based on solid lipid nanoparticles (SLN) with the chemotherapeutic agent gefitinib (GFT) and aluminum phthalocyanine (APhC) PS. GFT is a TKI and is widely used in the treatment of lung cancer both as monotherapy and in combination with other agents. GFT is poorly soluble in water, and therefore is used in clinical practice in the form of tablets, due to which it has insufficiently high bioavailability. This problem can be solved by developing a DF with GFT in the form of nanoparticles, ensuring the delivery of the drug to the tumor due to its nanosize, the effect of increased permeability and retention (EPR) based on tumor neovascularization [6], and controlled release of GFT from nanoparticles under photoexposure.

Materials and Methods

Materials

GFT (MSN Laboratories Private Limited), APhC (Merck Life Science LLC), stearic acid (SA, Himedia), sesame oil (SO, Merck Life Science LLC), Tween 80 (Montanox 80, Seppic), phosphatidylcholine S 100,

SPC (PhC, Lipoid), copolymer of lactic and glycolic acids Purasorb PDLG 5010 (CPLG, Corbion), chitosan extra pure (Ch, Sisco Research Laboratories), polyvinyl alcohol hydrolyzed 88% (PVA, Acros Organics), sucrose, pure for analysis, trehalose dihydrate, extra pure, mannitol, pure for analysis (Himmed), chloroform, chemically pure (Vekton).

Equipment

Laboratory scale DL-120 (AND), analytical scale OHAUS Analytical Plus AP 100S (OHAUS Corporation), magnetic stirrer IKA® C-MAG HS 4 (IKA Werke GmbH & Co KG), vacuum pump Büchi V-700 (BÜCHI Labortechnik AG), immersion homogenizer Polytron PT 1200 E (Kinematica), ultrasonic homogenizer Bandelin Sonopuls HD 2070 (Bandelin), freeze-dryer Edwards Minifast DO.2 (Ero Electronic SpA), pH meter HANNA pH 2211 (Hanna Instruments), spectrophotometer Cary 100 (Agilent Technologies).

Methods for obtaining model combinations

- 1) By hot homogenization [7] using SA and SO as the lipid phase and Tween 80 as the aqueous phase in various ratios (SLN-1). The preparation of the compositions began with melting SA at 70–100°C on a magnetic stirrer, then SO was added by weight and GFT and APhC were dissolved in the resulting mixture with stirring (300 rpm) and constant heating. A glass with the resulting composite was dispersed on an immersion homogenizer with the gradual addition of an aqueous solution of Tween 80 for 1 hour. The resulting particles were ground on an ultrasonic disperser and filtered under pressure. The scheme for producing is shown in Fig. 1.
- 2) By the method of one-stage dispersion [8, 9] with CPLG and PhC under vacuum, where chloroform was used as the organic phase, and a 1–2% solution of PVA with or without chitosan (SLN-2) as the aqueous phase. The method for obtaining particles involved prolonged mixing (for 24–32 h) of a chloroform solution of GFT and APhC and an aqueous solution of PVA and chitosan under vacuum. After evaporation of chloroform, the resulting dispersion was crushed and filtered under pressure. The scheme of obtaining SLN-2 models is shown in Fig. 2.

The particles were ground using a combination of homogenization (5,000 rpm, 60 min) and ultrasonic dispersion (5 min, 60%). To increase the shelf life of the nanoparticles, lyophilization was performed using the method [10].

Quality control of all obtained SLNs was carried out by measuring the quantitative content, pH, particle size, ζ-potential [10, 11] and studying the stability during storage. Analysis of the quantitative content of GFT and APhC in SLNs was carried out spectrophotometrically at

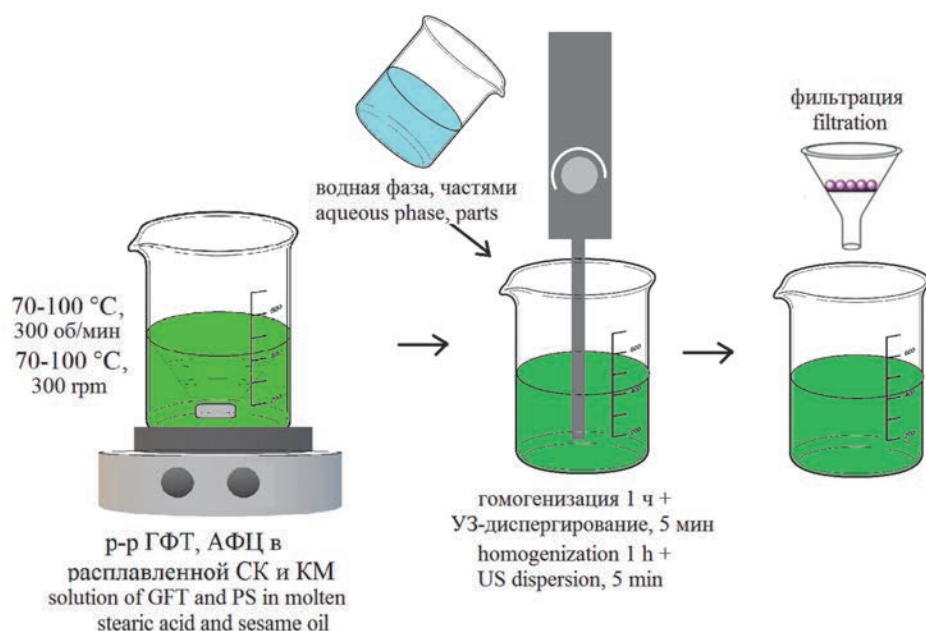


Рис. 1. Схема получения моделей ТЛН-1 методом горячей гомогенизации.
Fig. 1. Scheme for producing SLN-1 models by hot homogenization.

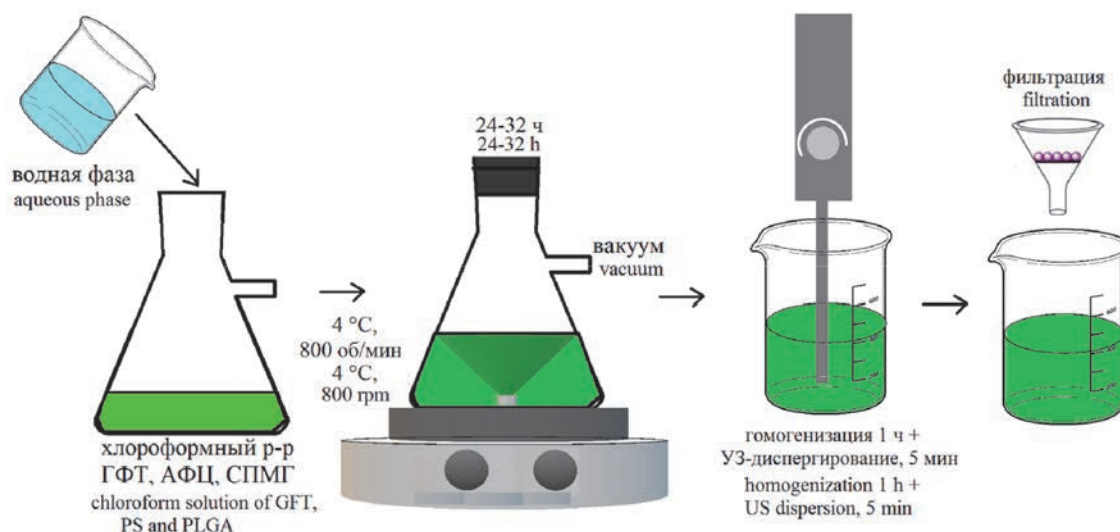


Рис. 2. Схема получения моделей ТЛН-1 методом горячей гомогенизации.
Fig. 2. Scheme for producing SLN-1 models by hot homogenization.

wavelengths of 338 ± 3 nm and 717 ± 3 nm, for GFT and APhC, respectively.

Cytotoxic activity

The study of the cytotoxic activity of SLN included the study of dark and photoinduced cytotoxicity on the lung carcinoma cell line A549 obtained from the Cell Line Bank of the N.N. Blokhin National Medical Research Center of Oncology of the Ministry of Health of the Russian Federation. The cell lines were cultured using the standard technique [12]. The MTT test was carried out using the routine method [13], irradiation was carried out 24 hours after the drug administration for 20 minutes with a LED source with a wavelength of 730 nm, then the cells were incubated for 24 hours.

Statistical processing was performed using standard Microsoft Excel 2007 packages and GraphPad Prism software (GraphPad Software Inc.). Each experiment was repeated at least three times, the results were presented as the mean \pm standard deviation (SD). IC_{50} concentrations were calculated by nonlinear regression. Statistical significance was determined at $p < 0.05$.

Results and discussion

The composition of SLN-1 is based on SA and SO, since the inclusion of liquid lipid in a solid lipid allows compounds to be embedded both between fatty acid chains and between lipid layers [7], which increases the loading capacity of active substances and reduces the explosive release of compounds. To select the optimal

composition of nanoparticles, model mixtures with different ratios of excipients were prepared (Table 1).

According to Table 1, it is evident that the content of surfactants and SA has a significant effect on the formation of a stable colloidal system, so an increase in the content of Tween 80 from 0.4% (No. 1) to 2.0% (No. 4) allows obtaining dispersion samples without sediment, and a decrease in SA from 2.0% (No. 1) to 0.7% (No. 4) prevents thickening, i.e. composition 4 with an average particle size of 236 ± 4 nm, ζ -potential of -20 ± 2.0 mV and pH = 6.1 turned out to be the most optimal. To stabilize the selected composition, lyophilization was carried out using cryoprotectors – mannitol, trehalose, and then the obtained samples were studied for the main quality indicators. The most optimal for forming a lyophilisate “tablet” was the use of 5% cryoprotector solutions (Table 2).

In the samples without cryoprotectant, the formation of a lyophilic structure did not occur, the samples with

mannitol and trehalose at a concentration of 5% not only formed a homogeneous dry porous mass during lyophilization, but also retained the SLN-1 indicators after rehydration of the lyophilisate (rehydration time is 1 min). However, the composition of SLN-1 with trehalose after rehydration remained stable for a longer time (about 30 days) in appearance (homogeneous suspension without signs of stratification and sedimentation).

SLN-2 was obtained using CPLG, which are currently widely studied due to their biocompatibility and biodegradability in the body. Based on the experience of preparing SLN-1 models, SLN-2 compositions were prepared in a ratio of GFT to APHC as 4:1 (Table 3, Fig. 3).

The data in Table 3 and Fig. 3 show that the stability of the resulting suspension directly depends on the amount of CPLG and PhC. Attempts to reduce the amount of CPLG and PhC led to a decrease in the inclusion of GFT and APHC by 6-30% and the precipitation of substances.

Таблица 1
Составы ТЛН-1

Table 1
Compositions of SLN-1

№	Массовое соотношение Ratio			Внешний вид Appearance of samples	
	ГФТ:АФЦ GFT: APHC	ГФТ:СК GFT:SA	СК:КМ:твин-80 SA:S.oil:twin- 80	после получения after receipt	через 24 ч after 24 h
1	4,5:1	1:11	2,2:1:0,4	неоднородная дисперсия с осадком, быстро загустевает heterogeneous dispersion with sediment, thickens quickly	неоднородная густая дисперсия с осадком heterogeneous thick dispersion with sediment
2	3,3:1	1:17	2,2:1:4,3	однородная дисперсия, быстро загустевает homogeneous dispersion, thickens quickly	густая дисперсия thick dispersion
3	3,7:1	1:10	2,2:1:4,3		
4	4:1	1:7	1,3:1:3,7	однородная дисперсия homogeneous dispersion	однородная дисперсия homogeneous dispersion

Таблица 2
Влияние криопротекторов на показатели качества ТЛН-1

Table 2
The influence of cryoprotectors on the quality indicators of SLN-1

Криопротектор Cryoprotector	Внешний вид лиофилизата Appearance of the lyophilisate	pH	Размер частиц, нм Nanoparticle size, nm	ζ -потенциал, мВ ζ -potential, mV	Эффективность включения ГФТ/ АФЦ, % Entrapment effi- ciency GFT/APHC, %
маннит 5% mannitol 5%	однородная сухая пористая масса светло-зеленого цвета homogeneous dry porous mass of light green color	6,4-6,8	220 ± 13	$-16 \pm 1,1$	100/40
трегалоза 5% trehalose 5%		7,3-7,4	245 ± 15	$-15 \pm 1,2$	92/44
-	прозрачная пленка transparent film	6,8-7,0	235 ± 11	$-14 \pm 0,9$	90/48

Таблица 3
Составы ТЛН-2
Table 3
Compositions of SLN-2

№	Массовое соотношение Ratio		Внешний вид Appearance of samples	
	ГФТ:СМПГ GFT:CPLG	СМПГ:ФХ:ПВС:Х CPLG:PhC:PA:Ch	после получения after receipt	через 24 ч after 24 h
1	1:30	60:40:40:1 ФХ — SPC PhC — SPC	однородная суспензия homogeneous suspension	однородная суспензия homogeneous suspension
2	1:30	60:16:40:1 ФХ — S100 PhC — S100		осадок sediment
3	1:20	40:15:40:1 ФХ — SPC PhC — SPC		однородная суспензия, осадок через 5 сут homogeneous suspension, sediment after 5 days
4	1:15	30:15:40:1 ФХ — SPC PhC — SPC		однородная суспензия, осадок через 3 сут homogeneous suspension, sediment after 3 days
5	1:15	30:15:20 ФХ — SPC, безХ PhC — SPC, without Ch		осадок sediment

The SLN-2 model of composition No. 1 turned out to be the most optimal with the inclusion of GFT at 87%, APhC at 99%, an average particle size of 243±11 nm, a neutral ζ-potential and a pH of 5.5. Monitoring this model over time using the above indicators showed its stability for 14 days at a storage temperature of 2-8°C. Lyophilization of this composition is planned for the future.

The cytotoxic activity of the selected models of SLN-1 (composition 4 with 5% trehalose) and SLN-2 (composition 1) was studied *in vitro* experiments on the A549 lung cancer cell model (Fig. 4, 5, Table 4).

In the study of dark and photoinduced cytotoxicity, combined SLN-1 and 2, as well as monodrugs (GFT substance and SLN-1 and SLN-2 models with only APhC)

were introduced into cells in concentrations of GFT at doses of 1.56-100 µg/ml. The GFT substance is not phototoxic, the difference between the IC₅₀ of the substance with and without irradiation is ~3%. According to IC₅₀, photoinduced cytotoxicity when exposed to a laser with a energy dose density of 33 J/cm² in both models was 3.5-4.6 times higher than dark toxicity, which indicates a synergistic effect of the drug and PDT. Compared with monotherapy, the combinations were 5.1-8.7 times more effective for GFT and 1.5-1.8 times more effective for APhC. Close IC₅₀ values between SLN-2 without irradiation and the GFT substance indicate photoinduced release of GFT from DF and low toxicity of excipients in this composition, while SLN-1 is sufficiently cytotoxic

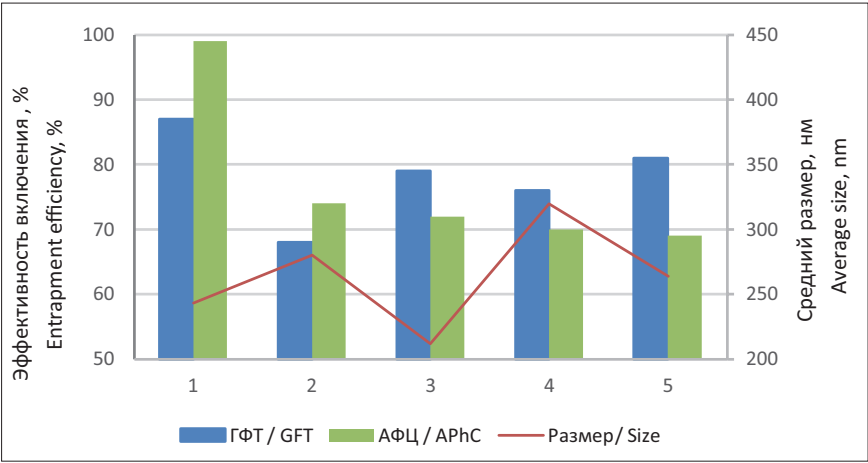


Рис. 3. Влияние состава вспомогательных веществ на эффективность включения ГФТ, АФЦ и на средний размер частиц в ТЛН-2.
Fig. 3. The influence of the composition of excipients on the efficiency of the inclusion of GFT, APhC and on the average particle size in SLN-2.

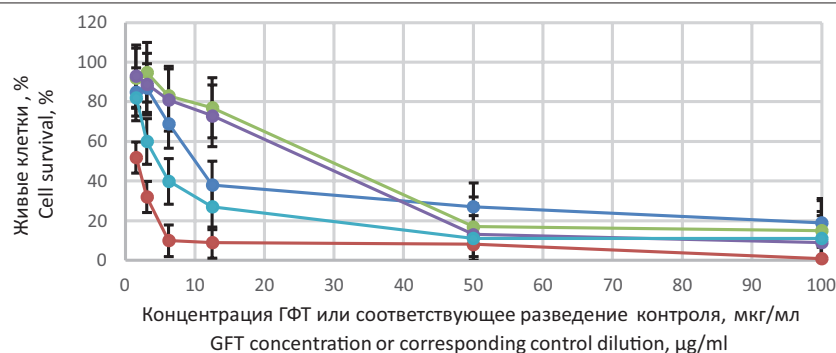


Рис. 4. Цитотоксическая активность ТЛН-1 на клетках A549, время инкубации 24 ч, для значений IC_{50} $p \leq 0,05$.

Fig. 4. Cytotoxic activity of SLN-1 on A549 cells, incubation time 24 h, for IC_{50} values $p \leq 0,05$.

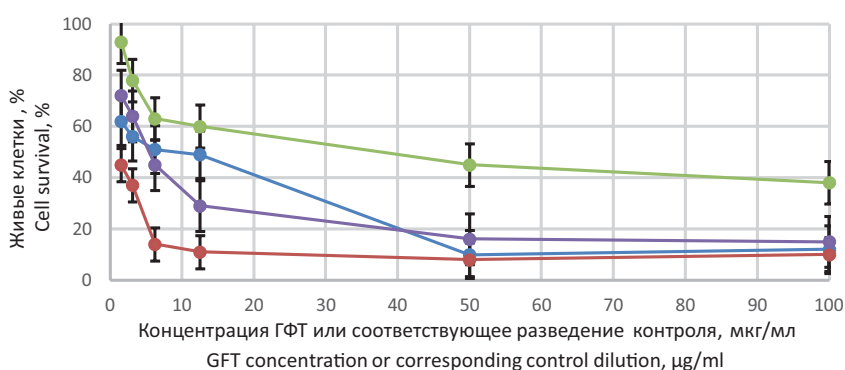


Рис. 5. Цитотоксическая активность ТЛН-2 на клетках A549, время инкубации 24 ч. Для значений $ТЛН-2IC_{50}$ и $ТЛН-2с$ АФЦ без ГФТ (без облучения и с облучением) $p \leq 0,05$.

Fig. 5. Cytotoxic activity of SLN-2 on A549 cells, incubation time 24 h, for IC_{50} values $p \leq 0,05$.

Таблица 4
 IC_{50} исследуемых образцов на модели A549
Table 4
 IC_{50} of tested samples on model A549

Образец препарата Drug sample	ТЛН-1*, мкг/мл SLN-1, µg/ml	ТЛН-2*, мкг/мл SLN-2, µg/ml
ТЛН без облучения SLN not illuminated	8,5	19,0
ТЛН с облучением SLN illuminated	2,4	4,1
Субстанция ГФТ без облучения GFT substance, not illuminated	21,6	
Субстанция ГФТ с облучением GFT substance, illuminated	20,9	
ТЛН с АФЦ без ГФТ без облучения SLN with APhC without GFT, not illuminated	-	22,5
ТЛН с АФЦ без ГФТ с облучением SLN with APhC without GFT, illuminated	4,3	6,2

* $p \leq 0,05$

even without irradiation. The presented data indicate the prospects for further study of the SLN-2 nanoparticle model on other cell lines.

Conclusion

As a result of complex studies on the creation of combined photoinduced nanosystems of GFT and PS with high cytotoxic activity, two models of SLN-1 and SLN-2 were obtained and studied with the IC_{50} indices of 2.4 and 4.1 µg/ml, respectively. In further studies, it is planned to improve the composition based on CPLG and PhC and study its phototoxicity on other cell lines, as well as select the optimal irradiation mode.

Data on the producing and study of SLN with photo-induced release can serve as a methodological approach for the development of various chemotherapeutic agents with stimulus-sensitive release.

The work was carried out with the financial support of the Russian Science Foundation grant No. 23-75-01026 "Development of targeted combined structures based on phospholipid nanosystems for the therapy of lung cancer."

REFERENCES

- Jampilek J., Kralova K. Insights into Lipid-Based Delivery Nanosystems of Protein-Tyrosine Kinase Inhibitors for Cancer Therapy. *Pharmaceutics*, 2022, vol. 14(12), pp. e2706. doi: 10.3390/pharmaceutics14122706.
- Nadaf S.J., Killedar S.G., Kumbhar V.M., Bhagwat D.A., Gurav S.S. Pazopanib-laden lipid based nanovesicular delivery with augmented oral bioavailability and therapeutic efficacy against non-small cell lung cancer. *International Journal of Pharmaceutics*, 2022, vol. 628, pp. e122287. doi: 10.1016/j.ijpharm.2022.122287.
- Kumar V., Khan I., Gupta U. Lipid-dendrimer nanohybrid system or dendrosomes: evidences of enhanced encapsulation, solubilization, cellular uptake and cytotoxicity of bortezomib. *ApplNanosci*, 2020, vol. 10, pp. 4049-4062. doi: 10.1007/s13204-020-01515-7.
- Gracias S., Ayyanar M., Peramaiyan G., Kalaskar M., Redasani V., Gurav N., Nadaf S., Deshpande M., Bhole R., Khan M.S., Chikhale R., Gurav S. Fabrication of chitosan nanocomposites loaded with biosynthetic metallic nanoparticles and their therapeutic investigation. *Environmental Research*, 2023, vol. 234, pp. e116609. doi: 10.1016/j.envres.2023.116609.
- Meerovich I., Nichols M.G., Dash A.K. Low-intensity light-induced paclitaxel release from lipid-based nano-delivery systems. *Journal of Drug Targeting*, 2019, vol. 27(9), pp. 971-983. doi: 10.1080/1061186X.2019.1571066.
- Yang T., Zhai J., Hu D., Yang R., Wang G., Li Y., Liang G. «Targeting Design» of Nanoparticles in Tumor Therapy. *Pharmaceutics*, 2022, vol. 14(9), pp. 1919. doi: 10.3390/pharmaceutics14091919.
- Makeen H.A., Mohan S., Al-Kasim M.A., Attafi I.M., Ahmed R.A., Syed N.K., Sultan M.H., Al-Bratty M., Alhazmi H.A., Safhi M.M., Ali R., Alam M.I. Gefitinib loaded nanostructured lipid carriers: characterization, evaluation and anti-human colon cancer activity in vitro. *Drug Delivery*, 2020, vol. 27(1), pp. 622-631. doi: 10.1080/10717544.2020.1754526.
- Sapelnikov M.D., Nikolskaya E.D., Morozova N.B., Plotnikova E.A., Efremenko A.V., Panov A.V., Grin M.A., Yakubovskaya R.I. Development of the technology for obtaining PLGA and dipropoxybateriopurpurinimide-based nanoparticles. Evaluation of physicochemical and biological properties of the obtained delivery system. *Biomedical Photonics*, 2019, vol. 8(1), pp. 4-17. doi:10.24931/2413-9432-2019-8-1-4-17.
- Kedik S.A., Omelchenko O.A., Suslov V.V., Shnyak E.A. Development of a method for the preparation of the naltrexone base encapsulated in polymeric microparticles. *Drug development & registration*, 2018, vol. 7(1), pp. 32-35.
- Kolpaksidi A. P., Dmitrieva M. V., Orlova O. L., Ektova L. V., Krasniuk I. I. Application of solid dispersion technology to obtain a model of injectable dosage form of indolocarbazole derivative. *Drug development & registration*, 2022, vol. 11(4), pp.73-78. doi:10.33380/2305-2066-2022-11-4-73-78.
- Sanarova E.V., Lantsova A.V., Nikolaeva L.L., Oborotova N.A., Litvinenko Ya.E., Solov'eva N.L. Creation of a Model of a Complex Delivery Nanosystem Containing a Tyrosine Kinase Inhibitor and a Photosensitizer. *Pharm Chem J*, 2023, vol. 57, pp. 1075-1079. doi:10.1007/s11094-023-02986-y.
- Abo Qoura L., Morozova E.A., Koval V.S., Kulikova V.V., Spirina T.S., Demidova E.A., Demidkina T.V., Pokrovsky V.S. Cytotoxic and antitumor properties of methionine γ -lyase conjugate in combination with S-alk(en)yl-L-cysteine sulfoxides. *Russian Journal of Biotherapy*, 2022, vol. 21(4), pp. 62-70. doi:10.17650/1726-9784-2022-21-4-62-70.
- Ionov N.S., Baryshnikova M.A., Bocharov E.V., Pogodin P.V., Lagunin A.A., Filimonov D.A., Karpova R.V., Kosorukov V.S., Stilidi I.S., Matveev V.B., Bocharova O.A., Poroikov V.V. Possibilities of in silico estimations for the development of pharmaceutical composition phytoladapto-gene cytotoxic for bladder cancer cells. *Biomed Khim*, 2021, vol. 67(3), pp. 278-288. doi:10.18097/PBMC20216703278.

ЛИТЕРАТУРА

- Jampilek J., Kralova K. Insights into Lipid-Based Delivery Nanosystems of Protein-Tyrosine Kinase Inhibitors for Cancer Therapy // *Pharmaceutics*. – 2022. – Vol. 14(12). – P. e2706. doi: 10.3390/pharmaceutics14122706.
- Nadaf S.J., Killedar S.G., Kumbhar V.M., Bhagwat D.A., Gurav S.S. Pazopanib-laden lipid based nanovesicular delivery with augmented oral bioavailability and therapeutic efficacy against non-small cell lung cancer // *International Journal of Pharmaceutics*. – 2022. – Vol. 628. – P. e122287. doi: 10.1016/j.ijpharm.2022.122287.
- Kumar V., Khan I., Gupta U. Lipid-dendrimer nanohybrid system or dendrosomes: evidences of enhanced encapsulation, solubilization, cellular uptake and cytotoxicity of bortezomib // *ApplNanosci*. – 2020. – Vol. 10. – P. 4049-4062. doi: 10.1007/s13204-020-01515-7.
- Gracias S., Ayyanar M., Peramaiyan G., Kalaskar M., Redasani V., Gurav N., Nadaf S., Deshpande M., Bhole R., Khan M.S., Chikhale R., Gurav S. Fabrication of chitosan nanocomposites loaded with biosynthetic metallic nanoparticles and their therapeutic investigation // *Environmental Research*. – 2023. – Vol. 234. – P. e116609. doi: 10.1016/j.envres.2023.116609.
- Meerovich I., Nichols M.G., Dash A.K. Low-intensity light-induced paclitaxel release from lipid-based nano-delivery systems // *Journal of Drug Targeting*. – 2019 – Vol. 27(9). – P. 971-983. doi: 10.1080/1061186X.2019.1571066.
- Yang T., Zhai J., Hu D., Yang R., Wang G., Li Y., Liang G. «Targeting Design» of Nanoparticles in Tumor Therapy // *Pharmaceutics*. – 2022. – Vol. 14(9). – P. 1919. doi: 10.3390/pharmaceutics14091919.
- Makeen H.A., Mohan S., Al-Kasim M.A., Attafi I.M., Ahmed R.A., Sultan M.H., Al-Bratty M., Alhazmi H.A., Safhi M.M., Ali R., Alam M.I. Gefitinib loaded nanostructured lipid carriers: characterization, evaluation and anti-human colon cancer activity in vitro // *Drug Delivery*. – 2020. – Vol. 27(1). – P. 622-631. doi: 10.1080/10717544.2020.1754526.
- Sapelnikov M.D., Nikolskaya E.D., Morozova N.B., Plotnikova E.A., Efremenko A.V., Panov A.V., Grin M.A., Yakubovskaya R.I. Development of the technology for obtaining PLGA and dipropoxybateriopurpurinimide-based nanoparticles. Evaluation of physicochemical and biological properties of the obtained delivery system // *Biomedical Photonics*. – 2019. – Vol. 8(1). – P. 4-17. doi:10.24931/2413-9432-2019-8-1-4-17.
- Кедик С.А., Омельченко О.А., Суслов В.В., Шняк Е.А. Разработка способа получения налтрексона основания, инкапсулированного в полимерные микрочастицы // Разработка и регистрация лекарственных средств. – 2018. – Т. 7(1). – С. 32-35. Kedik S.A., Omelchenko O.A., Suslov V.V., Shnyak E.A. Development of a method for the preparation of the naltrexone base encapsulated in polymeric microparticles // *Drug development & registration*. – 2018. – Vol. 7(1). – P.32-35.
- Kolpaksidi A. P., Dmitrieva M. V., Orlova O. L., Ektova L. V., Krasniuk I. I. Application of solid dispersion technology to obtain a model of injectable dosage form of indolocarbazole derivative // *Drug development & registration*. – 2022. – Vol. 11(4). – P.73-78. doi:10.33380/2305-2066-2022-11-4-73-78.
- Sanarova E.V., Lantsova A.V., Nikolaeva L.L., Oborotova N.A., Litvinenko Ya.E., Solov'eva N.L. Creation of a Model of a Complex Delivery Nanosystem Containing a Tyrosine Kinase Inhibitor and a Photosensitizer // *Pharm Chem J*. – 2023. – Vol. 57. – P. 1075-1079. doi:10.1007/s11094-023-02986-y.
- Abo Qoura L., Morozova E.A., Koval V.S., Kulikova V.V., Spirina T.S., Demidova E.A., Demidkina T.V., Pokrovsky V.S. Cytotoxic and antitumor properties of methionine γ -lyase conjugate in combination with S-alk(en)yl-L-cysteine sulfoxides // *Russian Journal of Biotherapy*. – 2022. – Vol. 21(4). – P. 62-70. doi:10.17650/1726-9784-2022-21-4-62-70.
- Ionov N.S., Baryshnikova M.A., Bocharov E.V., Pogodin P.V., Lagunin A.A., Filimonov D.A., Karpova R.V., Kosorukov V.S., Stilidi I.S., Matveev V.B., Bocharova O.A., Poroikov V.V. Possibilities of in silico estimations for the development of pharmaceutical composition phytoladapto-gene cytotoxic for bladder cancer cells // *Biomed Khim*. – 2021. – Vol. 67(3). – P. 278-288. doi:10.18097/PBMC20216703278.

BACTERICIDAL EFFECTIVENESS OF HIGH-INTENSITY PULSED BROADBAND IRRADIATION IN TREATING INFECTED WOUNDS

Abduvosidov Kh.A.^{1,2,3}, Chudnykh S.M.^{2,3,4}, Egorov V.S.^{3,4}, Filimonov A.Yu.³, Korolyova I.A.³, Kamrukov A.S.⁵, Bagrov V.V.⁵, Kondrat'ev A.V.⁵

¹FSBEI HE «Russian Biotechnological University», Moscow, Russia

²FSBEI HE «Tver State Medical University» of MOH of Russia, Tver, Russia

³FSBEI HE «Russian University Of Medicine» of MOH of Russia, Moscow, Russia

⁴Moscow Clinical Scientific Center n.a. A.S. Loginov, Moscow, Russia

⁵FSBEI HE «Bauman Moscow State Technical University», Moscow, Russia

Abstract

The study aimed to investigate the bactericidal efficacy of high-intensity pulsed broadband irradiation in the treatment of infected wounds. An experimental study was conducted on 90 mature male Wistar rats. An infected wound model was created by contaminating with *Staphylococcus aureus*, *Pseudomonas aeruginosa*, *Klebsiella pneumoniae*, and *Candida albicans*. Animals in Group 1 received high-intensity pulsed broadband irradiation. Animals in Group 2 received traditional UV irradiation. Animals in Group 3 had their wounds cleaned with 0.1% chlorhexidine solution. By the 3rd day of treatment, animals that received pulsed high-intensity broadband irradiation showed a significant reduction in contamination by *Staphylococcus aureus*, *Klebsiella pneumoniae*, and *Pseudomonas aeruginosa* compared to Group 3. By the 7th day of treatment, half or the majority of animals in Groups 1 and 2 showed complete decontamination of wounds concerning *Staphylococcus aureus* and *Klebsiella pneumoniae*. Most animals in Group 1 showed complete wound clearance of *Pseudomonas aeruginosa*. By the 10th day, nearly all animals in Group 1 demonstrated complete decontamination of wounds. Statistical analysis revealed a significant difference in the reduction of wound contamination with *Staphylococcus aureus* and *Klebsiella pneumoniae* by the 10th day in Groups 1 and 2 compared to Group 3. Thus, the use of high-intensity pulsed broadband irradiation of wounds reduces the degree of pathogenic microorganism contamination in a shorter time frame.

Keywords: infected wound, ultraviolet irradiation, high-intensity pulsed broad-spectrum irradiation, local wound treatment, bacteriological control.

Contacts: Abduvosidov Kh.A., e-mail: sogdiana99@gmail.com

For citations: Abduvosidov Kh.A., Chudnykh S.M., Egorov V.S., Filimonov A.Yu., Korolyova I.A., Kamrukov A.S., Bagrov V.V., Kondrat'ev A.V. Bactericidal effectiveness of high-intensity pulsed broadband irradiation in treating infected wounds, *Biomedical Photonics*, 2024, vol. 13, no. 2, pp. 26–33. doi: 10.24931/2413–9432–2023–13-2-26–33.

БАКТЕРИЦИДНАЯ ЭФФЕКТИВНОСТЬ ИСПОЛЬЗОВАНИЯ ВЫСОКОИНТЕНСИВНОГО ИМПУЛЬСНОГО ШИРОКОПОЛОСНОГО ОБЛУЧЕНИЯ ПРИ ЛЕЧЕНИИ ИНФИЦИРОВАННЫХ РАН

Х.А. Абдувосидов^{1,2,3}, С.М. Чудных^{2,3,4}, В.С. Егоров^{3,4}, А.Ю. Филимонов³, И.А. Королёва³, А.С. Камруков⁵, В.В. Багров⁵, А.В. Кондратьев⁵

¹ФГБОУ ВО Российский биотехнологический университет, Москва, Россия

²ФГБОУ ВО Тверской государственный медицинский университет Минздрава России, Тверь, Россия

³ГБУЗ Московский клинический научно-практический центр им. А.С. Логинова ДЗМ, Москва, Россия

⁴ФГБОУ ВО Российский университет медицины Минздрава России, Москва, Россия

⁵ФГБОУ Московский государственный технический университет имени Н.Э. Баумана (национальный исследовательский университет), Москва, Россия

Резюме

Целью исследования явилось изучение бактерицидной эффективности высокоинтенсивного импульсного широкополосного облучения при лечении инфицированных ран. Проведено экспериментальное исследование на 90 половозрелых крысах-самцах линии Wistar (3 группы). Моделировали инфицированную рану контаминированием *Staphylococcus aureus*, *Pseudomonas aeruginosa*, *Klebsiella pneumoniae*, *Candida albicans*. Животным 1-й группы проводили высокоинтенсивное импульсное широкополосное облучение. Животным 2-й группы проводили традиционное УФ облучение. Животным 3-й группы проводили туалет раны раствором хлоргексидина 0,1%. Проведенное исследование показало, что к 3-му дню лечения у животных, которым проводили импульсное высокоинтенсивное широкополосное облучение ран, имело место существенное уменьшение контаминации *Staphylococcus aureus*, *Klebsiella pneumoniae* и *Pseudomonas aeruginosa* по сравнению с 3-й группой. К 7-му дню лечения в 1-й и во 2-й группах у большинства животных наблюдали полную деконтаминацию ран в отношении *Staphylococcus aureus* и *Klebsiella pneumoniae*. У большинства животных 1-й группы выявлено полное очищение ран от *Pseudomonas aeruginosa*. К 10-му дню практически у всех животных 1-й группы отмечена полная деконтаминация ран. Статистический анализ показал, что к 10-му дню лечения у животных 1-й и 2-й групп по отношению к *Staphylococcus aureus* и *Klebsiella pneumoniae* выявлена существенная разница в снижении степени контаминации ран по сравнению с результатами у животных 3-й группы. Таким образом, применение импульсного высокоинтенсивного широкополосного облучения ран снижает степень контаминации патогенных микроорганизмов в более ранние сроки.

Ключевые слова: инфицированная рана, ультрафиолетовое облучение, импульсное высокоинтенсивное широкополосное облучение, местное лечение ран, бактериологический контроль.

Контакты: Абдувосидов Х.А., e-mail: sogdiana99@gmail.com

Для цитирования: Абдувосидов Х.А., Чудных С.М., Егоров В.С., Филимонов А.Ю., Корольова И.А., Камруков А.С., Багров В.В., Кондратьев А.В. Бактерицидная эффективность использования высокоинтенсивного импульсного широкополосного облучения при лечении инфицированных ран // Biomedical Photonics. – 2024. – Т. 13, № 2. – С. 26–33. doi: 10.24931/2413–9432–2024–13–2–26–33.

Introduction

In modern surgery, an important issue is the prevention and treatment of infections. In the first half of the 20th century, owing to the scientific works of A. Fleming, H.W. Florey and E.B. Chain, a new era in medicine began, which was marked by the emergence of antibiotics, for the discovery of which the scientists were awarded the Nobel Prize. Undoubtedly, the first and most important link in the treatment of infections, including wound infection, is antibacterial therapy. However the widespread use of antibacterial drugs has led to the evolution of microorganisms and the emergence of new types of pathogens with resistance to antibiotics.

According to WHO, there is an increase in antibacterial resistance to antibiotics. For instance, 50% of *Escherichia coli* strains are resistant to methicillin, *Staphylococcus aureus* (MRSA) and *Klebsiella pneumoniae* – to third-generation cephalosporins and fluoroquinolones [1, 2]. Many types of microorganisms, including fungi, produce a protective extracellular polymer matrix, the so-called biofilms, which are quite difficult for modern systemic antimicrobial drugs to penetrate. There is a need to prescribe high doses of antimicrobial drugs, which can increase the risk of side effects [3, 4, 5].

The literature contains many works devoted to the issue of antibacterial resistance and the search for new drugs for the treatment of infections with antibacterial resistance [2, 6, 7, 8, 9, 10, 11]. Nevertheless, the issue of treating wound infections remains relevant. At the same time, many authors emphasize additional treatment methods that can achieve complete decontamination of wounds or sufficiently reduce their contamination. These methods include the

effect of exogenous nitric oxide, vacuum therapy, hydrosurgical treatment of wounds, the use of ultrasonic cavitation, and photodynamic therapy [12, 13, 14, 15].

Light technologies are a set of developing methods in wound treatment. At the same time, low-frequency laser therapy and photodynamic therapy are currently widely used to treat wound infections [16, 17, 18, 19, 20]. The ultraviolet range includes electromagnetic radiation with wavelengths from 100 to 400 nm, which is divided into four independent spectral regions.

The wavelength range from 315 to 400 nm is defined as UVA, the range from 280 to 315 nm as UVB, radiation with wavelengths from 200 to 280 nm is classified as the UVC range, and the region from 100 to 200 nm is classified as vacuum ultraviolet. Short-wave UV radiation in the UV-C and UV-B ranges has a pronounced bactericidal effect with maximum efficiency at wavelengths from 250 to 270 nm and allows for the inactivation of various types of microorganisms, including antibiotic-resistant strains of pathogenic bacteria [21, 22, 23].

A large selection of methods of physical impact using light technologies on wound infection with increasing antibacterial resistance determine the relevance of improving phototherapy methods and selecting optimal effective modes of their use.

The aim of the study was to study the bactericidal effectiveness of high-intensity pulsed broadband irradiation in the treatment of infected wounds.

Materials and Methods

An experimental study approved by the Interuniversity Ethics Committee (extract from protocol No. 06-23

dated 15/06/23) was conducted. The experiment was performed on mature male Wistar rats weighing 220-250 g in the vivarium of the Russian University of Medicine of the Ministry of Health of the Russian Federation. All animals were quarantined for 2 weeks.

Manipulations on animals were performed under general anesthesia. Pre-medication with a 2% xylazine solution was performed. Then general anesthesia was performed with a solution of zoletil 100.

After achieving anesthesia, an infected wound was modeled under aseptic conditions. A skin incision 20x20 mm was made in the withers area. A trigger in the form of a gauze ball with a suspension of cultures from control strains of *Staphylococcus aureus*, *Pseudomonas aeruginosa*, *Klebsiella pneumoniae*, *Candida albicans* in equal volumes and dilutions, containing 10^9 microbial bodies in 1 ml, was introduced into the wound. The wound was sutured with a polypropylene thread by applying two interrupted sutures. In the postoperative period, all animals had access to liquid for drinking and received standard nutrition. One day after wound modeling, the sutures were removed. Then all animals were randomly divided into three Groups of thirty individuals.

Animals of the 1st Group (n=30) in the postoperative period after removal of sutures underwent daily wound cleaning with 0.1% chlorhexidine solution followed by high-intensity pulsed broadband irradiation and application of a dressing with 0.1% chlorhexidine solution to the wound. Irradiation was carried out for 10 days.

Animals of the 2nd Group (n=30) after daily wound cleaning with 0.1% chlorhexidine solution underwent traditional UV irradiation with application of a dressing with 0.1% chlorhexidine solution to the wound. Irradiation was carried out for 10 days.

Animals of the 3rd Group (n=30) underwent daily wound cleaning with 0.1% chlorhexidine solution and application of a dressing with 0.1% chlorhexidine solution to the wound.

High-intensity pulsed broadband irradiation was performed using a device developed by the Research Institute of Power Engineering of Bauman Moscow State Technical University. The operating principle of the device is based on pulsed irradiation of affected areas with high-intensity optical radiation of a continuous spectrum generated by a small-sized pulsed xenon lamp of the PPS 5/60 type. The lamp operates in a pulse-periodic mode with a pulse frequency of 5 Hz and an average electric power of 100 W. The average radiation power of the lamp in the UV-C range of the spectrum (200-280 nm) was 3 W, the pulsed power of UV-C radiation was 24 kW.

The device had three modes: mode 1 – irradiation cycle duration of 10 s (50 pulses); mode 2 – 20 s (100 pulses); mode 3 – 40 s (200 pulses). We selected the following wound treatment technique depending on the degree of contamination and the stage of the wound

process: during the first five days of treatment, mode 3 was used (200 pulses with an irradiation cycle duration of 40 s) with an irradiation distance of 5 cm from the wound, starting from the sixth day of treatment. Mode 2 was used for the next five days (100 pulses with a cycle duration of 20 s) at a distance of 10 cm.

Traditional UV irradiation was carried out using the IUVQ-01 "Solnyshko" – a UV quartz irradiator based on a mercury bactericidal lamp of the ACBU-7 type with an electric power of 7 W. The radiation power in the UV-C range was 1.2 W. Irradiation was carried out daily for 10 days for 3 minutes from a distance of 10 cm from the irradiator to the wound.

To assess the bactericidal effectiveness of high-intensity pulsed broadband radiation and traditional UV irradiation in the treatment of infected wounds, a bacteriological study was carried out on the day of suture removal (before treatment), on the 3rd, 7th, 10th, 14th and 21st days from the start of treatment.

The analysis of the degree of contamination and the dynamics of decontamination of wounds with various microflora was performed. For this purpose, at each control period, the number of animals with different degrees of contamination of four types of microorganisms (*Staphylococcus aureus*, *Klebsiella pneumoniae*, *Pseudomonas aeruginosa*, *Candida albicans*) 10^8 , 10^6 and $<10^4$ on the wound surface was taken into account. Samples were seeded using the sector seeding method (according to Gold-Rodman) on Petri dishes with blood agar, as well as with Endo and Saburo media.

The study was conducted in the bacteriological laboratory of the A.S. Loginov Moscow Medical Scientific Center of the Healthcare Department of the City of Moscow. The results are presented as a percentage. Comparative assessment of qualitative features within and between Groups was performed using the Pearson χ^2 criterion, for which conjugation tables were preliminarily constructed and evaluated. A feature was considered statistically different at $p < 0.05$. Multiple comparisons were performed using the Bonferroni correction. For comparisons between Groups, $k = 0.05/3 = 0.0167$.

Results

Before the treatment, bacteriological examination of the wound surface showed that there was no statistically significant difference between the study Groups in the degree of microflora contamination. Almost all animals were contaminated with *Staphylococcus aureus* 10^8 CFU. Wound contamination with *Pseudomonas aeruginosa* (10^8 CFU) was noted in 90% of animals in the three study Groups.

By the 3rd day of treatment, statistically significant decrease in the degree of wound contamination with *Staphylococcus aureus* was revealed in animals of the 1st Group compared to the 2nd and 3rd Groups (Table 1). Positive dynamics were observed in all Groups in relation

to the reduction in the degree of wound contamination with *Klebsiella pneumoniae* on the 3rd day. By the 3rd day of control, a significant difference in the treatment results was found between the 1st and 3rd Groups ($p=0.0025$, $\chi^2=14.3$ and $p=0.01$, $\chi^2=11$, respectively) in relation to the contamination of wounds with *Klebsiella pneumoniae* and *Pseudomonas aeruginosa*. Positive dynamics in the form of decontamination and a decrease in the degree of contamination of the wound surface with *Candida albicans* were also noted. No statistical difference was found between the Groups during this period in terms of *Candida albicans* contamination ($p=0.33$, $\chi^2=4.58$).

By the 7th day of treatment, positive dynamics were observed in relation to the reduction of the degree of contamination of all microorganisms (Table 2). Moreover, it was noted that there was no contamination of 10^8 CFU in any Group. Analysis of the contamination of

wounds with *Staphylococcus aureus* by this time showed that there was a significant difference in the results of decontamination and reduction of the degree of contamination between the 1st and 3rd Groups ($p<0.0001$, $\chi^2=41.14$), and a difference was also revealed between the 2nd and 3rd Groups ($p<0.0001$, $\chi^2=29.14$).

At the same time, the contamination of *Klebsiella pneumoniae* was reduced in all Groups of animals (Table 2). The rates of *Pseudomonas aeruginosa* contamination of wounds in animals of the 1st Group by the 7th day of treatment differed from those in the 2nd and 3rd Groups ($p=0.01$, $\chi^2=8.93$, $p<0.0001$, $\chi^2=25.84$, respectively). There was a positive trend with respect to *Candida albicans*; in all Groups, complete decontamination of wounds with *Candida albicans* was observed in most animals. However, no statistically significant difference was found between the Groups by this time (Table 2).

Таблица 1
Контаминация ран различной микрофлорой у животных в трех группах на 3-й день лечения

Table 1
Contamination of wounds by various microflora in animals across three groups on day 3 of treatment

Микрофлора Microflora	КОЕ CFU	Группы Groups						P
		1		2		3		
		Абс. Abs.	%	Абс. Abs.	%	Абс. Abs.	%	
Staphylococcus aureus	10 ⁸	2	6,67	6	20	11	36,67	p=0,0014, χ ² =21,64; P1-2 p=0,043, χ ² =8,13; P1-3 p=0,0003, χ ² =18,6; P2-3 p=0,25, χ ² =4,07
	10 ⁶	7	23,33	13	43,33	13	43,33	
	<10 ⁴	13	43,33	9	30	6	20	
	Нет роста No growth	8	26,67	2	6,67	0		
Klebsiella pneumoniae	10 ⁸	0		1	3,33	6	20	p=0,0071, χ ² =17,65; P1-2 p=0,26, χ ² =4; P1-3 p=0,0025, χ ² =14,3; P2-3 p=0,13, χ ² =5,5
	10 ⁶	4	13,33	8	26,67	10	33,33	
	<10 ⁴	12	40	13	43,33	10	33,33	
	Нет роста No growth	14	46,67	8	26,67	4	13,33	
Pseudomonas aeruginosa	10 ⁸	5	16,67	9	30	14	46,67	p=0,034, χ ² =13,48 P1-2 p=0,28, χ ² =3,82; P1-3 p=0,01, χ ² =11; P2-3 p=0,17, χ ² =4,95
	10 ⁶	8	26,67	6	20	9	30	
	<10 ⁴	8	26,67	11	36,67	6	20	
	Нет роста No growth	9	30	4	13,33	1	3,33	
Candida albicans	10 ⁸	0		0		0		p=0,33, χ ² =4,58
	10 ⁶	2	6,67	4	13,33	5	16,67	
	<10 ⁴	6	20	9	30	11	36,67	
	Нет роста No growth	22	73,33	17	56,67	14	46,67	

By the 10th day of treatment, the *Staphylococcus aureus* contamination differed significantly between the Groups (Table 3). The number of animals with wound decontamination with *Staphylococcus aureus* was significantly lower in Group 1 compared to Groups 2 and 3 ($p=0.01$, $\chi^2=6.4$ and $p<0.0001$, $\chi^2=22.33$, respectively). In Group 2, the results differed significantly compared to Group 3 ($p=0.01$, $\chi^2=9.13$). The decrease in the degree of *Klebsiella pneumoniae* contamination among animals in Group 1 was significantly greater than in Groups 2 and 3 ($p=0.01$, $\chi^2=9.23$ and $p<0.0001$, $\chi^2=25.71$, respectively).

Also, the wound cleansing indices in the 2nd Group differed significantly from those in the 3rd Group ($p=0.0002$, $\chi^2=17.01$). When analyzing the wound contamination with *Pseudomonas aeruginosa* by the 10th day of treatment, there was a statistically significant dif-

ference between the Groups ($p=0.0001$, $\chi^2=29.03$). The results in the 1st Group were significantly better compared to the 3rd Group ($p=0.0001$, $\chi^2=23.81$). By the 3rd day of control, decontamination of *Candida albicans* wounds was detected in all animals of the 1st and 2nd Groups, and only 2 (6.67%) animals of the 3rd Group had a contamination of 10^4 CFU.

On the 14th day of treatment, positive dynamics were observed compared to the previous days of control. In all animals of the 1st Group, complete decontamination of wounds was observed in relation to all microorganisms. In the 2nd Group, 27 animals showed complete decontamination in relation to *Staphylococcus aureus* and *Klebsiella pneumoniae*, and in 26 animals in relation to *Pseudomonas aeruginosa*. In the 3rd Group, positive dynamics were also observed, in most rats, complete cleansing of wounds was detected.

Таблица 2

Контаминация ран различной микрофлорой у животных в трех группах на 7-й день лечения

Table 2

Contamination of wounds by various microflora in animals across three groups on day 7 of treatment

Микрофлора Microflora	КОЕ CFU	Группы Groups						P
		1		2		3		
		Абс. Abs.	%	Абс. Abs.	%	Абс. Abs.	%	
Staphylococcus aureus	10 ⁸	0		0		0		p<0,0001, χ ² =54,62; P1-2 p=0,051, χ ² =5,8; P1-3 p<0,0001, χ ² =41,14; P2-3 p<0,0001, χ ² =29,14
	10 ⁶	0		4	13,33	24	80	
	<10 ⁴	8	26,67	11	36,67	0		
	Нет роста No growth	22	73,33	15	50	6	20	
Klebsiella pneumoniae	10 ⁸	0		0		6	20	p<0,0001, χ ² =48,82; P1-2 p=0,35, χ ² =0,88; P1-3 p<0,0001, χ ² =32,87; P2-3 p<0,0001, χ ² =28,68
	10 ⁶	0		0		10	33,33	
	<10 ⁴	5	16,67	8	26,67	10	33,33	
	Нет роста No growth	25	83,33	22	73,33	4	13,33	
Pseudomonas aeruginosa	10 ⁸	0		0		2	6,67	p<0,0001, χ ² =27,91 P1-2 p=0,01, χ ² =8,93; P1-3 p<0,0001, χ ² =25,84; P2-3 p=0,047, χ ² =7,94
	10 ⁶	0		7	23,33	14	46,67	
	<10 ⁴	9	30	10	33,33	9	30	
	Нет роста No growth	21	70	13	43,33	5	16,67	
Candida albicans	10 ⁸	0		0		0		p=0,052, χ ² =5,88
	10 ⁶	0		0		0		
	<10 ⁴	1	3,33	2	6,67	5	16,67	
	Нет роста No growth	29	96,67	28	93,33	25	83,33	

Таблица 3
Контаминация ран различной микрофлорой у животных в трех группах на 10-й день лечения

Table 3
Contamination of wounds by various microflora in animals across three groups on day 10 of treatment

Микрофлора Microflora	КОЕ CFU	Группы Groups						P
		1		2		3		
		Абс. Abs.	%	Абс. Abs.	%	Абс. Abs.	%	
Staphylococcus aureus	10 ⁸	0		0		0		p<0,0001, χ ² =26,86; P1-2 p=0,01, χ ² =6,4; P1-3 p<0,0001, χ ² =22,33; P2-3 p=0,01, χ ² =9,13
	10 ⁶	0		0		5	16,67	
	<10 ⁴	1	3,33	8	26,67	13	43,33	
	Нет роста No growth	29	96,67	22	73,33	12	40	
Klebsiella pneumoniae	10 ⁸	0		0		0		p<0,0001, χ ² =35,46; P1-2 p=0,01, χ ² =9,23; P1-3 p<0,0001, χ ² =25,71; P2-3 p=0,0002, χ ² =17,01
	10 ⁶	0		0		5	16,67	
	<10 ⁴	0		3	10	13	43,33	
	Нет роста No growth	30	100	27	90	12	40	
Pseudomonas aeruginosa	10 ⁸	0		0		1	3,33	p=0,0001, χ ² =29,03; P1-2 p=0,01, χ ² =8,93; P1-3 p=0,0001, χ ² =23,81; P2-3 p=0,026, χ ² =9,25
	10 ⁶	0		1	3,33	9	30	
	<10 ⁴	0		7	23,33	6	20	
	Нет роста No growth	30	100	22	73,33	14	46,67	
Candida albicans	10 ⁸	0		0		0		p=0,12, χ ² =4,09
	10 ⁶	0		0		0		
	<10 ⁴	0		0		2	6,67	
	Нет роста No growth	30	100	30	100	28	93,33	

By the 21st day, among the animals of the 2nd Group, only 1 animal showed growth of *Staphylococcus aureus*, in the remaining animals, complete decontamination of wounds was detected. In the 3rd Group, 1 animal had contamination of 10⁶ CFU, 5 animals had growth of *Staphylococcus aureus* and *Pseudomonas aeruginosa* of 10⁴ CFU, and 2 animals had growth of *Klebsiella pneumoniae* of 10⁴ CFU.

Discussion

There are scientific studies devoted to the effectiveness of pulsed high-intensity optical irradiation in experiments. Thus, some authors note the bactericidal effect of pulsed high-intensity optical irradiation for the treatment of linear wounds in experimental animals. It is worth noting that the modeled wounds were not subjected to initial infection, they were practically aseptic [24].

There is also information on the clinical effectiveness of using high-intensity optical irradiation in experiments *in vitro* and *in vivo* [25, 26]. The authors of the study claim that high-intensity optical irradiation has pronounced bactericidal and wound-healing effects and reliably provides higher rates of wound healing compared to the use of only a typical antibacterial and wound-healing agent – Levomekole (methylluracilum, chloramphenicol) ointment [25, 26]. It should be emphasized that the modeled wounds were infected with one microorganism in low contamination of 10³ CFU. At the same time, there is no data on wound contamination control and, moreover, antibacterial therapy was started immediately after the application of pathogenic flora to the wound.

In our study, experimental infection of the wound was performed with four pathogenic strains in equal volumes and dilutions containing 10⁹ microbial bodies in 1 ml.

Bacteriological control was carried out, which confirmed pathogenic infection of the wounds, after which the animals were divided into three Groups depending on the treatment method. We conducted a comparative analysis of the effectiveness of decontamination and reduction of the degree of contamination of infected wounds between pulsed high-intensity broadband irradiation, traditional ultraviolet irradiation and drug local treatment. Bacteriological control was performed during the treatment. It was revealed that pulsed high-intensity broadband irradiation has a higher antibacterial activity compared to traditional irradiation and local treatment.

Conclusion

Thus, the conducted bacteriological study showed that against the background of the treatment, positive dynamics were obtained at each control period in the form of a decrease in the degree of contamination or complete decontamination of wounds in all Groups. Moreover, by the 3rd day of treatment against the background of pulsed high-intensity broadband irradiation of wounds, there was a statistically significant decrease in the degree of contamination of wounds with *Staphylococcus aureus*, *Klebsiella pneumoniae*, and *Pseudomonas aeruginosa* compared to the Group where traditional local treatment of wounds with an antiseptic was carried out ($p = 0.0003$, $\chi^2 = 18.6$, $p = 0.0025$, $\chi^2 = 14.3$ and $p = 0.01$, $\chi^2 = 11$, respectively).

By the 3rd day of control, no significant difference was found in the results of treatment of infected wounds

between the Group of animals that underwent traditional ultraviolet irradiation of wounds and the Group of animals that received local drug therapy.

On the 7th day, the dynamics of treatment results between the Groups differed statistically significantly. In the 1st and 2nd Groups, as a result of treatment, most animals achieved complete decontamination of wounds with respect to *Staphylococcus aureus* and *Klebsiella pneumoniae*. Most animals treated with pulsed high-intensity broadband irradiation showed complete cleansing of wounds from *Pseudomonas aeruginosa*.

Compared with the previous control periods, by the 10th day, almost all animals in the 1st Group had complete decontamination of wounds from all types of microflora. During this period, in the 2nd Group, most animals showed a decrease in the degree of bacterial contamination, as well as complete cleansing of wounds. Statistical analysis showed that with pulsed high-intensity broadband or traditional UV irradiation of wounds on the 10th day, a reliable difference in the effectiveness of treatment with respect to *Staphylococcus aureus* and *Klebsiella pneumoniae* was revealed compared with local drug therapy.

Consequently, the use of pulsed high-intensity broadband irradiation of wounds by the claimed method reduces contamination of pathogenic microorganisms, both gram-negative and gram-positive, at an earlier time, in contrast to traditional drug methods of local treatment and traditional ultraviolet irradiation of wounds.

REFERENCES

1. Hariyanto H., Yahya C.Q., Cucunawangsih C., Pertiwi C.L.P. Antimicrobial resistance and mortality. // *Afr J Infect*, 2022, vol. 16 (2), pp. 13-20. doi: 10.21010/Ajid.v16i2.2.
2. Reyes J., Komarow L., Chen L., Ge L., Hanson B.M., et al. Antibacterial Resistance Leadership Group and Multi-Drug Resistant Organism Network Investigators. Global epidemiology and clinical outcomes of carbapenem-resistant *Pseudomonas aeruginosa* and associated carbapenemases (POP): a prospective cohort study. *Lancet Microbe*, 2023, vol. 4(3), pp. 159-170. doi: 10.1016/S2666-5247(22)00329-9.
3. Hall-Stoodley L., Costerton J.W., Stoodley P. Bacterial biofilms: from the natural environment to infectious diseases. *Nat Rev Microbiol*, 2004, vol. 2 (2), pp. 95-108. doi: 10.1038/nrmicro821.
4. Stewart P.S., Costerton J.W. Antibiotic resistance of bacteria in biofilms. *Lancet*, 2001, vol. 358 (9276), pp. 135-138. doi: 10.1016/S0140-6736(01)05321-1.
5. St Denis T.G., Dai T., Izikson L., Astrakas C., Anderson R.R., Hamblin M.R., Tegos G.P. All you need is light: antimicrobial photoinactivation as an evolving and emerging discovery strategy against infectious disease. *Virulence*, 2011, vol. 2 (6), pp. 509-20. doi: 10.4161/viru.2.6.17889. Epub 2011 Nov 1.
6. Karbalaee-Heidari H.R., Budisa N. Combating Antimicrobial Resistance With New-To-Nature Lanthipeptides Created by Genetic Code Expansion. *Front*, 2020, vol. 11, pp. 590522. doi: 10.3389/fmicb.2020.590522.
7. Aguda O.N., Lateef A. Recent advances in functionalization of nanotextiles: A strategy to combat harmful microorganisms and emerging pathogens in the 21st century. *Heliyon*, 2022, vol. 8(6), pp. e09761. doi: 10.1016/j.heliyon.2022.e09761.
8. Oli A.N., Eze D.E., Gugu T.H., Ezeobi I., Maduagwu U.N., Ihekwereme C.P. Multi-antibiotic resistant extended-spectrum beta-lactamase producing bacteria pose a challenge to the effective treatment of

ЛИТЕРАТУРА

1. Hariyanto H., Yahya C.Q., Cucunawangsih C., Pertiwi C.L.P. Antimicrobial resistance and mortality // *Afr J Infect Dis*. – 2022. – Vol. 16 (2). – P. 13-20. doi: 10.21010/Ajid.v16i2.2.
2. Reyes J., Komarow L., Chen L., Ge L., Hanson B.M., et al. Antibacterial Resistance Leadership Group and Multi-Drug Resistant Organism Network Investigators. Global epidemiology and clinical outcomes of carbapenem-resistant *Pseudomonas aeruginosa* and associated carbapenemases (POP): a prospective cohort study // *Lancet Microbe*. – 2023. – Vol. 4(3). – P. 159-170. doi: 10.1016/S2666-5247(22)00329-9.
3. Hall-Stoodley L., Costerton J.W., Stoodley P. Bacterial biofilms: from the natural environment to infectious diseases // *Nat Rev Microbiol*. – 2004. – Vol. 2 (2). – P. 95-108. doi: 10.1038/nrmicro821.
4. Stewart P.S., Costerton J.W. Antibiotic resistance of bacteria in biofilms // *Lancet*. – 2001. – Vol. 358 (9276). – P. 135-138. doi: 10.1016/S0140-6736(01)05321-1.
5. St Denis T.G., Dai T., Izikson L., Astrakas C., Anderson R.R., Hamblin M.R., Tegos G.P. All you need is light: antimicrobial photoinactivation as an evolving and emerging discovery strategy against infectious disease // *Virulence*. – 2011. – Vol. 2 (6). – P. 509-20. doi: 10.4161/viru.2.6.17889. Epub 2011 Nov 1.
6. Karbalaee-Heidari H.R., Budisa N. Combating Antimicrobial Resistance With New-To-Nature Lanthipeptides Created by Genetic Code Expansion // *Front Microbiol*. – 2020. – Vol. 11. – P. 590522. doi: 10.3389/fmicb.2020.590522.
7. Aguda O.N., Lateef A. Recent advances in functionalization of nanotextiles: A strategy to combat harmful microorganisms and emerging pathogens in the 21st century // *Heliyon*. – 2022. – Vol. 8(6). – P. e09761. doi: 10.1016/j.heliyon.2022.e09761.
8. Oli A.N., Eze D.E., Gugu T.H., Ezeobi I., Maduagwu U.N., Ihekwereme C.P. Multi-antibiotic resistant extended-spectrum beta-lactamase producing bacteria pose a challenge to the effective treatment of

- wound and skin infections. *Pan Afr Med J*, 2017, vol. 27, pp. 66. doi: 10.11604/pamj.2017.27.66.10226.
9. Park S.C., Nam J.P., Kim J.H., Kim Y.M., Nah J.W., Jang M.K. Antimicrobial action of water-soluble β -chitosan against clinical multi-drug resistant bacteria. *Int J Mol Sci*, 2015, vol. 16(4), pp. 7995-8007. doi: 10.3390/ijms16047995.
10. Sanyasi S., Majhi R.K., Kumar S., Mishra M., Ghosh A., et al. Polysaccharide-capped silver Nanoparticles inhibit biofilm formation and eliminate multi-drug-resistant bacteria by disrupting bacterial cytoskeleton with reduced cytotoxicity towards mammalian cells. *Sci Rep*, 2016, vol. 6, pp. 24929. doi: 10.1038/srep24929.
11. Kortright K.E., Chan B.K., Koff J.L., Turner P.E. Phage Therapy: A Renewed Approach to Combat Antibiotic-Resistant Bacteria. *Cell Host Microbe*, 2019, vol. 25 (2), pp. 219-232. doi: 10.1016/j.chom.2019.01.014.
12. Tabaldyev A.T. Modern methods of treatment of purulent wounds and their effectiveness. *Bulletin of science and practice*, 2022, vol. 8(12), pp. 311-319.
13. Chepuray Yu.L., Melkonyan G.G., Gulmuradova N.T., Sorokin A.A. Improving the results of treatment of patients with purulent diseases of the fingers and hand using laser radiation and photodynamic therapy. *Laser medicine*, 2021, vol. 25(2), pp. 28-40.
14. Topchiev M.A., Parshin D.S., Pyankov Yu.P., Topchiev A.M., Chukhnina Yu.G. Oxygenated drugs and exogenous nitric oxide in the complex treatment of purulent-necrotic lesions of diabetic foot syndrome. *Tavrchesky medico-biological Bulletin*, 2018, vol. 21(1), pp.148-152.
15. Chasnoyt A.Ch., Zhilinsky E.V., Serebryakov A.E., Leshchenko V.T. Mechanisms of action of vacuum therapy of the Russian Academy of Sciences. *Medical news*, 2015, vol.7, pp. 12-16.
16. Wang D., Kuzma M.L., Tan X., He T.C., Dong C. et al. Phototherapy and optical waveguides for the treatment of infection. *Adv Drug Deliv Rev*, 2021, vol. 179, pp. 114036. doi: 10.1016/j.addr.2021.114036.
17. Dai T., Huang Y.Y., Hamblin M.R. Photodynamic therapy for localized infections--state of the art. *Photodiagnosis Photodyn Ther*, 2009, vol. 6(3-4), pp. 170-88. doi: 10.1016/j.pdpdt.2009.10.008.
18. Cesar G.B., Winyk A.P., Sluchensci Dos Santos F., Queiroz E.F. et al. Treatment of chronic wounds with methylene blue photodynamic therapy: A case report. *Photodiagnosis Photodyn Ther*, 2022, vol. 39, pp. 103016. doi: 10.1016/j.pdpdt.2022.103016.
19. Permatasari P.A., Astuti S.D., Yaqubi A.K., Paisei E.A., Pujiyanto, Anuar N. Effectiveness of katuk leaf chlorophyll (Sauropus androgynus (L Merr) with blue and red laser a ctivation to reduce Aggregatibacter actinomycetemcomitans and Enterococcus faecalis biofilm. *Biomedical Photonics*, 2023, vol. 12(1), pp. 14-21. doi. org//10.24931/2413-9432-2023-12-1-14-21
20. Semyonov D.Yu., Vasil'ev Yu.L., Dydykin S.S., Stranadko E.F., Shubin V.K., Bogomazov Yu.K., Morokhotov V.A., Shcherbyuk A.N., Morozov S.V., Zakharov Yu.I. Antimicrobial and antimycotic photodynamic therapy (review of literature). *Biomedical Photonics*, 2021, vol. 10(1), pp. 25-31. doi.org/10.24931/2413-9432-2021-10-1-25-31
21. Yin R., Dai T., Avci P., Jorge A.E., de Melo W.C. et al. Light based anti-infectives: ultraviolet C irradiation, photodynamic therapy, blue light, and beyond. *Curr Opin Pharmacol*, 2013, vol. 13(5), pp.731-62. doi: 10.1016/j.coph.2013.08.009.
22. Song C, Wen R, Zhou J, Zeng X, Kou Z. et al. UV C Light from a Light-Emitting Diode at 275 Nanometers Shortens Wound Healing Time in Bacterium- and Fungus-Infected Skin in Mice. *Microbiol Spectr*, 2022, vol. 10 (6), pp. e0342422. doi: 10.1128/spectrum.03424-22.
23. Panzures A. 222-nm UVC light as a skin-safe solution to antimicrobial resistance in acute hospital settings with a particular focus on methicillin-resistant *Staphylococcus aureus* and surgical site infections: a review. *J Appl Microbiol*, 2023, vol. 134(3), pp. lxad046. doi: 10.1093/jambio/lxad046. PMID: 36869801.
24. Arkhipov V.P., Bagrov V.V., Byalovsky Yu.Yu., Kamrukov A.S., Kuspanalieva D.S., etc. Organization of preclinical studies of the bactericidal and wound healing effects of the pulsed phototherapy apparatus "Zarya". *Problems of social hygiene, healthcare and the history of medicine*, 2021, vol.2(5), pp. 1156-1162. doi 10.32687/0869-866X-2021-29-5-1156-1162.
25. Bagrov V.V., Bukhtiyarov I.V., Volodin L.Yu., etc. A high-intensity optical irradiation device for the treatment of wounds and wound infection. *Medical equipment*, 2023, vol. 2(338), pp. 1-4.
26. Bagrov V.V., Bukhtiyarov I.V., Volodin L.Y., Zibarev E.V., Kamrukov A.S. et al. Preclinical Studies of the Antimicrobial and Wound-Healing Effects of the High-Intensity Optical Irradiation "Zarnitsa-A" Apparatus. *Applied Sciences*. 2023. vol. 13(19), pp. 10794. https://doi.org/10.3390/app131910794
- wound and skin infections // *Pan Afr Med J*. – 2017. – Vol. 27. – P. 66. doi: 10.11604/pamj.2017.27.66.10226.
9. Park S.C., Nam J.P., Kim J.H., Kim Y.M., Nah J.W., Jang M.K. Antimicrobial action of water-soluble β -chitosan against clinical multi-drug resistant bacteria // *Int J Mol Sci*. – 2015. – Vol. 16(4). – P. 7995-8007. doi: 10.3390/ijms16047995.
10. Sanyasi S., Majhi R.K., Kumar S., Mishra M., Ghosh A., et al. Polysaccharide-capped silver Nanoparticles inhibit biofilm formation and eliminate multi-drug-resistant bacteria by disrupting bacterial cytoskeleton with reduced cytotoxicity towards mammalian cells // *Sci Rep*. – 2016. – Vol. 6. – P. 24929. doi: 10.1038/srep24929.
11. Kortright K.E., Chan B.K., Koff J.L., Turner P.E. Phage Therapy: A Renewed Approach to Combat Antibiotic-Resistant Bacteria // *Cell Host Microbe*. – 2019. – Vol. 25 (2). – P. 219-232. doi: 10.1016/j.chom.2019.01.014.
12. Табалдыев А.Т. Современные методы лечения гнойных ран и их эффективность // Бюллетень науки и практики. – 2022. – Т.8, №12. – С. 311-319.
13. Чепурная Ю.Л., Мелконян Г.Г., Гульмурадова Н.Т., Сорокин А.А. Улучшение результатов лечения пациентов с гнойными заболеваниями пальцев и кисти при использовании лазерного излучения и фотодинамической терапии // Лазерная медицина. – 2021. – Т.25, №2. – С. 28-40.
14. Топчиев М.А., Паршин Д.С., Пьянков Ю.П., Топчиев А.М., Чухнина Ю.Г. Оксигенированные лекарственные препараты и экзогенный оксид азота в комплексном лечении гнойно-некротических поражений синдрома диабетической стопы // Таврический медико-биологический вестник. – 2018. – Т.21, №1. – С.148-152.
15. Часнойть А.Ч., Жилинский Е.В., Серебряков А.Е., Лещенко В.Т. Механизмы действия вакуумной терапии ран // Медицинские новости. – 2015. – №7. – С. 12-16.
16. Wang D., Kuzma M.L., Tan X., He T.C., Dong C. et al. Phototherapy and optical waveguides for the treatment of infection // *Adv Drug Deliv Rev*. – 2021. – Vol. 179. – P. 114036. doi: 10.1016/j.addr.2021.114036.
17. Dai T., Huang Y.Y., Hamblin M.R. Photodynamic therapy for localized infections--state of the art // *Photodiagnosis Photodyn Ther*. – 2009. – Vol. 6(3-4). – P. 170-88. doi: 10.1016/j.pdpdt.2009.10.008.
18. Cesar G.B., Winyk A.P., Sluchensci Dos Santos F., Queiroz E.F. et al. Treatment of chronic wounds with methylene blue photodynamic therapy: A case report // *Photodiagnosis Photodyn Ther*. – 2022. – Vol. 39. – P. 103016. doi: 10.1016/j.pdpdt.2022.103016. Epub 2022 Jul 14.
19. Permatasari P.A., Astuti S.D., Yaqubi A.K., Paisei E.A., Pujiyanto, Anuar N. Effectiveness of katuk leaf chlorophyll (Sauropus androgynus (L Merr) with blue and red laser a ctivation to reduce Aggregatibacter actinomycetemcomitans and Enterococcus faecalis biofilm // *Biomedical Photonics*. – 2023. – Vol. 12(1). – P. 14-21. doi. org//10.24931/2413-9432-2023-12-1-14-21
20. Semyonov D.Yu., Vasil'ev Yu.L., Dydykin S.S., Stranadko E.F., Shubin V.K., Bogomazov Yu.K., Morokhotov V.A., Shcherbyuk A.N., Morozov S.V., Zakharov Yu.I. Antimicrobial and antimycotic photodynamic therapy (review of literature) // *Biomedical Photonics*. – 2021. – Vol. 10(1). – P. 25-31. doi.org/10.24931/2413-9432-2021-10-1-25-31
21. Yin R., Dai T., Avci P., Jorge A.E., de Melo W.C. et al. Light based anti-infectives: ultraviolet C irradiation, photodynamic therapy, blue light, and beyond // *Curr Opin Pharmacol*. – 2013. – Vol. – 13(5). – P. 731-62. doi: 10.1016/j.coph.2013.08.009.
22. Song C, Wen R, Zhou J, Zeng X, Kou Z. et al. UV C Light from a Light-Emitting Diode at 275 Nanometers Shortens Wound Healing Time in Bacterium- and Fungus-Infected Skin in Mice // *Microbiol Spectr*. – 2022. – Vol. 10 (6). – P. e0342422. doi: 10.1128/spectrum.03424-22.
23. Panzures A. 222-nm UVC light as a skin-safe solution to antimicrobial resistance in acute hospital settings with a particular focus on methicillin-resistant *Staphylococcus aureus* and surgical site infections: a review // *J Appl Microbiol*. – 2023. – Vol. 134 (3). – P. lxad046. doi: 10.1093/jambio/lxad046. PMID: 36869801.
24. Архипов В.П., Багров В.В., Бяловский Ю.Ю., Камруков А.С., Куспаналиева Д.С. и др. Организация доклинических исследований бактерицидного и ранозаживляющего действия импульсного фототерапевтического аппарата «Заря» // Проблемы социальной гигиены, здравоохранения и истории медицины. – 2021. – Т.29, №5. – С. 1156-1162. doi 10.32687/0869-866X-2021-29-5-1156-1162.
25. Багров В.В., Бухтияров И.В., Володин Л.Ю. и др. Аппарат высокоинтенсивного оптического облучения для терапии ран и раневой инфекции // Медицинская техника. – 2023. – № 2(338). – С. 1-4.
26. Bagrov V.V., Bukhtiyarov I.V., Volodin L.Y., Zibarev E.V., Kamrukov A.S. et al. Preclinical Studies of the Antimicrobial and Wound-Healing Effects of the High-Intensity Optical Irradiation "Zarnitsa-A" Apparatus // *Applied Sciences*. – 2023. – Vol. 13(19). – P. 10794. doi. org/10.3390/app131910794

EFFECTIVENESS OF PALLIATIVE PHOTODYNAMIC THERAPY FOR UNRESECTABLE BILIARY CANCER. SYSTEMATIC REVIEW AND META-ANALYSIS

Tseimakh A.E.¹, Mitshenko A.N.², Kurtukov V.A.², Shoikhet Ia.N.¹, Kuleshova I.V.¹

¹Altai State Medical University, Barnaul, Russia

²State hospital №5, Barnaul, Russia

Abstract

A systematic review and meta-analysis was aimed to assess the effectiveness of palliative photodynamic therapy for unresectable malignant tumors of the biliary system in order to justify the feasibility of including photodynamic therapy (PDT) in the complex treatment of this category of patients. Publications in the databases PubMed Central, the bibliographic database of scientific citations of the RSCI, and the Cochrane library were considered. Heterogeneity was assessed graphically using forest plots and statistically using τ^2 and I^2 statistics. A meta-analysis of 5-year survival revealed a statistically significantly longer pooled estimate of the survival period in groups where PDT was used – 339 ± 161 days (95% CI 25-710; $p < 0.001$) compared to groups where PDT was not used – 83 ± 16 days (95% CI 33-100; $p < 0.001$). Heterogeneity among studies was found to be statistically insignificant ($I^2 = 29\%$, $p = 0.23$). A meta-analysis of the risk difference for adverse events revealed a statistically significantly lower risk (-0.2306 ; 95% CI -0.3917 – 0.0696 ; $p = 0.005$) of adverse events after PDT compared with the comparison group. Heterogeneity among studies was found to be statistically insignificant ($I^2 = 0\%$, $p = 0.35$). There were no significant publication biases in either meta-analysis. The presented meta-analysis demonstrated that PDT may be the method of choice in the palliative complex treatment of patients with unresectable cholangiocarcinomas, increasing the five-year survival of patients along with the absence of increased risks of postoperative complications in comparison with other methods of palliative surgical treatment.

Key words: cholangiocarcinoma, photodynamic therapy, meta-analysis.

Contacts: Tseimakh A.E., e-mail: alevtsei@rambler.ru

For citations: Tseimakh A.E., Mitshenko A.N., Kurtukov V.A., Shoikhet Ia.N., Kuleshova I.V. Effectiveness of palliative photodynamic therapy for unresectable biliary cancer. Systematic review and meta-analysis, *Biomedical Photonics*, 2024, vol. 13, no. 2, pp. 34–42. doi: 10.24931/2413–9432–2024–13–2–34–42.

ЭФФЕКТИВНОСТЬ ПАЛЛИАТИВНОЙ ФОТОДИНАМИЧЕСКОЙ ТЕРАПИИ У ПАЦИЕНТОВ С НЕРЕЗЕКТАБЕЛЬНЫМИ ЗЛОКАЧЕСТВЕННЫМИ НОВООБРАЗОВАНИЯМИ ЖЕЛЧЕВЫВОДЯЩЕЙ СИСТЕМЫ. СИСТЕМАТИЧЕСКИЙ ОБЗОР И МЕТААНАЛИЗ

А.Е. Цеймах¹, А.Н. Мищенко², В.А. Куртуков², Я.Н. Шойхет¹, И.В. Кулешова¹

¹Алтайский государственный медицинский университет, Барнаул, Россия

²Городская больница №5, Барнаул, Россия

Резюме

Систематический обзор и метаанализ направлены на оценку эффективности паллиативной фотодинамической терапии (ФДТ) у пациентов с нерезектабельными злокачественными новообразованиями желчевыводящей системы с целью обоснования целесообразности включения ФДТ в комплексное лечение данной категории пациентов. Рассмотрены публикации в базах PubMed Central, библиографической базе данных научного цитирования РИНЦ, библиотеке Cochrane. Гетерогенность оценивали графически, используя лесные диаграммы, и статистически, используя статистику τ^2 и I^2 . Метаанализ пятилетней выживаемости выявил статистически значимо большую общую выживаемость при объединенной оценке в группах, где применяли ФДТ – 339 ± 161 дней (95% ДИ 25-710; $p < 0,001$) по сравнению с группами, где ФДТ не применяли – 83 ± 16 дней (95% ДИ 33-100; $p < 0,001$). Гетерогенность исследований была признана статистически незначимой ($I^2 = 29\%$, $p = 0,23$). Метаанализ разницы рисков нежелательных явлений выявил статисти-

чески значимо меньший риск (-0,2306; 95% ДИ -0,3917-0,0696; $p = 0,005$) нежелательных явлений после ФДТ по сравнению с группой сравнения. Гетерогенность исследований была признана статистически незначимой ($I^2 = 0\%$, $p = 0,35$). Значимых публикационных ошибок и предвзятости в обоих метаанализах выявлено не было. Представленный метаанализ продемонстрировал, что ФДТ может быть методом выбора при паллиативном комплексном лечении пациентов с нерезектабельными злокачественными новообразованиями желчевыводящих протоков, увеличивающим пятилетнюю выживаемость пациентов наряду с отсутствием повышенных рисков послеоперационных осложнений в сравнении с другими методами паллиативного хирургического лечения.

Ключевые слова: злокачественные новообразования желчевыводящей системы, фотодинамическая терапия, метаанализ.

Контакты: Цеймах А.Е., e-mail: alevtsei@rambler.ru

Для цитирования: Цеймах А.Е., Мищенко А.Н., Куртуков В.А., Шойхет Я.Н., Кулешова И.В. Эффективность паллиативной фотодинамической терапии нерезектабельных злокачественных новообразований желчевыводящей системы. Систематический обзор и мета-анализ // Biomedical Photonics. – 2024. – Т. 13, № 2. – С. 34–42. doi: 10.24931/2413–9432–2024–13–2–34–42.

Introduction

Biliary tract cancer is a rare oncological pathology, which includes distal and proximal cholangiocarcinoma and gallbladder cancer [1, 2, 3]. The structure of incidence and mortality in biliary cancer is assessed together with hepatocellular cancer [1]. Being one of the rarest oncological pathologies, assessed together with hepatocellular cancer with a prevalence of only 6.7 cases per 100 thousand population, malignant neoplasms of the bile ducts have one of the highest overall mortality (35.2%) and mortality in the first year from the date of diagnosis (66.8%) [1, 2, 3, 4, 5].

Despite the development of radiation and chemotherapy methods, surgery remains the main method of treating biliary cancer. However, at the time of diagnosis, 57.3% of patients already have advanced stage IV of the underlying disease, and 80.3% of patients have an advanced or locally advanced process [1, 2]. Thus, more than 80% of patients can only undergo palliative treatment, the main component of which is the elimination of life-threatening complications of the underlying disease, such as obstructive jaundice and cholangitis [4, 5, 6].

One of the methods of palliative treatment that complements surgical treatment is photodynamic therapy (PDT). PDT is a method of treating malignant neoplasms, which involves irradiating the tumor with light of a certain wavelength, which causes molecules of a special substance, a photosensitizer, selectively accumulated in the tumor tissue, to an excited state in the presence of oxygen. The resulting active oxygen species cause tumor cells to die through apoptosis, necrosis, and autophagy. The first successful application of PDT in the palliative treatment of biliary tract cancer was a clinical example published by McCaughan et al. [7], which began the study of the effect of PDT on malignant neoplasms of the bile ducts. Conducted in 2015–2023 years studies of the effectiveness of PDT in biliary tract cancer have yielded encouraging results, indicating the promise of the PDT method in palliative treatment of this category of patients [8, 9, 10, 11, 12, 13]. The main advantages of PDT

include its safety and the absence of side effects compared to chemotherapeutic treatment methods in the presence of a therapeutic effect that exceeds the results of treatment without PDT.

This systematic review and meta-analysis are aimed at assessing the effectiveness of palliative PDT in patients with unresectable malignant neoplasms of the biliary system in order to substantiate the feasibility of including PDT in the complex treatment of this category of patients. To achieve the goal set during the preparation of the systematic review and meta-analysis, it was necessary to solve the following problems:

- 1) to evaluate the safety of PDT in palliative treatment of patients with unresectable malignant neoplasms of the biliary system;
- 2) to evaluate five-year survival after the use of palliative PDT in patients with unresectable malignant neoplasms of the biliary system.

Materials and Methods

The systematic review was conducted in accordance with the Preferred Reporting Items for Systematic reviews and Meta-Analyses (PRISMA) guidelines [15]. For inclusion in the systematic review, we reviewed open-source publications in Russian and English in the PubMed Central database (Internet address: <https://www.ncbi.nlm.nih.gov/pmc/>), the bibliographic database of scientific citations RSCI (Internet resource: e-library.ru), and the Cochrane Library (Internet address: <https://www.cochranelibrary.com/>). The search for articles in these databases was conducted using the following keywords: photodynamic therapy, cholangiocarcinoma. The search strategy included identifying full-text articles presenting the materials and results of clinical studies. The titles, abstracts, and full texts of potentially eligible articles were independently reviewed by two researchers. Disagreements were resolved by a third investigator.

At the identification stage, 422 published full-text articles published between March 1998 and January 2024 were selected (Fig. 1). At the screening stage, 395

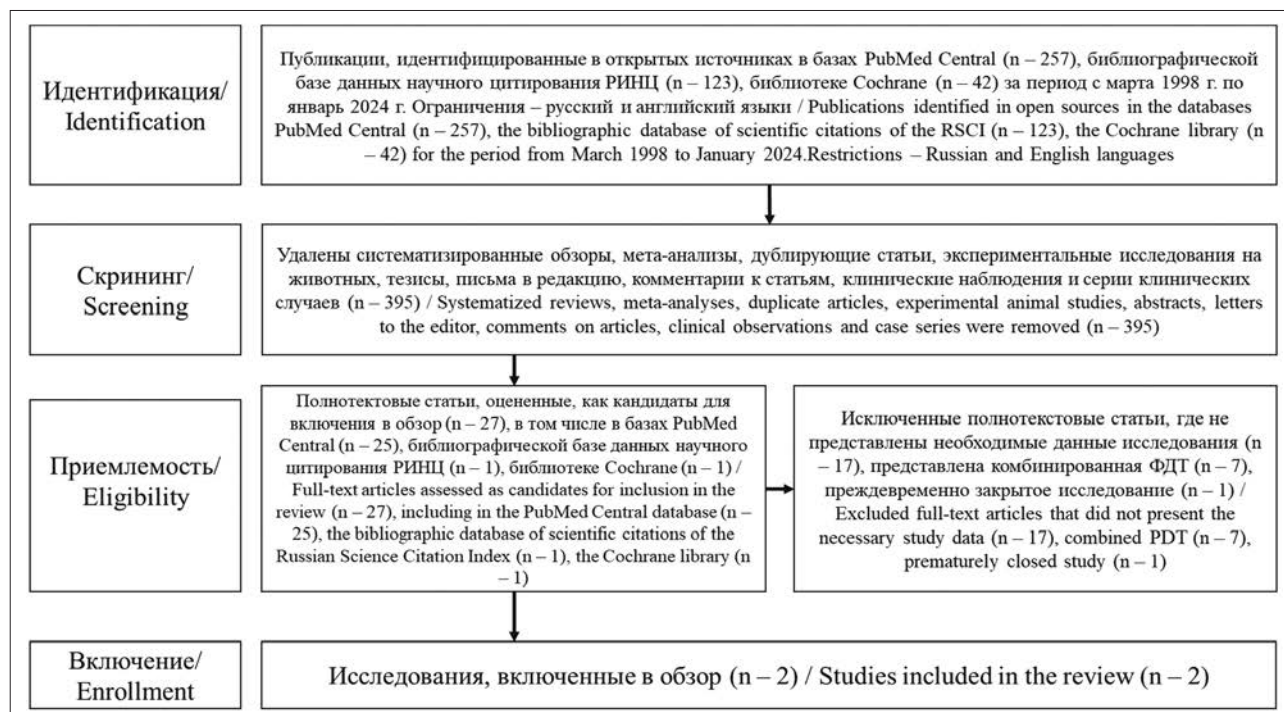


Рис. 1. Схема проведения систематического обзора и метаанализа в соответствии с рекомендациями PRISMA [15].
Fig. 1. Scheme for conducting a systematic review and meta-analysis according to PRISMA guidelines [15].

publications were excluded: systematic reviews, meta-analyses, duplicate articles, experimental animal studies, abstracts, letters to the editor, comments on articles, clinical observations and clinical case series were removed. As a result of multi-stage selection, 27 scientific publications were included.

Published studies that met the following inclusion criteria were considered eligible:

- 1) the study assessed the efficacy of PDT in the palliative treatment of unresectable cholangiocarcinoma in the adjuvant setting. Studies of PDT in the neoadjuvant setting or in patients with resectable cholangiocarcinoma were excluded;
- 2) the study assessed the efficacy of PDT monotherapy. Studies of the combined effects of PDT and other modalities such as chemotherapy and radiotherapy without PDT monotherapy were excluded;
- 3) the study provided sufficient data to assess 5-year survival, analyze adverse events according to the meta-analysis methodology, assess the risk of systematic errors, and describe all parameters of the PDT.

At the stage of assessing the eligibility criteria, 25 articles were excluded, including 17 publications due to missing data (recruitment to the studies was not completed, adverse events were not specified, five-year survival was not controlled, the full study design was not presented); 7 publications – in connection with the study of PDT in combination with chemotherapy and/or other radiation exposure; 1 study – due to premature closure of the study and the impossibility of correct calculation

of five-year survival. Thus, 2 scientific publications were analyzed in a systematic review and meta-analysis.

When assessing the methodological quality of the studies, an analysis of the design's compliance with the study objectives, an assessment of the correctness of the statistical analysis and its compliance with the study design, and an assessment of the risk of systematic errors in the study were performed. The risk of systematic errors (bias of results) in randomized studies was assessed using the adapted and validated Russian version of the Cochrane Collaboration questionnaire [16]. The risk of systematic errors in non-randomized comparative case-control studies was analyzed using the corresponding Newcastle-Ottawa questionnaires [17].

Statistical analysis was performed using the Sigma Plot software package, version 14.0 (Registration number 775400014), the meta-analysis was performed with the additional use of the Cochrane RevMan Web Version: 7.5.0 graphical editor. The proportions of individual studies with survival rates (in days) and adverse events were combined using the double arcsine transformation (Freeman-Tukey transformation). Heterogeneity was assessed graphically using forest plots and statistically using τ^2 and I^2 statistics.

A fixed effects model was used because heterogeneity was not statistically significant. The τ^2 statistic reflects the degree of variation in prevalence observed across studies. An I^2 of 0%–39% was considered statistically insignificant heterogeneity, 40–75% as moderate heterogeneity, and 76%–100% as significant hetero-

geneity among the compared studies. A p-value ≥ 0.05 was taken to reject the null hypothesis that the studies are heterogeneous. Publication effect and selection bias in pooled estimates were tested using the Begg and Mazumdar test. Publication bias was assessed by constructing funnel plots. A p-value < 0.05 was taken to be statistically significant to support the null hypothesis.

Results

All studies that met the selection criteria were comparative prospective. Of the two studies included in the systematic review and meta-analysis, one was randomized and one was a cohort non-randomized study. When assessing the risk of systematic errors, all studies were characterized by high methodological quality (Table 1). All studies were characterized by adequate methods of statistical processing of research

results in accordance with the objectives and design of their implementation.

The characteristics of PDT methods in the studies included in the systematic review and meta-analysis are presented in Table 2.

In the study by Tseimakh A.E. *et al.* (2023), the efficacy of intraluminal local and systemic PDT in patients with unresectable malignant neoplasms of the biliary tract was studied. The main group included 5 patients with stage III and 5 patients with stage IV according to the TNM classification. Of these, 5 patients had proximal cholangiocarcinoma: 2 patients – of type II, 2 patients – of type IIIa/IIIb, and 1 patient – of type IV according to the Bismuth-Corlette classification. The comparison group included 14 patients with stage III and 6 patients with stage IV according to the TNM classification. Of these, 6 patients had proximal cholangiocarcinoma: 1 patient –

Таблица 1
Оценка риска систематических ошибок в исследованиях эффективности исследований эффективности ФДТ
нерезектабельных злокачественных новообразований желчевыводящей системы

Table 1
Assessing the risk of bias in efficacy studies of PDT efficacy studies of unresectable biliary tumors

Критерий риска систематической ошибки (оценка в баллах) в когортных нерандомизированных исследованиях [17] / Risk of bias criterion (score) in non-randomized cohort studies [17]	Цеймах А.Е. и др. (2023) / Tseimakh A.E. and others (2023)	Критерий риска систематической ошибки (оценка в баллах) в рандомизированных исследованиях [16] / Risk of bias criterion (score) in randomized trials [16]	Ortner M.E.J. et al. (2003)
Является ли экспонированная когорта репрезентативной? / Is the exposed cohort representative?	1	Метод рандомизации (систематическая ошибка распределения пациентов по группам) / Randomization method (systematic error in the distribution of patients into groups)	Низкий риск / Low risk
Каким образом была сформирована неэкспонированная когорта? / How was the unexposed cohort formed?	1	Соккрытие рандомизационной последовательности (систематическая ошибка распределения пациентов по группам) / Concealment of the randomization sequence (systematic error in the allocation of patients to groups)	Низкий риск / Low risk
Каким образом был установлен факт воздействия изучаемого фактора? / How was the fact of the influence of the studied factor established?	1	«Ослепление» пациентов и медперсонала (маскирование/сокрытие вмешательства от пациентов и медперсонала) в процессе лечения (систематическая ошибка исполнения; может оцениваться отдельно от каждого исхода) / Blinding of patients and staff (masking/concealing the intervention from patients and staff) during treatment (performance bias; may be assessed separately for each outcome)	Низкий риск / Low risk
Было ли подтверждено отсутствие интересующего исхода в начале исследования? / Was the absence of the outcome of interest confirmed at baseline?	1		
Являются ли сравниваемые когорты сопоставимыми? / Are the comparing cohorts comparable?	1	Пропуски в данных об исходах (систематическая ошибка пропуска данных; может оцениваться отдельно для каждого исхода) / Missing outcome data (missing data bias; may be assessed separately for each outcome)	Низкий риск / Low risk
Какой источник информации об исходах использовался? / What source of outcome information was used?	1	Представление результатов исследования (систематическая ошибка представления результатов исследования) / Presentation of research results (systematic error in the presentation of research results)	Низкий риск / Low risk

Была ли продолжительность наблюдения достаточной для возникновения интересующих исходов? / Was the duration of follow-up sufficient for the outcomes of interest to occur?	1	Другие возможные источники систематических ошибок / Other possible sources of systematic errors	Низкий риск / Low risk
Каково было выбывание пациентов? / What was the patient attrition rate?	1	Дополнительный источник систематических ошибок: конфликт интересов / Additional source of bias: conflict of interest	Неопределенный риск / Uncertain risk
Общая оценка методологического качества / Overall assessment of methodological quality	Высокое / High	Общая оценка методологического качества / Overall assessment of methodological quality	Высокое / High
Высокое методологическое качество – 8-9 баллов / High methodological quality – 8-9 points	Высокое методологическое качество, при низком риске всех ошибок или неопределенном риске одной систематической ошибки / High methodological quality, with low risk of all biases or uncertain risk of one bias		
Удовлетворительное методологическое качество – 6-7 баллов / Satisfactory methodological quality – 6-7 points	Удовлетворительное методологическое качество, при неопределенном риске двух и более систематических ошибок / Satisfactory methodological quality, with an uncertain risk of two or more systematic errors		
Низкое методологическое качество – 0-5 баллов / Low methodological quality – 0-5 points	Низкое методологическое качество, при высоком риске одной и более систематической ошибки / Low methodological quality, with a high risk of one or more systematic errors		

Таблица 2

Характеристика исследований эффективности ФДТ нерезектабельных злокачественных новообразований желчевыводящей системы, включенных в систематический обзор и метаанализ

Table 2

Characteristics of studies on the effectiveness of PDT for unresectable malignant tumors of the biliary system included in the systematic review and meta-analysis

Исследование/Дизайн/ Study/Design	Доза фотосенсибилизатора и техника ФДТ/ Photosensitizers dose and PDT technique	Выживаемость основной группы/группы сравнения и нежелательные явления основной группы/группы сравнения/ Survival of main/comparison group and adverse events of main/comparison group
1. Цеймах А.Е. и др. (2023) [18] / Открытое нерандомизированное сравнительное / 1. Tseimakh A.E. et al. (2023) [18] / Open non-randomized comparative	Фотодитазин 1-1,4 мг/кг за 5 ч до экспозиции с длиной волны 662 нм с экспозиционной дозой света 220 Дж/см ² , плотностью мощности излучения 0,22 Вт/см ² / Photoditazine 1-1.4 mg/kg 5 hours before exposure to a wavelength of 662 nm with an exposure light dose of 220 J/cm ² , radiation power density 0.22 W/cm ²	170±100 (95% ДИ/CI 25-365)/ 66±17 (95% ДИ/CI 33-99) p < 0,05 1/3
2. Ortnier M.E.J. et al. (2003) [19] / Открытое рандомизированное сравнительное / 2. Ortnier M.E.J. et al. (2003) [19] / Open randomized comparative	Фотофрин 2 мг/кг за 48 ч до экспозиции с длиной волны 630 нм с экспозиционной дозой света 180 Дж/см ² , плотностью мощности излучения 0,24 Вт/см ² / Photofrin 2 mg/kg 48 hours before exposure to a wavelength of 630 nm with an exposure light dose of 180 J/cm ² , radiation power density 0.24 W/cm ²	493±217 (95% ДИ/CI 276-710)/ 98±15 днями (95% ДИ/CI 83-100) p < 0,001 9/13 Серьезные нежелательные явления: 2 случая холангита, осложненного сепсисом. / Serious adverse events: 2 cases of cholangitis complicated by sepsis.

Примечание: p – статистическая значимость различий между основной группой и группой сравнения.
Note: p – statistical significance of differences between the main group and the comparison group.

of type II and 5 patients – of type IIIa/IIIb according to the Bismuth-Corlette classification. A statistically significant increase in survival was found in patients who received PDT with a median overall survival of 170±100 days (95% CI 25-365; p < 0.05) compared to the comparison group

that did not receive PDT with a median overall survival of 66±17 days (95% CI 33-99; p < 0.05). No adverse events associated with PDT were identified [18]. One patient had acute posthemorrhagic anemia after percutaneous transhepatic monobar drainage of the bile ducts

for mechanical jaundice. In the comparison group, 2 patients had loss of percutaneous transhepatic drainage with the development of bile peritonitis; 1 patient had postoperative acute hemorrhagic anemia after percutaneous transhepatic monolobar drainage of the bile ducts for mechanical jaundice [18].

In the study by Ortner M.E.J. et al. (2003), 20 patients with unresectable malignant neoplasms of the bile ducts received intraluminal local and systemic monotherapy with PDT, 19 patients in the comparison group did not receive PDT. The main group included 4 patients with stage III and 16 patients with stage IV according to the TNM classification. Of these, 20 patients had proximal cholangiocarcinoma: 4 patients – of type IIIa/IIIb and 16 patients – of type IV according to the Bismuth-Corlette classification. The comparison group included 3 patients with stage III and 16 patients with stage IV according to the TNM classification. Of these, 19 patients had proximal cholangiocarcinoma: 2 patients – of type II, 2 patients – of type IIIa/IIIb, 15 patients – of type IV according to the Bismuth-Corlette classification. A statistically significant increase in overall survival was found in patients who received PDT, with a median overall survival of 493 ± 217 days (95% CI 276-710; $p < 0.05$) compared with 98 ± 15 days (95% CI 83-100; $p < 0.05$) with PDT monotherapy [19]. In the main group, there were 2 cases of photosensitivity reaction, 5 cases of cholangitis (including 2 chol-

angitis complicated by sepsis), and 2 cases of stenosis after PDT. In the comparison group, there were 13 cases of cholangitis.

A meta-analysis with fixed effects of the proportions of individual studies and a pooled estimate of overall survival after PDT monotherapy was performed (Fig. 2).

The meta-analysis revealed a statistically significantly higher overall survival in the pooled assessment in the main groups where PDT was used – 339 ± 161 days (95% CI 25-710; $p < 0.001$) compared to the comparison groups where PDT was not used – 83 ± 16 days (95% CI 33-100; $p < 0.001$). The heterogeneity of the studies was considered statistically insignificant ($I^2 = 29\%$, $p = 0.23$).

The probability of publication bias was assessed by visual analysis of the funnel plot (Fig. 3), where no visually significant asymmetry or disruption of the plot structure was detected, and the crossover point is in the area of no asymmetry ($p < 0.01$). The Begg and Mazumdar test also showed the absence of publication bias (Kendall's tau b -1.0000; $p = 0.3173$).

Then, a meta-analysis of the difference in the risks of adverse events in the compared groups was performed (Fig. 4), which revealed a statistically significantly lower risk (-0.2306; 95% CI -0.3917-0.0696; $p = 0.005$) of adverse events after PDT monotherapy compared to the comparison group. The heterogeneity of the studies was considered statistically insignificant ($I^2 = 0\%$, $p = 0.35$).

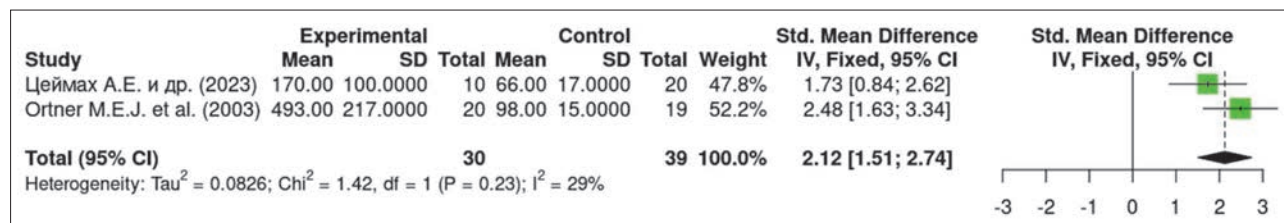


Рис. 2. Древовидная диаграмма с фиксированными эффектами, демонстрирующая анализ пропорций отдельных исследований и объединенную оценку общей выживаемости после монотерапии ФДТ.

Fig. 2. Forest plot of fixed effects demonstrating analysis of individual study proportions and pooled estimates of survival time following PDT monotherapy.

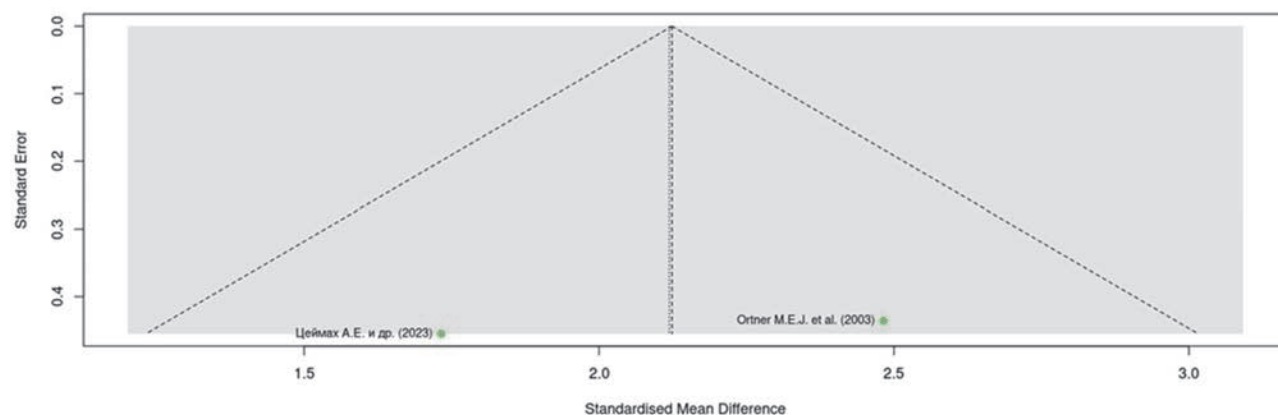


Рис. 3. Воронкообразный график для оценки вероятности наличия публикационной ошибки в объединенной оценке общей выживаемости после монотерапии ФДТ.

Fig. 3. Funnel plot to assess the likelihood of a publication error in pooled estimates of survival time following PDT monotherapy.

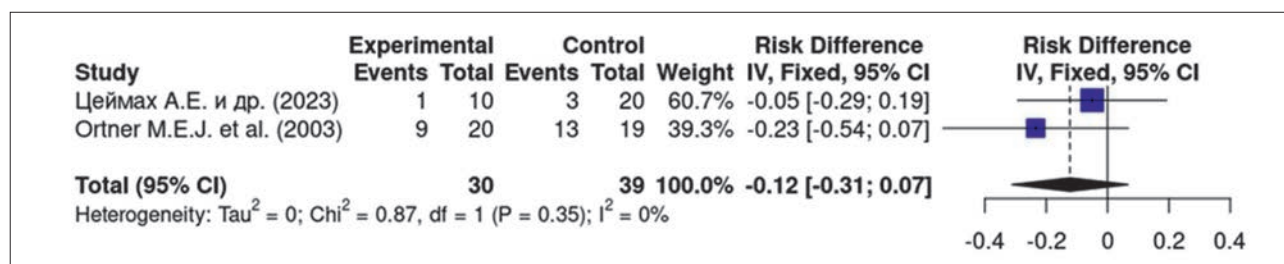


Рис. 4. Древоидная диаграмма с фиксированными эффектами, демонстрирующая анализ пропорций отдельных исследований и объединенного риска нежелательных явлений после монотерапии ФДТ.

Fig. 4. Forest plot of fixed effects demonstrating analysis of individual study proportions and pooled risk of adverse events after PDT monotherapy.

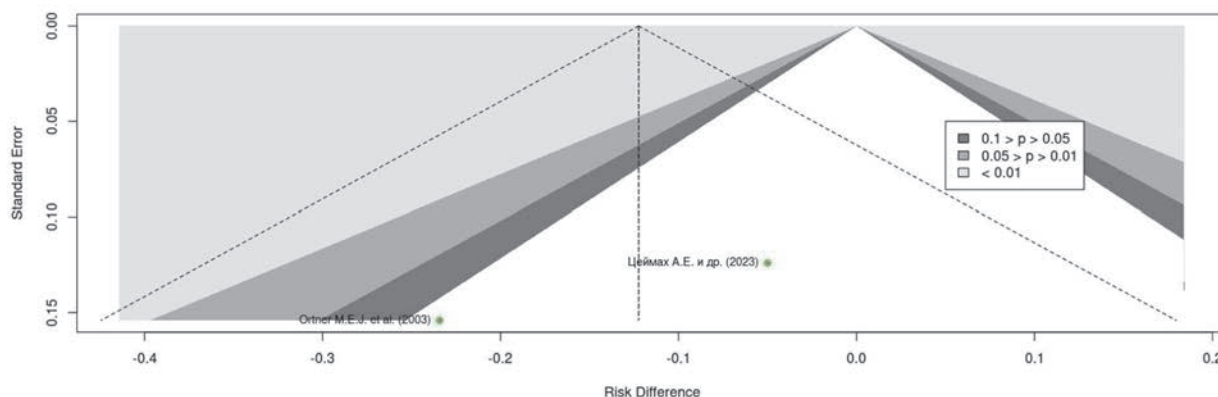


Рис. 5. Воронкообразный график для оценки вероятности наличия публикационной ошибки в объединенной оценке разницы рисков нежелательных явлений после монотерапии ФДТ.

Fig. 5. Funnel plot to assess the likelihood of a publication error in pooled estimates of risk difference of adverse events after PDT monotherapy.

The probability of the presence of a publication bias was assessed by visual analysis of the funnel plot (Fig. 5). No visually significant asymmetry or disruption of the graph structure was detected, and the crossover point is in the area of no asymmetry ($p < 0.01$). The Begg and Mazumdar test also showed the absence of a publication bias (Kendall's tau b – 1.0000; $p = 0.3173$).

Discussion

Cholangiocarcinoma is a rare malignant neoplasm characterized by one of the worst prognoses among tumors of the digestive system [1, 3-5, 22-24]. About 80% of cholangiocarcinoma cases are diagnosed at a late stage, when radical surgical treatment is impossible [1, 3-5, 22-24, 25-26]. Chemotherapy and radiation therapy without surgery do not contribute to a significant increase in overall survival of patients [1, 3-5, 22-24]. Effective palliative treatment by decompression of the bile ducts to eliminate the clinical picture of mechanical jaundice and prevent cholangitis and sepsis are the main goal of surgical treatment and are the final intervention for most patients [1, 3-5, 22]. PDT is a promising treatment method for unresectable cholangiocarcinoma. Patients with unresectable cholangiocarcinoma have a median overall survival of 3 months without intervention

and 4-10 months with bile duct decompression [1, 3-5, 22]. The presented systematic review and meta-analysis show that PDT can increase overall survival of patients with unresectable cholangiocarcinoma along with the absence of increased risks of adverse events compared with other methods of minimally invasive surgical treatment. A special role is played by targeted action on the tissue by performing choledochoscopy with intraluminal laser delivery to cholangiocarcinoma under visual control.

The aim of this meta-analysis was to evaluate the efficacy of palliative PDT for unresectable biliary tract malignancies. Survival meta-analysis revealed statistically significantly higher overall survival in the pooled assessment in the main groups where PDT was used – 332 ± 229 days (95% CI 25-710; $p < 0.001$) compared to the comparison groups where PDT was not used – 82 ± 23 days (95% CI 33-100; $p < 0.001$).

Meta-analysis of the difference in the risks of adverse events in the compared groups revealed a statistically significantly lower risk (-0.2306; 95% CI -0.3917-0.0696; $p = 0.005$) of adverse events after PDT monotherapy compared to the comparison group. The strength of the conducted meta-analysis is the high homogeneity and reliability of the obtained results, achieved by careful selec-

tion of studies with a homogeneous, clearly described design, study results and the same target access for local PDT – intraluminal under visual control.

Thus, the conducted meta-analysis allows to say with high statistical reliability that PDT is a promising and safe method of surgical intervention that can increase overall survival in patients with unresectable cholangiocarcinoma, and can be included in the complex treatment of this category of patients. The disadvantage of the conducted meta-analysis is the small number of patients in the study samples due to the rare occurrence of malignant neoplasms of the biliary system. Another weakness of the meta-analysis is the small number of studies included in the systematic review and meta-analysis. This is due to the fact that most published studies of the effectiveness of PDT evaluate PDT in combination with chemotherapy and/or radiation therapy.

At the same time, the synergy of PDT and chemotherapy, their possible antagonism associated with immunosuppression during chemotherapy treatment and the involvement of mechanisms of immune response stimulation in PDT have not been fully studied, and there is no consensus on PDT irradiation protocols in combination

with radiation therapy. All these factors led to the inclusion of combined PDT as an exclusion criterion in the systematic review and meta-analysis. Another weakness of the meta-analysis is the differences in the PDT technique, which are characteristic of all studies in this area. This is due to both different photosensitizers and different parameters of cholangiocarcinoma irradiation.

Thus, given the above shortcomings, in order to obtain more reliable results and improve the quality of subsequent meta-analyses, large randomized studies of the effectiveness of PDT in unresectable cholangiocarcinoma are required. At the same time, the conducted meta-analysis proves the promise of PDT in the treatment of this category of patients.

Conclusion

The conducted meta-analysis demonstrated that PDT can be a method of choice in palliative complex treatment of patients with unresectable malignant neoplasms of the bile ducts, increasing the five-year survival of patients along with the absence of increased risks of postoperative complications in comparison with other methods of palliative surgical treatment.

REFERENCES

1. The state of oncological care for the population of Russia in 2020 / edited by Kaprin A.D., Starinsky V.V., Petrova G.V. M.: Herzen Moscow State Medical Research Institute – branch of the Federal State Budgetary Institution «NMIRC» of the Ministry of Health of Russia, 2021, pp. 239.
2. Zhang X. et al. Comparison of current guidelines and consensus on the management of patients with cholangiocarcinoma: 2022 update. *Intractable Rare Dis Res*, 2022, vol. 11(4), pp. 161-172.
3. All-Russian National Union «Association of Oncologists of Russia». Cancer of the biliary system. *Clinical recommendations*, 2020, pp. 51.
4. Zerem E., Imširović B., Kunosić S. et al. Percutaneous biliary drainage for obstructive jaundice in patients with inoperable, malignant biliary obstruction. *Clin Exp Hepatol*, 2022, vol. 8(1), pp. 70-77.
5. Shah R., John S. Cholestatic Jaundice. In: StatPearls [Internet]. Treasure Island (FL): StatPearls Publishing, 2022, PMID: 29489239.
6. Tseimakh A.E., Lazarev A.F., Kurtukov V.A. and coauthors. A method of complex mini-invasive treatment of mechanical jaundice, cholangitis, intrahepatic abscesses of tumor genesis using local and systemic photodynamic therapy. Patent of the Russian Federation No.2704474, 2019.
7. McCaughan J.S. Jr., McCaughan J.S., Mertens B.F. et al. Photodynamic therapy to treat tumors of the extrahepatic biliary ducts. A case report. *Arch Surg*, 1991, vol. 126(1), pp. 111-113. doi: 10.1001/archsurg.1991.01410250119022.
8. Haider H., Chapman C.G., Siddiqui U.D. Maximizing survival in hilar cholangiocarcinoma patients using multi-modality therapy: photodynamic therapy (pdt) with stenting, chemotherapy, and radiation. *Gastrointestinal Endoscopy*, 2020, vol. 91(6), pp. 1-5. doi: 10.1016/j.gie.2020.03.2226
9. Lu Y et al. Efficacy and safety of photodynamic therapy for unresectable cholangiocarcinoma: A meta-analysis. *Clinics and research in hepatology and gastroenterology*, 2015, vol. 39(6), pp. 718-724. doi: 10.1016/j.clinre.2014.10.015.
10. Li Z. et al. Long-Term Results of ERCP- or PTCS-Directed Photodynamic Therapy for Unresectable Hilar Cholangiocarcinoma. *Surg Endosc*, 2021, vol. 35(10), pp. 5655-5664. doi: 10.1007/s00464-020-08095-1

ЛИТЕРАТУРА

1. Состояние онкологической помощи населению России в 2020 году / под ред. А. Д. Каприна, В. В. Старинского, Г. В. Петровой // М.: МНИОИ им. П.А. Герцена – филиал ФГБУ «НМИЦ» Минздрава России. – 2021. – С. 239.
2. Zhang X. et al. Comparison of current guidelines and consensus on the management of patients with cholangiocarcinoma: 2022 update // *Intractable Rare Dis Res*. – 2022. – Vol. 11(4). – P. 161-172.
3. Общероссийский национальный союз «Ассоциация онкологов России». Рак желчевыводящей системы // Клинические рекомендации. – 2020. – С. 51.
4. Zerem E., Imširović B., Kunosić S. et al. Percutaneous biliary drainage for obstructive jaundice in patients with inoperable, malignant biliary obstruction // *Clin Exp Hepatol*. – 2022. – Vol. 8(1). – P. 70-77.
5. Shah R., John S. Cholestatic Jaundice // In: StatPearls [Internet]. Treasure Island (FL): StatPearls Publishing. – 2022. – PMID: 29489239.
6. Цеймах А.Е., Лазарев А.Ф., Куртуков В.А. и соавт. Способ комплексного мини-инвазивного лечения механической желтухи, холангита, внутрипеченочных абсцессов опухолевого генеза с применением локальной и системной фотодинамической терапии. – Патент РФ №2704474. – 2019.
7. McCaughan J.S. Jr., McCaughan J.S., Mertens B.F. et al. Photodynamic therapy to treat tumors of the extrahepatic biliary ducts. A case report // *Arch Surg*. – 1991. – Vol. 126(1). – P. 111-113. doi: 10.1001/archsurg.1991.01410250119022.
8. Haider H., Chapman C.G., Siddiqui U.D. Maximizing survival in hilar cholangiocarcinoma patients using multi-modality therapy: photodynamic therapy (pdt) with stenting, chemotherapy, and radiation // *Gastrointestinal Endoscopy*. – 2020. – Vol. 91(6). – P. 1-5. doi: 10.1016/j.gie.2020.03.2226
9. Lu Y et al. Efficacy and safety of photodynamic therapy for unresectable cholangiocarcinoma: A meta-analysis // *Clinics and research in hepatology and gastroenterology*. – 2015. – Vol. 39(6). – P. 718-724. doi: 10.1016/j.clinre.2014.10.015.
10. Li Z. et al. Long-Term Results of ERCP- or PTCS-Directed Photodynamic Therapy for Unresectable Hilar Cholangiocarcinoma // *Surg Endosc*. – 2021. – Vol. 35(10). – P. 5655-5664. doi: 10.1007/s00464-020-08095-1

11. Moole H. et al. Success of Photodynamic Therapy in Palliating Patients With Nonresectable Cholangiocarcinoma: A Systematic Review and Meta-Analysis. *World J Gastroenterol*, 2017, vol. 23(7), pp. 1278-88. doi: 10.3748/wjg.v23.i7.1278
12. Pereira S.P. et al. PHOTOSTENT-02: Porfimer Sodium Photodynamic Therapy Plus Stenting Versus Stenting Alone in Patients With Locally Advanced or Metastatic Biliary Tract Cancer. *ESMO Open*, 2018, vol. 3(5), pp. e000379. doi: 10.1136/esmoopen-2018-000379
13. Maswikiti E.P., Chen H. Photodynamic therapy combined with systemic chemotherapy for unresectable extrahepatic cholangiocarcinoma: A systematic review and meta-analysis. *Photodiagnosis Photodyn Ther*, 2023, vol. 2 (41), pp. 103318. doi: 10.1016/j.pdpdt.2023.103318.
14. Tseimakh A.E., Mishchenko A.N., Kurtukov V.A., Shoikhet Ya.N. Palliative surgical treatment using photodynamic therapy in patients with malignant neoplasms of the biliary system complicated by obstructive jaundice. *Biomedical Photonics*, 2023, vol. 12 (2), pp. 4-10. doi: 10.24931/2413-9432-2023-12-2-4-10.
15. Moher D., Liberati A., Tetzlaff J. et al. PRISMA Group. Preferred reporting items for systematic reviews and meta-analyses: the PRISMA statement. *PLoS Med*, 2009, vol. 6(7), pp. e1000097. doi: 10.1371/journal.pmed.1000097.
16. Rebrova O.Yu., Fedyaeva V.K., Khachatryan G.R. Adaptation and validation of the questionnaire to assess the risk of systematic errors in randomized controlled trials. *Medical technologies. Assessment and selection*, 2015, vol. 19(1), pp. 9-17.
17. Rebrova O. Yu., Fedyaeva V. K. Questionnaire for assessing the risk of systematic errors in non-randomized comparative studies: the Russian version of the Newcastle-Ottawa scale. *Medical technologies. Assessment and selection*, 2016, vol. (3), pp. 14-19.
18. Tseimakh A.E., Mishchenko A.N., Kurtukov V.A., Shoikhet Ya.N. Palliative surgical treatment using photodynamic therapy in patients with malignant neoplasms of the biliary system complicated by obstructive jaundice. *Biomedical Photonics*, 2023, vol. 12(2), pp. 4-10. doi: 10.24931/2413-9432-2023-12-2-4-10.
19. Ortner M.E., Caca K., Berr F. et al. Successful photodynamic therapy for nonresectable cholangiocarcinoma: a randomized prospective study. *Gastroenterology*, 2003, vol.125(5), pp. 1355-1363. doi: 10.1016/j.gastro.2003.07.015.
20. Surya H., Abdullah M., Nelwan E.J., et al. Current Updates on Diagnosis and Management of Cholangiocarcinoma: from Surgery to Targeted Therapy. *Acta Med Indones*, 2023, vol. 55(3), pp. 361-370.
21. Peirce V., Paskow M., Qin L., et al. A Systematised Literature Review of Real-World Treatment Patterns and Outcomes in Unresectable Advanced or Metastatic Biliary Tract Cancer. *Target Oncol*, 2023, vol. 18(6), pp. 837-852.
22. Vogel A., Bridgewater J., Edeline J., Kelley R.K., Klumpen H.J., Malka D., et al. Biliary tract cancer: ESMO clinical practice guideline for diagnosis, treatment and follow-up. *Ann Oncol*, 2023, vol. 34(2), pp. 127-40.
23. Trifylli E.M., Kriebardis A.G., Koustas E., et al. The Arising Role of Extracellular Vesicles in Cholangiocarcinoma: A Rundown of the Current Knowledge Regarding Diagnostic and Therapeutic Approaches. *Int J Mol Sci*, 2023, vol. 24(21), pp. 15563.
24. Zhao D.Y., Lim K.H. Current biologics for treatment of biliary tract cancers. *J Gastrointest Oncol*, 2017, vol. 8(3), pp. 430-40.
25. Baria K., De Toni E.N., Yu B., Jiang Z., Kabadi S.M., Malvezzi M. Worldwide incidence and mortality of biliary tract cancer. *Gastro Hep Adv*, 2022, vol. 1(4), pp. 618-26.
26. Zamani Z., Fatima S. Biliary tract cancer. *Treasure Island: Stat-Pearls*, 2021.
11. Moole H. et al. Success of Photodynamic Therapy in Palliating Patients With Nonresectable Cholangiocarcinoma: A Systematic Review and Meta-Analysis // *World J Gastroenterol*. – 2017. – Vol. 23(7). – P. 1278-88. doi: 10.3748/wjg.v23.i7.1278
12. Pereira S.P. et al. PHOTOSTENT-02: Porfimer Sodium Photodynamic Therapy Plus Stenting Versus Stenting Alone in Patients With Locally Advanced or Metastatic Biliary Tract Cancer // *ESMO Open*. – 2018. – Vol. 3(5). – P. e000379. doi: 10.1136/esmoopen-2018-000379
13. Maswikiti E.P., Chen H. Photodynamic therapy combined with systemic chemotherapy for unresectable extrahepatic cholangiocarcinoma: A systematic review and meta-analysis // *Photodiagnosis Photodyn Ther*. – 2023. – Vol. 2 (41). – P. 103318. doi: 10.1016/j.pdpdt.2023.103318.
14. Цеймах А.Е., Мищенко А.Н., Куртуков В.А., Шойхет Я.Н. Паллиативное хирургическое лечение с применением фотодинамической терапии больных со злокачественными новообразованиями желчевыводящей системы, осложненными обструктивной желтухой // *Biomedical Photonics*. – 2023. – Т. 12, № 2. – С. 4-10. doi: 10.24931/2413-9432-2023-12-2-4-10.
15. Moher D., Liberati A., Tetzlaff J. et al. PRISMA Group. Preferred reporting items for systematic reviews and meta-analyses: the PRISMA statement // *PLoS Med*. – 2009. – Vol. 6(7). – P. e1000097. doi: 10.1371/journal.pmed.1000097.
16. Реброва О.Ю., Федяева В.К., Хачатрян Г.Р. Адаптация и валидизация вопросника для оценки риска систематических ошибок в рандомизированных контролируемых испытаниях // *Медицинские технологии. Оценка и выбор*. – 2015. – Т. 19, №1. – С. 9-17.
17. Реброва О. Ю., Федяева В. К. Вопросник для оценки риска систематических ошибок в нерандомизированных сравнительных исследованиях: русскоязычная версия шкалы Ньюкасл-Оттава. *Медицинские технологии. Оценка и выбор*. 2016. – Т. 25, № 3. – С. 14-19.
18. Цеймах А.Е., Мищенко А.Н., Куртуков В.А., Шойхет Я.Н. Паллиативное хирургическое лечение с применением фотодинамической терапии больных со злокачественными новообразованиями желчевыводящей системы, осложненными обструктивной желтухой // *Biomedical Photonics*. – 2023. – Т. 12, № 2. – С. 4-10. doi: 10.24931/2413-9432-2023-12-2-4-10.
19. Ortner M.E., Caca K., Berr F. et al. Successful photodynamic therapy for nonresectable cholangiocarcinoma: a randomized prospective study // *Gastroenterology*. – 2003. – Vol. 125(5). – P. 1355-1363. doi: 10.1016/j.gastro.2003.07.015.
20. Surya H., Abdullah M., Nelwan E.J., et al. Current Updates on Diagnosis and Management of Cholangiocarcinoma: from Surgery to Targeted Therapy // *Acta Med Indones*. – 2023. – Vol. 55(3). – P. 361-370.
21. Peirce V., Paskow M., Qin L., et al. A Systematised Literature Review of Real-World Treatment Patterns and Outcomes in Unresectable Advanced or Metastatic Biliary Tract Cancer // *Target Oncol*. – 2023. – Vol. 18(6). – P. 837-852.
22. Vogel A., Bridgewater J., Edeline J., Kelley R.K., Klumpen H.J., Malka D., et al. Biliary tract cancer: ESMO clinical practice guideline for diagnosis, treatment and follow-up // *Ann Oncol*. – 2023. – Vol. 34(2). – P. 127-40.
23. Trifylli E.M., Kriebardis A.G., Koustas E., et al. The Arising Role of Extracellular Vesicles in Cholangiocarcinoma: A Rundown of the Current Knowledge Regarding Diagnostic and Therapeutic Approaches // *Int J Mol Sci*. – 2023. – Vol. 24(21). – P. 15563.
24. Zhao D.Y., Lim K.H. Current biologics for treatment of biliary tract cancers // *J Gastrointest Oncol*. – 2017. – Vol. 8(3). – P. 430-40.
25. Baria K., De Toni E.N., Yu B., Jiang Z., Kabadi S.M., Malvezzi M. Worldwide incidence and mortality of biliary tract cancer. *Gastro Hep Adv*. – 2022. – Vol. 1(4). – P. 618-26.
26. Zamani Z., Fatima S. Biliary tract cancer // *Treasure Island: Stat-Pearls*. – 2021.

THE ROLE OF MEMBRANE TRANSPORT PROTEINS IN 5-ALK-INDUCED ACCUMULATION OF PROTOPORPHYRIN IX IN TUMOR CELLS

Ivanova-Radkevich V.I.¹, Kuznetsova O.M.¹, Filonenko E.V.²

¹Peoples' Friendship University of Russia (RUDN University), Moscow, Russia

²P.A. Herzen Moscow Oncology Research Center – branch of FSBI NMRRС of the Ministry of Health of the Russian Federation, Moscow, Russia

Abstract

Features of the expression of membrane importers of 5-ALA, as well as transporters involved in the removal of photoactive precursors of protoporphyrin IX (PPIX) (uro-, copro- and protoporphyrinogens), may cause differences in the effectiveness of photodynamic therapy of malignant neoplasms using 5-aminolevulinic acid (5-ALA). Increased expression of ALA transporters is associated with an increase in the intensity of PPIX synthesis. When the expression of PPIX exporters increases, there is a decrease in PPIX concentration. The review describes the main transporters of 5-ALA, uro-, copro- and protoporphyrinogens, provides data on their expression in various tissues, and discusses the possibility of predicting the effectiveness of photodynamic therapy considering the expression of the corresponding transport proteins in malignant tissues.

Key words: photodynamic therapy, 5-aminolevulinic acid, protoporphyrin IX, transmembrane transporters.

Contacts: Ivanova-Radkevich V.I., e-mail: ivanova-radkevich-vi@rudn.ru

For citations: Ivanova-Radkevich V.I., Kuznetsova O.M., Filonenko E.V. The role of membrane transport proteins in 5-ALA-induced accumulation of protoporphyrin IX in tumor cells, *Biomedical Photonics*, 2024, vol. 13, no. 2, pp. 43–48. doi: 10.24931/2413-9432-2024-13-2-43-48.

РОЛЬ МЕМБРАННЫХ ПЕРЕНОСЧИКОВ В НАКОПЛЕНИИ 5-АЛК-ИНДУЦИРОВАННОГО ПРОТОПОРФИРИНА IX В ОПУХОЛЕВЫХ КЛЕТКАХ

В.И. Иванова-Радкевич¹, О.М. Кузнецова¹, Е.В. Филоненко²

¹Российский Университет дружбы народов, Москва, Россия

²«Московский научно-исследовательский онкологический институт им. П.А. Герцена – филиал ФГБУ «Национальный медицинский исследовательский центр радиологии» Министерства здравоохранения Российской Федерации, Москва, Россия

Резюме

Одной из причин различий в эффективности фотодинамической терапии с применением 5-аминолевулиновой кислоты (5-АЛК) при различных типах злокачественных новообразований могут быть особенности экспрессии в этих тканях мембранных транспортеров, участвующих в переносе самой 5-АЛК в опухолевые и нормальные клетки, а также в выведении из клеток предшественников фотоактивного протопорфирина IX (ППИХ) – уро-, копро- и протопорфириногенов. Повышенная экспрессия первых связана с увеличением интенсивности синтеза ППИХ. При повышении экспрессии вторых наблюдается снижение скорости синтеза ППИХ. В настоящем обзоре описаны основные транспортеры 5-АЛК, уро-, копро- и протопорфириногенов, приведены данные об их экспрессии в различных тканях, обсуждены возможности прогнозирования эффективности фотодинамической терапии с учетом экспрессии указанных транспортеров в злокачественных тканях.

Ключевые слова: фотодинамическая терапия, 5-аминолевулиновая кислота, протопорфин IX, трансмембранные переносчики.

Контакты: Иванова-Радкевич В.И., e-mail: ivanova-radkevich-vi@rudn.ru

Для цитирования: Иванова-Радкевич В.И., Кузнецова О.М., Филоненко Е.В. Роль трансмембранных переносчиков в накоплении 5-АЛК-индуцированного протопорфирина IX в опухолевых клетках // *Biomedical Photonics*. – 2024. – Т. 13, № 2. – С. 43–48. doi: 10.24931/2413-9432-2024-13-2-43-48.

Introduction

Photodynamic therapy (PDT) is widely used in Russia and around the world for the treatment of tumor and other diseases [1,2,3,4,5]. Antitumor PDT is based on the selective accumulation of a photosensitizer in pathological tissue. When irradiated with light of a certain wavelength, the photosensitizer causes the formation of singlet oxygen and other cytotoxic compounds that damage the structural elements of tumor tissue [1,6]. A photosensitizer as part of a drug can be introduced into the patient's body, or it can be synthesized inside target cells from an exogenous precursor. Such precursors (pro-photosensitizers) include 5-aminolevulinic acid (5-ALA). 5-ALA is an endogenous non-photoactive compound, an intermediate metabolite of heme biosynthesis. 5-ALA enters tumor cells and is included in heme synthesis after administration into the patient's body. 5-ALA is quickly converted into heme and is used to build hemoproteins in normal cells. While in tumor cells the synthesis is inhibited at the last stage due to a deficiency of the enzyme ferrochelatase, which catalyzes the last reaction of heme synthesis. An intermediate product, photoactive protoporphyrin IX (PPIX) accumulates in the cell as a result [1,6].

The ability of exogenous 5-ALA to induce the synthesis of photoactive PPIX depends on the tissue type (in particular, how well the tissue is vascularized) and the cell type. One possible explanation for the different intensity of PPIX accumulation in different cells may be the difference in the rate of uptake of 5-ALA by cells and elimination of intermediate products of heme synthesis (uroporphyrinogens, coproporphyrinogens, protoporphyrinogens) by cells [7].

Exogenous 5-ALA can enter the cell by active transport through several transporters, including the peptide transporters PEPT1 and PEPT2, the amino acid transporter PAT1, as well as TauT and GAT2 [7]. The question arises: does increased expression of these transporters affect the uptake of 5-ALA by tumor cells compared to normal cells? Will this affect the intensity of PPIX accumulation? In addition, the role of transporters that remove intermediate metabolites of heme synthesis from cells cannot be neglected [7]. In our review, we would like to discuss the role of various transmembrane transporters in the accumulation of photoactive PPIX.

PEPT1 (SLC15A1)

The peptide transporter PEPT1 is most widely known as the transporter of dipeptides and tripeptides formed during the digestion of proteins through the apical membrane into enterocytes [8]. Theoretically, all chemical compounds that have sufficient steric similarity to dipeptides or tripeptides are potential substrates for PEPT1 [8]. As a result, PEPT1 may be involved in the transmembrane transport of many drugs. As a result, PEPT1 may be involved in the transmembrane transport of many drugs. 5-ALA does not have a peptide bond but is a high-affinity substrate for PEPT1/2 due to its ketomethylene group [8].

A direct transfer of 5-ALA across the membrane of *Xenopus laevis* oocytes and *Pichia pastoris* yeast cells expressing PEPT1 was demonstrated by Döring et al. in 1998 [9].

PEPT1 is thought to be the largest contributor to the transport of 5-ALA across the intestinal epithelium [10]. In 2016, studies on wild-type mice with the *Pept1* gene showed significant permeability of cells in the duodenum, jejunum and ileum to 5-ALA when taken orally. Moreover, in mice with *Pept1* knockout, the permeability of small intestinal cells was reduced by 10 times, and the peak concentration of 5-ALA in plasma was reduced by 2 times compared to wild-type animals [11]. The study authors noted that the transport of 5-ALA into small intestinal cells occurred without apparent contributions from other transporters, including proton-associated amino acid transporter 1 (PAT1). However, PEPT1 had a slight effect on the distribution of 5-ALA along the periphery tissue [11]. This may indicate that in peripheral tissues the contribution of other transporters to the supply of 5-ALA may be more significant.

Interestingly, in wild-type mice, the rate of 5-ALA membrane transport in the duodenum, jejunum and ileum was 9-14 times lower than in the colon, and this difference is consistent with the PEPT1 protein expression pattern observed in mice [11,12].

In addition to enterocytes, PEPT1 is also expressed in other tissues: the stomach, bladder, and extrahepatic bile ducts.

In 2003, 5-ALA was shown to enter cells in human cholangiocarcinoma SK-ChA-1 cells via the PEPT1 transporter [13]. Ten years later, Chung et al. confirmed the transmembrane transfer of 5-ALA with the participation of PEPT1 in cholangiocyte cell lines derived from bile duct carcinoma [14].

In studies on human gastric cancer cells KKLS, NKPS and TMK-1, the effectiveness of 5-ALA-induced PDT was also associated with high expression of PEPT1 and simultaneously low expression of the ATP-binding cassette transporter ABCG2 (involved in the clearance of PPIX through the membrane). The expression of these transporters together determines the efficient formation and accumulation of PPIX after exogenous administration of 5-ALA [15]. Similar results were obtained in a study of bladder tumor samples: the accumulation of PPIX was due to increased expression of PEPT1 and decreased expression of ABCG2 [10].

An interesting observation was made by Lai et al. [16]: while PEPT1 was highly expressed in normal lung cells WI38, PEPT1 was not expressed in non-small cell lung cancer cells A549.

PEPT2 (SLC15A2)

PEPT2 is widely expressed in the tissues, especially kidney, brain and lung [11]. PEPT2 has been shown to play a central role in the reabsorption of 5-ALA from the glomeru-

lar filtrate in human renal proximal tubular cells [17] and is also involved in the uptake of 5-ALA by astrocytes in newborn mice [18].

PAT1 (SLC36A1)

The amino acid transporter PAT1 is involved in the membrane transport of small neutral amino acids such as proline and γ -aminobutyric acid (GABA). In its chemical structure, 5-ALA is like GABA. This is the basis for the possibility of 5-ALA transport through the GABA membrane transporters [19]. Several experimental studies provide evidence for the involvement of PAT1 in 5-ALA transport. Thus, *Xenopus laevis* oocytes expressing PAT1 more actively absorb 5-ALA [20].

In a study by Lai et al. [16], as well as for PEPT1, showed a difference in the expression of PAT1 in normal and malignant cells originating from the same organ: expression was quite high in healthy prostate cells PrEC, while it was almost absent in prostate cancer cells DU145.

TauT (SLC6A6) and GAT2 (SLC6A13)

In addition to PAT1, GABA is also a substrate for the TauT and GAT2 transporters, raising questions about whether they are involved in the transmembrane transport of 5-ALA [7]. According to some data, both transporters are highly expressed in many human tissues, especially in brain and liver cells [21]. Studies by others show that the highest levels of GAT2 mRNA are found in the liver and kidneys, whereas levels in the cerebellum and cerebral cortex are low [22]. In addition, high levels of the transporters are found in the stomach and retina [23].

In their study, Tran et al. assessed 5-ALA-induced protoporphyrin accumulation in DLD-1 colon cancer cells, HeLa cells, and HEK293. PPIX was not synthesized in the absence of exogenous 5-ALA. The authors used GABA homologs to evaluate the efficiency of 5-ALA transfer. The inhibitory effect of GABA homologs on 5-ALA-induced PPIX accumulation in HeLa cells was less than that observed in DLD-1 cells. Knockdown of GAT2 in HeLa cells resulted in a slight decrease in PPIX levels, suggesting the presence of alternative transporters in these cells. Simultaneous knockdown of TauT and GAT2 in HeLa cells resulted in a significant decrease in PPIX levels, indicating an important role of TauT in 5-ALA transport in these cells [24]. The authors also note that HEK293 renal adenocarcinoma cells, when overexpressed with either TauT or GAT2, induced a significant increase in PPIX production. The results of the described experiments confirm the significant contribution of the TauT and GAT2 transporters to the penetration of 5-ALA into the cell [24,25].

Neoplastic cells exhibit an increased requirement for certain metabolites, including amino acids, and adapt to this requirement not only through increased expression of transporters, but also through the expression of isoforms not found in normal tissues. Based on the overlapping specificities of amino acid transporters and neurotransmitters, increased expression of these transporters may

explain the greater accumulation of PPIX in various cancer cells, including HeLa cells [24].

TSPO1/2

The TSPO protein is also involved in the transmembrane transport of 5-ALA. It exists as two isoforms: TSPO1 is mainly localized in the outer membrane of mitochondria, while TSPO2 is found in the plasma membrane of red blood cells. The work of Manceau et al. [26] showed that the intensity of 5-ALA-induced accumulation of PPIX in erythroleukemia cells (UT-7 and K562) decreased when a specific competitive inhibitor TSPO1/2 was added to the medium (inhibitor code PK 11195). PK 11195 did not change the activity of heme biosynthetic enzymes. From the data obtained, the study authors concluded that the limiting factor in heme synthesis was the penetration of 5-ALA through the plasma membrane. However, PK 11195 had no effect on porphobilinogen (PBG)-induced PPIX accumulation, suggesting that TSPO2 is a selective 5-ALA transporter. Further evidence for the role of TSPO2 in membrane transport of 5-ALA is the fact that overexpression of TSPO2 on the plasma membrane of erythroleukemia cells increased 5-ALA-induced accumulation of PPIX [26]. The described patterns are rather important for determining the mechanism and the possibility of influencing the development of congenital sideroblastic anemia, however, potentially, data on the expression of TSPO2 in other tissues can be used to predict the effectiveness of PDT in tissues expressing TSPO.

ABCG2

ABCG2, a protein used to transport compounds against their concentration gradient using ATP hydrolysis as an energy source, has been identified as an exporter of PPIX and heme in mammals [27]. These data are supported by experiments with ectopically expressed ABCG2, which exports ZnMP (zinc-containing mesoporphyrin, used as a heme analog in experimental models) into K562 cells [28]. ABCG2 is expressed in a wide range of tissues, including hematopoietic stem cells and erythroid progenitor cells. High protein concentrations are found in the duodenum, small and large intestines, rectum, seminal vesicles and endometrium. The distribution of the transporter in tissues that have a predominantly secretory or barrier function leads to the idea that ABCG2 plays an essential role in controlling the distribution and tissue exposure of the different chemical compounds, such as antibiotics, sterols, immunosuppressants (including anti-HIV drugs), fluorescent dyes (for example, Hoechst 33342), photosensitizers (pheophorbide A and PPIX). Increased expression of ABCG2 has been associated with multidrug resistance in cancer [29].

The level of ABCG2 expression is especially high in the early stages of hematopoiesis [30]. Like FLVCR1-mediated heme export, ABCG2 possibly exports and transfers heme to extracellular heme-binding proteins such as albumin [31]. However, unlike FLVCR1, ABCG2 has a wide range of substrates, including porphyrin and non-porphyrin sub-

strates, suggesting that ABCG2 may not be a functional backup to FLVCR1.

The activity of ABCG2, which is used for PPIX transport, also affects the fluorescence intensity of PPIX. Thus, the combined use of 5-ALA and Ko143, a specific inhibitor of ABCG2, on a model of cultured cancer cells MCF-7 and MDA-MB 231 increased the fluorescence intensity of PPIX compared to cultured non-cancerous MCF10A cells [32]. And in the study by Hagiya et al. [10] showed that the selective accumulation of PPIX in bladder cancer cells is caused precisely by an increase in the expression of PEPT1 and a decrease in the expression of ABCG2.

ABCB6

ABCB6 is a heme-binding ATP-dependent transport protein that can interact with various tetrapyrroles, such as heme, coproporphyrin III, PPIX and plant porphyrin, pheophorbide A. ABCB6 can be localized both in the outer mitochondrial membrane and in the plasma membrane [33]. The basal level of metabolites of heme synthesis metabolites is maintained by ATP-independent transporters, this level is sufficient for the survival of the organism. But under stress conditions, the work of ATP-dependent transporters, such as ABCB6, is necessary. When the level of the transporter is low, the synthesis of zinc protoporphyrin IX occurs, so it can be assumed that this transporter is also involved in iron homeostasis [33].

High concentrations of the transporter are found in the gallbladder, testes and epididymis [23].

FLVCR1

FLVCR1 is an export protein and has a narrow spectrum of substrates, including heme, PPIX and coproporphyrin. FLVCR1 is localized on the surface of the plasma membrane [34]. FLVCR1 is actively expressed in various hematopoietic cells, and low-level expression is found in the fetal liver, pancreas, and kidneys [35]. Ectopic expression of FLVCR1 reduces intracellular concentrations of PPIX. This is supported by experiments using ZnMP, which mediates PPIX efflux in K562 rat kidney epithelial and hematopoietic cells [34]. FLVCR1 is predicted to normally export heme when macrophages phagocytose senescent erythrocytes. Given that PPIX is also a substrate of FLVCR1, it is possible that PPIX efflux is mediated by this transport protein. Alves et al. showed that in nucleated erythrocyte progenitors from human bone marrow, FLVCR1 expression increased during erythropoiesis and reached a maximum level at an intermediate stage of maturation under conditions in which the heme oxygenase system was defective [36]. It is possible that FLVCR1 may export excess PPIX or heme to prevent toxicity under conditions in which heme degradation is not fully induced.

In addition to full-length FLVCR1 (FLVCR1a), there is another isoform, FLVCR1b, which is a smaller protein possibly localized to mitochondria [37]. Overexpression of FLVCR1b increases cytosolic heme concentration, whereas knockdown of FLVCR1b results in heme accumulation in

mitochondria, indicating that FLVCR1b is an exporter of mitochondrial heme and possibly PPIX [37].

Increased expression of FLVCR1, according to several authors, is found in hepatocellular carcinoma and is associated with a higher stage of the disease and vascular invasion. FLVCR1 also plays a key role in cell survival, growth and migration in esophageal squamous cell carcinoma [38]. Given the high degree of homology between FLVCR2 and FLVCR1 [39], it is possible that FLVCR2 also promotes PPIX and heme efflux. FLVCR2 is expressed in a wide range of human tissues, including fetal liver, brain, and kidney [40]. However, the direct physiological role of FLVCR2 in PPIX and heme transport is currently unclear.

MFRN

Mitoferrins (MFRN) are transporters involved in the transport of iron ions into mitochondria. Transported iron ions are also used for intramitochondrial heme synthesis. According to Hayashi et al. [41], the level of iron in the mitochondria of tumor cells can be significantly lower than in normal cells. This is one of the reasons (besides the low activity of ferrochelatase) why the excess PPIX formed upon exogenous administration of 5-ALA is quickly utilized in normal cells and persists for a longer period in tumor cells. This difference in iron levels can be explained by decreased expression in tumor cells of mitoferrins, which transport iron across the mitochondrial membrane. A practical application of the results of this study may be to increase the effectiveness of PDT by additionally introducing iron supplements during the treatment period: in normal cells this can lead to a decrease in PPIX induced by exogenous administration of 5-ALA, but in tumor cells (due to low expression of mitoferrins) there is no such effect will be [41].

Practical use

Assessment of the expression level of the transporter proteins genes for 5-ALA and porphyrinogens (primarily PEPT1 and ABCG2) under certain conditions can be used to predict the rate and intensity of accumulation of 5-ALA-induced PPIX [8]. And in tumor tissues this may correlate with the effectiveness of PDT.

In addition, as some studies have shown [16], the expression of 5-ALA transporters in normal cells may be higher or like that in tumor cells of similar origin. For example, normal lung cells (WI38) express much more PEPT1 than their malignant counterparts (A549) [16]. According to the authors of the study [16], for such cells PDT can be less effective and the risk of developing phototoxicity can be higher. The study authors suggest that the application of appropriate transporter inhibitors to be used with PDT may be promising. Experimental results show that this strategy leads to an increase in the fluorescent contrast between malignant and normal cells: in normal cells with high expression of the transporter, the inhibitory effect is more pronounced [16].

REFERENCES

1. Filonenko E.V. Clinical implementation and scientific development of photodynamic therapy in Russia in 2010-2020, *Biomedical Photonics*, 2021, Vol. 10, pp. 4-22.
2. Zharkova N.N. et al. Fluorescence observations of patients in the course of photodynamic therapy of cancer with the photosensitizer PHOTOSENS, *Photodynamic Therapy of Cancer II, SPIE*, 1995, Vol. 2325, pp. 400-403.
3. Sokolov V.V. et al. Clinical fluorescence diagnostics in the course of photodynamic therapy of cancer with the photosensitizer PHOTOGEN, *Photodynamic Therapy of Cancer II, SPIE*, 1995, Vol. 2325, pp. 375-380.
4. Filonenko E.V. et al. Photodynamic therapy in the treatment of intraepithelial neoplasia of the cervix, vulva and vagina, *Biomedical Photonics*, 2021, Vol. 9(4), pp. 31-39. <https://doi.org/10.24931/2413-9432-2020-9-4-31-39>.
5. Filonenko E.V., Ivanova-Radkevich V.I. Photodynamic therapy of psoriasis, *Biomedical Photonics*, 2023, Vol. 12(1), pp. 28-36. doi: 10.24931/2413-9432-2023-12-1-28-36.
6. Ivanova-Radkevich V. I. Biochemical basis of selective accumulation and targeted delivery of photosensitizers to tumor tissues, *Biochemistry (Moscow)*, 2022, Vol. 87(11), pp. 1226-1242. <https://doi.org/10.1134/S0006297922110025>.
7. Lai H. W., Nakayama T., Ogura S. Key transporters leading to specific protoporphyrin IX accumulation in cancer cell following administration of aminolevulinic acid in photodynamic therapy/diagnosis, *International Journal of Clinical Oncology*, 2021, Vol. 26, pp. 26-33.
8. Brandsch M. Drug transport via the intestinal peptide transporter PepT1, *Current opinion in pharmacology*, 2013, Vol. 13(6), pp. 881-887.
9. Döring F. et al. Delta-aminolevulinic acid transport by intestinal and renal peptide transporters and its physiological and clinical implications, *The Journal of clinical investigation*, 1998, Vol. 101(12), pp. 2761-2767.
10. Hagiya Y. et al. Expression levels of PEPT1 and ABCG2 play key roles in 5-aminolevulinic acid (ALA)-induced tumor-specific protoporphyrin IX (PpIX) accumulation in bladder cancer, *Photodiagnosis and photodynamic therapy*, 2013, Vol. 10(3), pp. 288-295.
11. Xie Y., Hu Y., Smith D. E. The proton-coupled oligopeptide transporter 1 plays a major role in the intestinal permeability and absorption of 5-aminolevulinic acid, *British journal of pharmacology*, 2016, Vol. 173(1), pp. 167-176.
12. Jappard D. et al. Significance and regional dependency of peptide transporter (PEPT) 1 in the intestinal permeability of glycylsarcosine: in situ single-pass perfusion studies in wild-type and Pept1 knockout mice, *Drug metabolism and disposition*, 2010, Vol. 38(10), pp. 1740-1746.
13. Neumann J., Brandsch M. δ -Aminolevulinic acid transport in cancer cells of the human extrahepatic biliary duct, *Journal of Pharmacology and Experimental Therapeutics*, 2003, Vol. 305(1), pp. 219-224.
14. Chung C. W. et al. Aminolevulinic acid derivatives-based photodynamic therapy in human intra- and extrahepatic cholangiocarcinoma cells, *European Journal of Pharmacology and Biopharmaceutics*, 2013, Vol. 85(3), pp. 503-510.
15. Hagiya Y. et al. Pivotal roles of peptide transporter PEPT1 and ATP-binding cassette (ABC) transporter ABCG2 in 5-aminolevulinic acid (ALA)-based photocytotoxicity of gastric cancer cells in vitro, *Photodiagnosis and photodynamic therapy*, 2012, Vol. 9(3), pp. 204-214.
16. Lai H. W. et al. Novel strategy to increase specificity of ALA-Induced PpIX accumulation through inhibition of transporters involved in ALA uptake, *Photodiagnosis and Photodynamic Therapy*, 2019, Vol. 27, pp. 327-335.
17. Tchernitchko D. et al. A variant of peptide transporter 2 predicts the severity of porphyria-associated kidney disease, *Journal of the American Society of Nephrology*, 2017, Vol. 28(6), pp. 1924-1932.
18. Xiang J. et al. PEPT2-mediated transport of 5-aminolevulinic acid and carnosine in astrocytes, *Brain research*, 2006, Vol. 1122(1), pp. 18-23.
19. Anderson C. M. H. et al. Transport of the photodynamic therapy agent 5-aminolevulinic acid by distinct H⁺-coupled nutrient car-

ЛИТЕРАТУРА

1. Filonenko E. V. Clinical implementation and scientific development of photodynamic therapy in Russia in 2010-2020 // *Biomed. Photonics*. – 2021. – Т. 10. – С. 4-22.
2. Zharkova N. N. et al. Fluorescence observations of patients in the course of photodynamic therapy of cancer with the photosensitizer PHOTOSENS // *Photodynamic Therapy of Cancer II. – SPIE*, 1995. – Т. 2325. – С. 400-403.
3. Sokolov V. V. et al. Clinical fluorescence diagnostics in the course of photodynamic therapy of cancer with the photosensitizer PHOTOGEN // *Photodynamic Therapy of Cancer II. – SPIE*, 1995. – Т. 2325. – С. 375-380.
4. Filonenko E. V. et al. Photodynamic therapy in the treatment of intraepithelial neoplasia of the cervix, vulva and vagina // *Biomedical Photonics*. – 2021. – Т. 9. – №. 4. – С. 31-39. <https://doi.org/10.24931/2413-9432-2020-9-4-31-39>.
5. Filonenko E.V., Ivanova-Radkevich V.I. Photodynamic therapy of psoriasis // *Biomedical Photonics*. – 2023. – Т. 12. – №. 1. – С. 28-36. doi: 10.24931/2413-9432-2023-12-1-28-36.
6. Ivanova-Radkevich V. I. Biochemical basis of selective accumulation and targeted delivery of photosensitizers to tumor tissues // *Biochemistry (Moscow)*. – 2022. – Т. 87. – №. 11. – С. 1226-1242. <https://doi.org/10.1134/S0006297922110025>.
7. Lai H. W., Nakayama T., Ogura S. Key transporters leading to specific protoporphyrin IX accumulation in cancer cell following administration of aminolevulinic acid in photodynamic therapy/diagnosis // *International Journal of Clinical Oncology*. – 2021. – Т. 26. – С. 26-33.
8. Brandsch M. Drug transport via the intestinal peptide transporter PepT1 // *Current opinion in pharmacology*. – 2013. – Т. 13. – №. 6. – С. 881-887.
9. Döring F. et al. Delta-aminolevulinic acid transport by intestinal and renal peptide transporters and its physiological and clinical implications // *The Journal of clinical investigation*. – 1998. – Т. 101. – №. 12. – С. 2761-2767.
10. Hagiya Y. et al. Expression levels of PEPT1 and ABCG2 play key roles in 5-aminolevulinic acid (ALA)-induced tumor-specific protoporphyrin IX (PpIX) accumulation in bladder cancer // *Photodiagnosis and photodynamic therapy*. – 2013. – Т. 10. – №. 3. – С. 288-295.
11. Xie Y., Hu Y., Smith D. E. The proton-coupled oligopeptide transporter 1 plays a major role in the intestinal permeability and absorption of 5-aminolevulinic acid // *British journal of pharmacology*. – 2016. – Т. 173. – №. 1. – С. 167-176.
12. Jappard D. et al. Significance and regional dependency of peptide transporter (PEPT) 1 in the intestinal permeability of glycylsarcosine: in situ single-pass perfusion studies in wild-type and Pept1 knockout mice // *Drug metabolism and disposition*. – 2010. – Т. 38. – №. 10. – С. 1740-1746.
13. Neumann J., Brandsch M. δ -Aminolevulinic acid transport in cancer cells of the human extrahepatic biliary duct // *Journal of Pharmacology and Experimental Therapeutics*. – 2003. – Т. 305. – №. 1. – С. 219-224.
14. Chung C. W. et al. Aminolevulinic acid derivatives-based photodynamic therapy in human intra- and extrahepatic cholangiocarcinoma cells // *European Journal of Pharmacology and Biopharmaceutics*. – 2013. – Т. 85. – №. 3. – С. 503-510.
15. Hagiya Y. et al. Pivotal roles of peptide transporter PEPT1 and ATP-binding cassette (ABC) transporter ABCG2 in 5-aminolevulinic acid (ALA)-based photocytotoxicity of gastric cancer cells in vitro // *Photodiagnosis and photodynamic therapy*. – 2012. – Т. 9. – №. 3. – С. 204-214.
16. Lai H. W. et al. Novel strategy to increase specificity of ALA-Induced PpIX accumulation through inhibition of transporters involved in ALA uptake // *Photodiagnosis and Photodynamic Therapy*. – 2019. – Т. 27. – С. 327-335.
17. Tchernitchko D. et al. A variant of peptide transporter 2 predicts the severity of porphyria-associated kidney disease // *Journal of the American Society of Nephrology*. – 2017. – Т. 28. – №. 6. – С. 1924-1932.
18. Xiang J. et al. PEPT2-mediated transport of 5-aminolevulinic acid and carnosine in astrocytes // *Brain research*. – 2006. – Т. 1122. – №. 1. – С. 18-23.
19. Anderson C. M. H. et al. Transport of the photodynamic therapy agent 5-aminolevulinic acid by distinct H⁺-coupled nutrient car-

- rriers coexpressed in the small intestine, *Journal of Pharmacology and Experimental Therapeutics*, 2010, Vol. 332(1), pp. 220-228.
20. Boll M. et al. Functional characterization of two novel mammalian electrogenic proton-dependent amino acid cotransporters, *Journal of Biological Chemistry*, 2002, Vol. 277(25), pp. 22966-22973.
21. Kristensen A. S. et al. SLC6 neurotransmitter transporters: structure, function, and regulation, *Pharmacological reviews*, 2011, Vol. 63(3), pp. 585-640.
22. Zhou Y. et al. Deletion of the γ -aminobutyric acid transporter 2 (GAT2 and SLC6A13) gene in mice leads to changes in liver and brain taurine contents, *Journal of Biological Chemistry*, 2012, Vol. 287(42), pp. 35733-35746.
23. <https://www.proteinatlas.org/ENSG00000115657-ABCB6/tissue>
24. Tran T. T. et al. Neurotransmitter Transporter Family Including SLC 6 A 6 and SLC 6 A 13 Contributes to the 5-Aminolevulinic Acid (ALA)-Induced Accumulation of Protoporphyrin IX and Photodamage, through Uptake of ALA by Cancerous Cells, *Photochemistry and photobiology*, 2014, Vol. 90(5), pp. 1136-1143.
25. Bermudez Moretti M. et al. δ -aminolevulinic acid transport in murine mammary adenocarcinoma cells is mediated by BETA transporters, *British journal of cancer*, 2002, Vol. 87(4), pp. 471-474.
26. Manceau H. et al. TSP02 translocates 5-aminolevulinic acid into human erythroleukemia cells, *Biology of the Cell*, 2020, Vol. 112(4), pp. 113-126.
27. Krishnamurthy P., Schuetz J. D. The ABC transporter Abcg2/Bcrp: role in hypoxia mediated survival, *Biometals*, 2005, Vol. 18, pp. 349-358.
28. Desuzinges-Mandon E. et al. ABCG2 transports and transfers heme to albumin through its large extracellular loop, *Journal of biological chemistry*, 2010, Vol. 285(43), pp. 33123-33133.
29. Horsey A. J. et al. The multidrug transporter ABCG2: still more questions than answers, *Biochemical Society Transactions*, 2016, Vol. 44(3), pp. 824-830.
30. Wu X. G., Peng S. B., Huang Q. Transcriptional regulation of breast cancer resistance protein, *Yi Chuan= Hereditas*, 2012, Vol. 34(12), pp. 1529-1536.
31. Krishnamurthy P. et al. The stem cell marker Bcrp/ABCG2 enhances hypoxic cell survival through interactions with heme, *Journal of Biological Chemistry*, 2004, Vol. 279(23), pp. 24218-24225.
32. Morita M. et al. Fluorescence-based discrimination of breast cancer cells by direct exposure to 5-aminolevulinic acid, *Cancer medicine*, 2019, Vol. 8(12), pp. 5524-5533.
33. Boswell-Casteel R. C., Fukuda Y., Schuetz J. D. ABCB6, an ABC transporter impacting drug response and disease, *The AAPS journal*, 2018, Vol. 20, pp. 1-10.
34. Quigley J. G. et al. Identification of a human heme exporter that is essential for erythropoiesis, *Cell*, 2004, Vol. 118(6), pp. 757-766.
35. Quigley J. G. et al. Cloning of the cellular receptor for feline leukemia virus subgroup C (FeLV-C), a retrovirus that induces red cell aplasia, *Blood, The Journal of the American Society of Hematology*, 2000, Vol. 95(3), pp. 1093-1099.
36. Alves L. R. et al. Heme-oxygenases during erythropoiesis in K562 and human bone marrow cells, *PLoS One*, 2011, Vol. 6(7), e21358.
37. Chiabrando D. et al. The mitochondrial heme exporter FLVCR1b mediates erythroid differentiation, *The Journal of clinical investigation*, 2012, Vol. 122(12), pp. 4569-4579.
38. Zhou S. et al. FLVCR1 predicts poor prognosis and promotes malignant phenotype in esophageal squamous cell carcinoma via upregulating CSE1L, *Frontiers in Oncology*, 2021, Vol. 11, pp. 660955.
39. Brown J. K., Fung C., Taylor C. S. Comprehensive mapping of receptor-functioning domains in feline leukemia virus subgroup C receptor FLVCR1, *Journal of virology*, 2006, Vol. 80(4), pp. 1742-1751.
40. Duffy S. P. et al. The Fowler syndrome-associated protein FLVCR2 is an importer of heme, *Molecular and cellular biology*, 2010, Vol. 30(22), pp. 5318-5324.
41. Hayashi M. et al. The effect of iron ion on the specificity of photodynamic therapy with 5-aminolevulinic acid, *PLoS One*, 2015, Vol. 10(3), e0122351.
- ers coexpressed in the small intestine // *Journal of Pharmacology and Experimental Therapeutics*. – 2010. – T. 332. – №. 1. – C. 220-228.
20. Boll M. et al. Functional characterization of two novel mammalian electrogenic proton-dependent amino acid cotransporters // *Journal of Biological Chemistry*. – 2002. – T. 277. – №. 25. – C. 22966-22973.
21. Kristensen A. S. et al. SLC6 neurotransmitter transporters: structure, function, and regulation // *Pharmacological reviews*. – 2011. – T. 63. – №. 3. – C. 585-640.
22. Zhou Y. et al. Deletion of the γ -aminobutyric acid transporter 2 (GAT2 and SLC6A13) gene in mice leads to changes in liver and brain taurine contents // *Journal of Biological Chemistry*. – 2012. – T. 287. – №. 42. – C. 35733-35746.
23. <https://www.proteinatlas.org/ENSG00000115657-ABCB6/tissue>
24. Tran T. T. et al. Neurotransmitter Transporter Family Including SLC 6 A 6 and SLC 6 A 13 Contributes to the 5-Aminolevulinic Acid (ALA)-Induced Accumulation of Protoporphyrin IX and Photodamage, through Uptake of ALA by Cancerous Cells // *Photochemistry and photobiology*. – 2014. – T. 90. – №. 5. – C. 1136-1143.
25. Bermudez Moretti M. et al. δ -aminolevulinic acid transport in murine mammary adenocarcinoma cells is mediated by BETA transporters // *British journal of cancer*. – 2002. – T. 87. – №. 4. – C. 471-474.
26. Manceau H. et al. TSP02 translocates 5-aminolevulinic acid into human erythroleukemia cells // *Biology of the Cell*. – 2020. – T. 112. – №. 4. – C. 113-126.
27. Krishnamurthy P., Schuetz J. D. The ABC transporter Abcg2/Bcrp: role in hypoxia mediated survival // *Biometals*. – 2005. – T. 18. – C. 349-358.
28. Desuzinges-Mandon E. et al. ABCG2 transports and transfers heme to albumin through its large extracellular loop // *Journal of biological chemistry*. – 2010. – T. 285. – №. 43. – C. 33123-33133.
29. Horsey A. J. et al. The multidrug transporter ABCG2: still more questions than answers // *Biochemical Society Transactions*. – 2016. – T. 44. – №. 3. – C. 824-830.
30. Wu X. G., Peng S. B., Huang Q. Transcriptional regulation of breast cancer resistance protein // *Yi Chuan= Hereditas*. – 2012. – T. 34. – №. 12. – C. 1529-1536.
31. Krishnamurthy P. et al. The stem cell marker Bcrp/ABCG2 enhances hypoxic cell survival through interactions with heme // *Journal of Biological Chemistry*. – 2004. – T. 279. – №. 23. – C. 24218-24225.
32. Morita M. et al. Fluorescence-based discrimination of breast cancer cells by direct exposure to 5-aminolevulinic acid // *Cancer medicine*. – 2019. – T. 8. – №. 12. – C. 5524-5533.
33. Boswell-Casteel R. C., Fukuda Y., Schuetz J. D. ABCB6, an ABC transporter impacting drug response and disease // *The AAPS journal*. – 2018. – T. 20. – C. 1-10.
34. Quigley J. G. et al. Identification of a human heme exporter that is essential for erythropoiesis // *Cell*. – 2004. – T. 118. – №. 6. – C. 757-766.
35. Quigley J. G. et al. Cloning of the cellular receptor for feline leukemia virus subgroup C (FeLV-C), a retrovirus that induces red cell aplasia // *Blood, The Journal of the American Society of Hematology*. – 2000. – T. 95. – №. 3. – C. 1093-1099.
36. Alves L. R. et al. Heme-oxygenases during erythropoiesis in K562 and human bone marrow cells // *PLoS One*. – 2011. – T. 6. – №. 7. – C. e21358.
37. Chiabrando D. et al. The mitochondrial heme exporter FLVCR1b mediates erythroid differentiation // *The Journal of clinical investigation*. – 2012. – T. 122. – №. 12. – C. 4569-4579.
38. Zhou S. et al. FLVCR1 predicts poor prognosis and promotes malignant phenotype in esophageal squamous cell carcinoma via upregulating CSE1L // *Frontiers in Oncology*. – 2021. – T. 11. – C. 660955.
39. Brown J. K., Fung C., Taylor C. S. Comprehensive mapping of receptor-functioning domains in feline leukemia virus subgroup C receptor FLVCR1 // *Journal of virology*. – 2006. – T. 80. – №. 4. – C. 1742-1751.
40. Duffy S. P. et al. The Fowler syndrome-associated protein FLVCR2 is an importer of heme // *Molecular and cellular biology*. – 2010. – T. 30. – №. 22. – C. 5318-5324.
41. Hayashi M. et al. The effect of iron ion on the specificity of photodynamic therapy with 5-aminolevulinic acid // *PLoS One*. – 2015. – T. 10. – №. 3. – C. e0122351.


ФОТОСЕНСИБИЛИЗАТОРЫ НОВОГО ПОКОЛЕНИЯ ДЛЯ ФОТОДИНАМИЧЕСКОЙ ТЕРАПИИ



«ФОТОДИТАЗИН®» концентрат для приготовления раствора для инфузий — лекарственное средство (РУ № ЛС 001246 от 18.05.2012 г.)
«ФОТОДИТАЗИН®» гель — изделие медицинского назначения (РУ № ФСР 2012/13043 от 03.02.2012 г.)
«ФОТОДИТАГЕЛЬ®» — косметическое средство (ДС ЕАЭС № RU Д-РУ.НВ42.В.06108/20 от 24.09.2020 г.)

Препараты применяются для флюоресцентной диагностики и фотодинамической терапии злокачественных новообразований, а так же патологий не онкологического характера в следующих областях медицины:

- | | |
|------------------------|--------------------|
| ✓ гинекология | ✓ ортопедия |
| ✓ урология | ✓ комбустиология |
| ✓ нейрохирургия | ✓ гнойная хирургия |
| ✓ торакальная хирургия | ✓ дерматология |
| ✓ офтальмология | ✓ косметология |
| ✓ травматология | ✓ стоматология |

 www.fotoditazin.com
www.фотодитазин.рф

ООО «ВЕТА-ГРАНД»

123056, г. Москва, ул. Красина, д. 27, стр. 2
Тел.: +7 (499) 250-40-00, +7 (929) 971-44-46
E-mail: veta-grand@mail.ru



@FOTODITAZIN



@FOTODITAGEL_FDT

